INFORMATION TO USERS

This manuscript has been reproduced from the microfilm master. UMI films the text directly from the original or copy submitted. Thus, some thesis and dissertation copies are in typewriter face, while others may be from any type of computer printer.

The quality of this reproduction is dependent upon the quality of the copy submitted. Broken or indistinct print, colored or poor quality illustrations and photographs, print bleedthrough, substandard margins, and improper alignment can adversely affect reproduction.

In the unlikely event that the author did not send UMI a complete manuscript and there are missing pages, these will be noted. Also, if unauthorized copyright material had to be removed, a note will indicate the deletion.

Oversize materials (e.g., maps, drawings, charts) are reproduced by sectioning the original, beginning at the upper left-hand corner and continuing from left to right in equal sections with small overlaps.

Photographs included in the original manuscript have been reproduced xerographically in this copy. Higher quality 6" x 9" black and white photographic prints are available for any photographs or illustrations appearing in this copy for an additional charge. Contact UMI directly to order.

ProQuest Information and Learning
300 North Zeeb Road, Ann Arbor, MI 48106-1346 USA
800-521-0600

Université d'Ottawa • University of Ottawa

Application of GAC Adsorption in Pulp and Paper Mill Effluent Treatment

by
Jing Zheng

A thesis
submitted under the supervision of
Dr. R.L.Droste

in partial fulfillment of the
requirements for the degree of
Master of Applied Science
in
Civil Engineering

Department of Civil Engineering
University of Ottawa
Ottawa, Ontario
K1N 6N5
Canada

ACKNOLEDGMENT

Many thanks to the members of the Department of Civil Engineering for their advice and guidance in this work: Drs. Ron L. Droste, Roberto M. Narbaitz, Kevin J. Kennedy, and Leta F. Fernandes.

I also express my gratitude to the following persons: Mr. Francisco Aposaga for technical assistance, Mr. Brian R. Graham and many other fellow students for their support and friendship, and staff in the Department of Civil Engineering.

Thanks to my husband Fulei Yang for his support and the example of a work ethic.

ABSTRACT

Aerated stabilization basins (ASB) and activated sludge treatment (AST) are the most popular unit processes in the treatment of Pulp and paper mill effluents. However, these traditional biological processes can only provide partially satisfactory treatment because many components in pulp and paper mill wastes are persistent under the conditions of these processes. This study evaluated the application of granular activated carbon (GAC) adsorption using fixed-bed columns in the post-treatment of the whole-plant effluent of a Kraft and fine paper manufacturer. A mathematical model, the branched pore or dual rate model, was used to simulate the GAC column adsorption process. The computer program PRECOS was used to solve the model.

The wastewater was first treated using a traditional AST system and then filtered and passed through a small-scale GAC column to obtain data for estimating mass transfer coefficients of the model. Calgon® F400 GAC was used. Isotherm studies were carried out for column influents to determine the adsorption capacity of the GAC. A simplified form of the dual rate model was used to predict the column performance in terms of treatment efficiency, consumption of carbon, and organic removal. The mass transfer coefficients of the model were determined based on microcolumn experimental data. The performance of AST system followed by GAC column adsorption process was compared to that of a PACT™ system in the treatment of a similar wastewater.

It was found that for an overall COD removal of 80%, the carbon usage rate of the PACT™ system was 30% lower than that of the GAC column system. The lower performance of the GAC column system was attributed to a possible low efficiency in terms of carbon usage in the microcolumn experiment. A direct comparison between the two systems based on experiments is also needed.

TABLE OF CONTENTS

LIST OF TABLES

LIST OF FIGURES

GLOSSARY

Parameters (typical units in parentheses):

A	cross sectional area of the column (m^2 or cm^2)
B	constant in BET isotherm
a_p	specific external surface area of adsorbent (cm^2/cm^3)
c	equilibrium concentration of adsorbate in solution (mg/L)
c_0	influent or liquid phase initial concentration (mg/L)
c_e	liquid phase equilibrium concentration (mg/L)
c_r	non-adsorbable matter (mg/L)
c_s	liquid phase equilibrium concentration at particle surface (g/cm^3)
D	length of the column (m)
D_p	effective pore diffusion coefficient (cm^2/s)
D_s	effective surface diffusion coefficient (cm^2/s)
D_z	axial dispersion coefficient (cm^2/s)
f	fraction of total capacity available in macropores
k_b	micropore rate coefficient (s^{-1})
k_f	external film transfer coefficient (cm/s)
K_F	Freundlich isotherm constant
k_m	macropore pseudo mass transfer coefficient (cm/s)
k_p	pseudo mass transfer coefficient (cm/s)
M	mass of carbon in the bottle used in isotherm experiments (g)
n	Freundlich isotherm exponent
N	total number of data
Q	volumetric loading rate of reactors or carbon columns (m^3/d or cm^3/d)
q	solid phase concentration, (g/g)
$\bar{q}$	mean solid phase concentration in the particle (g/g)
q_b	branch pore solid phase concentration (g/g)
$\bar{q}_b$	mean branch pore solid phase concentration (g/g)
q_m	micropore solid phase concentration (g/g)
$\bar{q}_m$	mean macropore solid phase concentration (g/g)
q_s	solid phase concentration at the particles' external surface (g/g)
q_∞	solid phase concentration at initial concentration (g/g)
η	average error
ρ_b	packed density of adsorbent (kg/m^3 or g/cm^3)
ρ_c	apparent adsorbent particle density (g/cm^3)
θ_H	hydraulic loading rate (d)
ε	liquid phase volume fraction
ε_p	internal porosity of the adsorbent particle
ρ_p	packed density of the carbon (mg/cm^3)

Q_m	constant in BET isotherm
Q_w	wastage rate of AST reactors (cm^3/d)
R	radius of adsorbent particle (cm)
r	radius variable (cm)
R_b	rate of transfer from macropores to micropores (mg/g/s)
R_e	carbon exhaustion rate (kg/m^3)
$R_{e,mim}$	theoretical minimum carbon exhaustion rate (kg/m^3)
t	time (s)
V	aeration tank volume (cm^3)
v_s	interstitial liquid phase velocity (cm/s)
W	mass of carbon (g)
X	mixed liquor *VSS* (g/cm^3)
x	adsorption bed length variable (cm)
X_e	effluent TSS (g/cm^3)
$x_{predicted}$	predicted effluent concentration
$x_{observed}$	experimental data

Abbreviations/Acronyms (typical units in parentheses)

AOX	Adsorbable organic halide.
AST	Activated sludge treatment.
ASB	Aerated stabilization basin.
BOD	Biochemical oxygen demand (mg/L).
CL	Column length (cm).
COD	Chemical oxygen demand (mg/L).
EBCT	Empty bed contact time (min).
F/M	Food to microorganism ratio (mg TOC/(mg VSS × d)).
GAC	Granular activated carbon.
HLR	Hydraulic loading rate (m/h).
SRT	Sludge age (d).
HRT	Hydraulic retention time (h).
MEP	Metabolic end product.
ML	Mixed liquor.
PAC	Powdered activated carbon.
PACT™	Powered activated carbon treatment. A patented process in which PAC is mixed into the mixed liquor of activated sludge.
QDF	Quadratic driving force.
SRT	Solids retention time (d).
TOC	Total organic carbon (mg/L).
TSS	Total suspended solids (mg/L).

Chapter 1

INTRODUCTION

The pulp and paper industry is one of the oldest and most economically important industries in Canada. It produces large quantities of organic and chlorinated wastes. Since the 1970s, it has become increasingly regulated for its effluent discharges. Increasing environmental concern and international competition have led to research and development of new pulping procedures and high-efficiency treatment facilities.

Pulp is an intermediate product in the manufacture of pulp and paper products. Pulping processes are divided into two principal categories: chemical and mechanical. The Kraft process, also known as the sulfate process, is the dominant chemical pulping process in Canada and the rest of the world. Kraft pulp is manufactured by separating the wood into its individual fibers by cooking wood chips under pressure and high temperature in a digester with strong alkali. The pulp is usually then bleached by molecular chlorine, chlorine compounds and related chemicals. These processes consume large amounts of energy and water and form the major sources of organic wastes, particularly chlorinated organic wastes and other toxic substances discharged to the environment. These wastes pose a serious human health hazard and are difficult to degrade.

The federal and provincial governments have promulgated regulations since 1971 to control the quality and limit the quantity of effluent discharged to Canadian waterways. To comply with the regulations, all Canadian pulp and paper mills had installed and put in operation their biological treatment systems by the end of 1995 (Kantardjieff and Jones,

1997). Among the existing treatment systems, aerated stabilization basins (ASB) and activated sludge treatment (AST) are the most popular unit processes. However, these traditional biological processes can only provide partial treatment because many components in pulp and paper mill wastes are persistent under the conditions of these processes and can upset biological treatment systems. Therefore, improvement of effluent quality is often achieved by adding additional advanced treatment stages.

A whole-plant effluent of a Kraft and fine paper manufacturer was used as the source wastewater in this study. Objectives of this study were to evaluate the adsorptive capacity of granular activated carbon (GAC) in the treatment of the waste and to compare the performance of AST system followed by GAC column process with that of a PACT™ process in terms of treatment efficiency, consumption of carbon, and organic removal.

Chapter 2

LITERATURE REVIEW

2.1 Pulp and Paper Industry as A Pollution Source

Pulp is an intermediate product in the manufacture of paper. The primary raw material of paper making, wood contains about 45% cellulose fiber, 25% hemicellulose, 20–30% lignin, and 1.5–5% extractives. The purpose of pulping is to free the cellulose fibers from the other wood components to obtain individual fibers that will be suitable for paper or related products.

There are a number of different pulping processes with varying effluent characteristics. Traditionally, these processes have been divided into two principal categories: mechanical and chemical. In mechanical pulping, the fibers are separated by application of mechanical energy under wet conditions. The yield, i.e., the weight of pulp produced from a unit weight of oven dry wood, of mechanical pulping is high, ranging from 90 to 96%; however, since the fibers are literally torn apart in the process, they become weak. This process decreased in popularity when chemical pulping, which separated the wood fibers by breaking down the bonds between them with chemical reactants and produced longer stronger fibers, was developed. During the early half of the 20^{th} century, sulfite pulping predominated, which was replaced by Kraft pulping. Today, Kraft pulp accounts for a very large share of the total pulp production (Sinclair, 1990; McCubbin, 1992).

Kraft pulping process begins by treating wood chips at 160–180°C in a sodium sulfide and sodium hydroxide solution, referred to as "white liquor". This process cleaves lignin

ether bonds and dissolves 90–95% of the lignin and essentially all hemicellulose and wood extractives. Approximately 55% of the original wood is dissolved in the spent cooking liquor, known as "black liquor". The yield of Kraft pulping ranges from 40 to 55% (Kringsted and Lindstrom, 1984, McCubbin, 1992).

Byproducts are recovered. The black liquor is evaporated to a high concentration and then burned for recovery of energy and inorganic chemicals. The evaporated phase that may contain inorganic sulfur in the form of sulfate, sulfite, or dithionite, is trapped in a condenser. The content, termed as the evaporator condensate, forms a concentrated sulfur wastewater stream. Air contamination is caused by the highly volatile fugitive emissions from the condenser and volatile compounds and gases from the burnt concentrated black liquor (Kringsted and Lindstrom, 1984).

The pulping process is terminated when the pulp still contains 5–10% lignin, as further delignification would harm fiber quality. In the bleaching process, the unwanted lignin is dissolved from the pulp in order to obtain a high and permanent brightness of the pulp. The lignin is first converted to compounds that are soluble in alkali by treatment with molecular chlorine and/or chlorine dioxide and then washed out with sodium hydroxide. Subsequent bleaching treatments may vary, but usually proceed through a series of hypochlorite, chlorine dioxide, alkali, and chlorine dioxide processing steps. After this treatment stage, the pulp is filtered, and the process liquids are combined as bleachery effluent. The conventional bleaching process is the source of about half the BOD, all the chlorinated organic compounds, most of the color, and much of the toxicity in the effluent from a typical bleached kraft mill (Kringsted and Lindstrom, 1984; McCubbin, 1992).

2.2 Pulp and Paper Industry Effluent Control

Ranking third in the world in terms of freshwater withdrawal, the pulp and paper industry is believed to become the largest manufacturing user of water by the year 2000 (Kallas and Munter, 1994). In Canada, it has been estimated that this industry is responsible for 50% of all the waste dumped into the nation's waters (Sinclair, 1990). The large quantities of organic, especially organic chlorine compounds in the pulp and paper mill effluents are toxic, difficult to degrade, and have a propensity to bioaccumulate.

2.2.1 Effluent Regulations in Canada

Promulgated in 1971 under the Fisheries Act, the Pulp and Paper Effluent Regulations limits the quantities of certain substances – specifically, total suspended solids (TSS) and BOD matter– that may be discharged into waterways. These substances can affect the food chain. In addition, mills are prohibited from discharging any acutely lethal effluent that kills fish under specified laboratory test conditions. The regulations applied to mills built after 1971, which account for about 10% of all mills. In 1992, the regulations were amended to cover all Canadian mills and two off-site treatment facilities (Environment Canada, 1996).

The traditional wastewater parameters, TSS, BOD, and acute lethality, provide a basis for examining the short term and local effects of effluent discharges. In recent years attention has shifted to the longer term effects, requiring consideration of the content of persistent and/or bioaccumulative substances in the effluents. Chemical oxygen demand (COD) and adsorbable organic halogens (AOX) provide indications of the total quantities of non- and poorly biodegradable substances in the effluent (McCubbin, 1992).

AOX is an analysis of organohalogens that are adsorbable on activated charcoal. In a pulp mill effluent AOX is an approximate measure of total organic chlorine compounds. It consists of approximately 80% high-molecular mass materials, 19% relatively hydrophilic low-molecular mass compounds, and 1% others. The exact composition varies considerably

depending on its origin (McCubbin, 1992). Many countries are now legislating effluent discharge limits based on the amount of chlorine bound to organic matter in the effluent stream. In Canada a number of provinces have developed regulations to limit discharges of organic chlorine compounds from Kraft mills to levels as low as 1.4 kg AOX/t ADP (air dry pulp) (Hall and Randle, 1992).

In 1992, the Pulp and Paper Mill Chlorinated Dioxins and Furans Regulations were promulgated under the Canadian Environmental Protection Act (CEPA). Dioxins and furans are persistent and tend to accumulate in sediments and in human and animal tissues. They were found to be produced when certain compounds were present in the materials used to manufacture wood pulp. The regulations require all mills that use chlorine or chlorine dioxide in bleaching to take measures to prevent the formation of dioxins and furans and prohibit the discharge of measurable amounts of the most toxic forms of dioxins and furans, i.e., 2,3,7,8-TCDD and 2,3,7,8-TCDF (Environment Canada, 1996).

2.2.2 Environmental Significance of Process Modification

Many existing pulp and paper manufacturing processes can be modified to reduce the consumption of energy and raw materials at the source. These modifications result in reduced effluent discharges and always lower the need for external effluent treatment. Technologies for this purpose have been developed at an increasing rate. Of primary concern has been the modification of bleaching processes, namely the utilization of oxygen delignification and the substitution of molecular chlorine with chlorine dioxide.

Since the early 1970s, the oxygen delignification stage has been added to the conventional bleach plant in many European mills, as well as a growing number of mills in the US and in Canada. The filtrate from an oxygen delignification stage may be recycled to the chemical recovery system. The installation of an oxygen stage will allow most bleached Kraft mills to reduce bleach plant BOD discharges by approximately 50% and color by 60%.

Discharges of organic chlorine compounds will be reduced by approximately 30–50% (McCubbin, 1992).

Chlorine dioxide is used increasingly to replace the traditional molecular chlorine in the first chlorination stage of the bleach plant. Chlorine dioxide substitution is defined as the percentage of "equivalent chlorine" or "active chlorine" used in the form of chlorine dioxide in the chlorination stage. In the past, the advantages of this process modification were most concerned with improvements in pulp quality, but the principal driving force to increased substitution is AOX and PCDD/PCDF reductions. Since 1 kg of chlorine dioxide can replace approximately 2.63 kg molecular chlorine, there is a net reduction in the amount of chlorine used, and a reduction in discharges of organic chlorine compounds.

For most mills, chlorine dioxide substitution is the simplest and lowest capital cost approach for reducing organic chlorine compounds. Compared to a mill with neither oxygen delignification nor chlorine dioxide substitution, this process modification can reduce discharges of chlorinated organic compounds by up to 70%, if all of the molecular chlorine is replaced (McCubbin, 1992). In practice, oxygen delignification and chlorine dioxide substitution are often used simultaneously.

2.2.3 Biological Treatment of Pulp and Paper Mill Effluents

There are many forms of biological treatment used to treat municipal and industrial effluents. ASB and AST have been the most popular treatment processes in the pulp and paper industry. There are approximately 600 installations in the North American pulp and paper mills, and increasing numbers are being installed in Scandinavia and other pulp and paper producing regions (McCubbin, 1992).

The existing treatment facilities at paper mills were designed to control conventional pollutants, such as TSS and BOD. The dissolved BOD fraction of pulp and paper mill

effluents consists largely of wood extractives and cellulose decomposition products. Since these substances are readily amenable to bacterial attack, the removal of BOD through ASB and AST is usually greater than 90% (Bryant et al., 1992; Hall and Randle, 1992; Çeçen et al., 1992). However, the COD removals were reported below 60% in both ASBs and AST systems (Saunamäki et al., 1991; Hall and Randle, 1992; Çeçen et al., 1992; Möbius and Gordes-Tolle, 1994).

The abilities of ASB and AST systems to remove organic chlorine compounds have been studied by various researchers (Randle et al., 1991; Saunamäki et al., 1991; Bryant et al., 1992; Hall and Randle, 1992; Çeçen et al., 1992). The hypothesized mechanism of AOX removal in ASB was adsorption onto virgin biomass and subsequent settling to the benthal layer, and the settled adsorbed AOX has been reported to undergo dehalogenation (Bryant et al., 1988, 1992). In AST systems, studies indicated that the removal of organic chlorine compounds was largely the result of biological degradation (Saunamäki et al., 1991; Çeçen et al., 1992). In a survey conducted for eight full-scale wastewater treatment systems operated at pulp and paper mills in North America, the average removals of AOX were 34% in five ASBs and 46% in two AST systems (Bryant et al., 1992). Both the ASBs and AST facilities on average removed over half of the influent low molecular weight AOX, and the average removal of high molecular weight AOX varied among mill sites from 1 to 47%.

2.2.4 Activated Carbon Adsorption in the Treatment of Pulp And Paper Mill Effluents

Since over half of the pollutants in pulp and paper mill effluents measured by COD and AOX are non-degradable during conventional biological treatment, advanced treatment methods have been studied and put into practice in the effort to improve the treatment results and to meet the increasingly stringent environmental regulations. Some studies have emphasized alternative secondary treatment processes, while the others have explored additional treatment stages following the widely used biological treatment processes.

Activated carbon adsorption has been evaluated in both manners in the treatment of pulp and paper mill effluents. Unit operations utilized include fixed bed GAC columns, fluidized GAC columns, and powdered activated carbon (PAC) treatment. The treatment processes have often been tested using pilot plants.

2.2.4.1 Adsorption as A Secondary Treatment Process

In a pilot-scale study conducted in Canada, downflow GAC columns were used to treat the whole-plant effluent of a Kraft mill that produced bleached, semi-bleached, and unbleached Kraft pulp from a combination of 90% softwood and 10% hardwood (Wasserlauf, 1975). The effluent was clarified and then passed through four GAC columns operated in series. The average BOD, COD, suspended solids (SS), and color of the column influent were 335, 784, and 85 mg/L, and 2600 color units, respectively. The corresponding overall removals were 36, 57, 65, and 58% while the loading was 0.0625 g BOD per g carbon used (Wasserlauf, 1975).

In Fitchburg, Massachusetts, a full-scale GAC filter system has been in operation since 1976 to treat the pulp and paper effluent mixed with municipal wastewater (Callahan and Pincince, 1977). The system consists of 12 GAC columns, each 6.1 m in diameter and 4.7 m in bed depth, operated in parallel. The performance of the system reported in 1977 indicated that, pre-treated by flocculation (lime and alum added) and clarification, the mixed wastewater entering the GAC filters had average BOD, COD, and SS values of 97, 200, and 24 mg/L, respectively. The average BOD, COD, and SS values in the filter effluent were 5, 12, and 7 mg/L respectively. About 0.25 g of COD had been removed per g of carbon. It was also concluded that bacterial growth on carbon effectively extended the life of the carbon by degrading the organic material in the applied wastewater (Callahan and Pincince, 1977).

2.2.4.2 Adsorption of Bio-treated Effluents

Adsorption studies of biologically treated pulp and paper mill effluents have been conducted to evaluate adsorption capacity of activated carbon for non-biodegradable matter. In pilot plant studies carried out at two integrated pulp and paper mills in the U.S. with biological treatment facilities, the feasibility of using GAC columns for the post treatment of the mill effluents was investigated (Chen, 1981). The effluent of one mill was pretreated with an AST system and the other with an ASB. Then both effluents were filtered with sand filters before entering the pilot plant. Four adsorption columns were operated in series in the pilot plant. Different contact times, ranging from 35 to 140 minutes, were tested. It was observed that the carbon columns continued removing chloroform for many days after becoming exhausted for the adsorption of COD and color. With 70 minutes of contact time, to remove 80% influent COD, the carbon dosages were 6.2 kg/m^3 and 20.4 kg/m^3; to remove 80% influent chloroform, the carbon dosage was 0.34 kg/m^3, which was much lower than the dosage needed for the same percentage of COD removal (Chen, 1981).

Several isotherm studies for biologically treated pulp and paper mill effluents have been reported in recent years (Çeçen et al., 1992, 1993; Kallas et al., 1994). Çeçen et al. conducted isotherm studies for bleaching effluents from the chlorination and extraction steps of a sulfate pulp mill. The combined effluent was first treated with an AST system in the laboratory. Several different carbons were tested. The biotreated effluent showed poor adsorbability in terms of COD, dissolved organic carbon (DOC), $color_{436}$, and UV_{254} within the carbon dosage range of 20-2000 mg/L. When the carbon dosage exceeded 10,000 mg/L, the removal levels of the above parameters and AOX increased to over 90%. The isotherms could be expressed by a Freundlich equation, and the shapes of the isotherms were strongly dependent on the carbon dosages (Çeçen, 1993).

2.2.4.3 Activated Carbon Based Biological Treatment

Treatment processes using activated carbon to intensify biological reaction rates through accumulation of high concentrations of active biomass have been explored for the treatment of pulp and paper effluents (Ball, 1996; Graham, 1996; Rovel et al., 1994; Vuoriranta and Remo, 1994; Jackson-Moss et al., 1992; Verreault, 1992; LaFond et al., 1991). The activated carbon based biological fluidized bed is one of the process configurations (Vuoriranta and Remo, 1994). A secondary effluent from a bleached Kraft mill activated sludge plant was treated in a pilot scale fluidized bed to remove residual organic carbon and AOX. GAC was used as an adsorbent and support material for biomass. The average daily loading of the system was 0.9 g DOC per kg GAC. The overall reduction of DOC in the system through the 18-week operation was 57%. AOX removal was more efficient, ranging between 70 to 90%. Removal rates decreased in the course of time but could be partly recovered with addition of nutrients to the nutrient deficient feed, a process called bioregeneration. It was believed that 20–30% of the DOC removal was due to biodegradation and bioregeneration (Vuoriranta and Remo, 1994). Other processes of this kind include anaerobic biological GAC process (LaFond et al., 1991; Jackson-Moss et al., 1992), biofiltration (Rovel et al., 1994), and PACT® (Verreault, 1992; Graham, 1996; Ball, 1996).

2.3 Activated Carbon Adsorption and Process Modeling

Adsorption is a complicated surface phenomenon. It is a process by which material accumulates at the interface between two phases. The driving force for surface adsorption is the reduction in surface tension when the adsorbing molecule enters the interface. Adsorption on solids, particularly activated carbons, has become a widely used process for water and wastewater treatment. Due to the high degree of purification that can be achieved, this process is often used at the end of a treatment sequence.

In wastewater treatment, either powdered activated carbon (PAC), consisting of particles at and below U.S. Sieve Series No. 50, or granular activated carbon (GAC), consisting of larger particles, can be used. The adsorptive properties of PAC and GAC are not fundamentally different since they depend on pore size and the internal surface area of the pores, which are independent of overall particle size. The addition of PAC to an activated sludge process to enhance the removal of organic compounds for industrial wastewater is a very common practice. However, in terms of the adsorption process, the batch mode is inefficient compared to continuous plug flow configurations.

2.3.1 Adsorption Theory

In water and wastewater treatment, the activated carbon adsorption is normally assessed in two aspects: how much pollutant can be loaded onto an adsorbent, and how long it will take for this loading to occur. These two phenomena are described by adsorption equilibria and kinetics. The feasibility of the process depends on the equilibrium parameters, but the system's efficiency is usually a strong function of the rate of adsorption.

2.3.1.1 Adsorption Equilibria and Isotherm

Adsorption in a solid-liquid system results in the removal of solutes, or adsorbate, from solution. Their concentration at the surface of the solid, or adsorbent, continuously increases until the concentration of the solute remaining in solution is in a dynamic equilibrium with that at the surface. The equilibrium isotherm describes the relation between the amount or concentration of adsorbate that accumulates on the adsorbent and the equilibrium concentration of dissolved adsorbate. It may be a function of multiple factors including the molecular size and structure and polarity of the solute, the concentration of the solute, the nature and concentration of competing solutes, the nature of the solution, and so on. The term "isotherm" arises because the equilibrium relationship is measured at constant temperature

and it is generally given the mathematical expression by fitting the experimental data to empirical or semi-empirical functions (Weber, 1972; Droste, 1997). In addition to the mathematical expression, the isotherm is also used to refer to the experiments that quantify the equilibrium conditions and the plots of the experimental data.

Isotherm studies fall into two categories, one is the single solute isotherm, and the other one is the multicomponent isotherm. The single solute isotherm is used to describe the adsorption of an individual compound or the adsorption of complex mixtures of compounds described in terms of a gross organic parameter such as COD or TOC. The latter approach has been used to describe many water and wastewater applications (Narbaitz, 1985). Four types of single solute isotherms are most commonly used in solid-liquid systems (Figure 2.1). They are:

1) linear $q_e = Mc_e$

2) irreversible $q_e = M$

3) favorable $q_e = f(c_e)$

4) unfavorable $q_e = f(c_e)$

where:

q_e is the equilibrium concentration of solute in solid, defined as the number of moles or mass of adsorbate per unit weight of adsorbent at concentration of solute in solution when equilibrium exists

c_e is the equilibrium concentration of solute in solution

M is a constant

Irreversible isotherms can only be determined by conducting desorption isotherms. The majority of isotherms found in aqueous systems are of the favorable type.

Three common forms of isotherm found in the literature are:

1) Freundlich isotherm $$q_e = K_F c_e^n \quad (2\text{-}1)$$

where:

K_F and n are empirical constants dependent on the nature of adsorbate and adsorbent, and on the temperature

2) Langmuir isotherm $$q_e = \frac{Q_0 K c_e}{K c_e + 1} \quad (2\text{-}2)$$

where:

Q_0 is the maximum amount of solute that can be adsorbed

K is a constant

3) BET isotherm $$q_e = \frac{B c_e Q_m}{(c_s - c)\left[1 + \frac{(B-1)c_0}{c_s}\right]} \quad (2\text{-}3)$$

where:

B and Q_m are constants

c_S is the saturation concentration of the solute in solution

The Langmuir isotherm can be derived theoretically based on the assumptions of constant adsorption site energy, no interaction between adsorbed molecules, and that there is a maximum adsorption capacity corresponding to a monolayer coverage. Since the activated carbon surface is heterogeneous, it would appear to be most compatible with the Freundlich description and in fact the majority of liquid phase systems are found to be quite well described by the Freundlich isotherm (Peel, 1980). The EBT is rarely used to describe liquid-phase adsorption.

Figure 2-1 Four Types of Isotherm

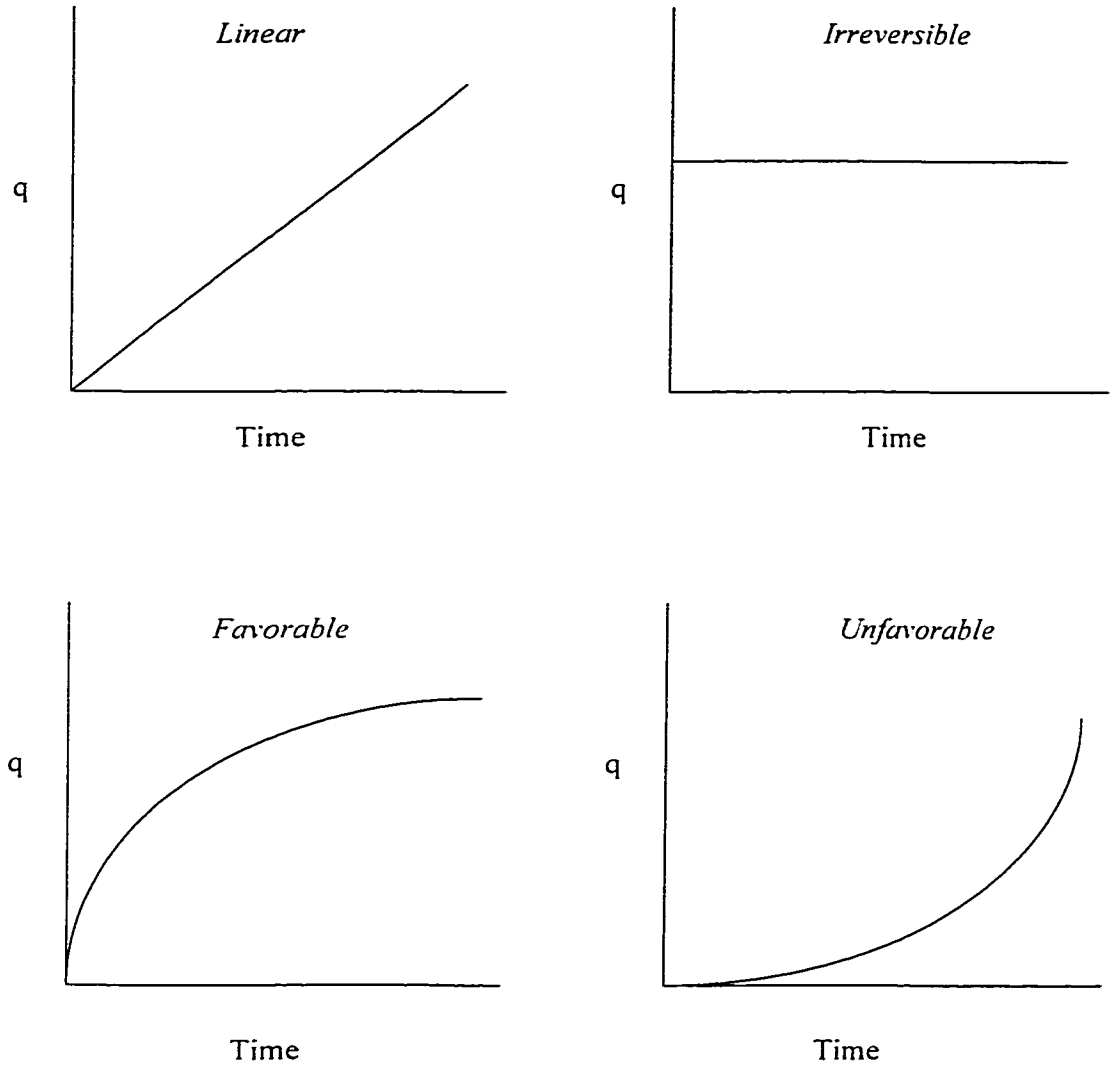

2.3.1.2 Adsorption Kinetics

Adsorption onto an activated carbon particle can be considered to occur in three steps:

1. Film resistance or film diffusion: The mass transfer by diffusion of the adsorbate molecules from the bulk fluid phase through a stagnant boundary layer surrounding each adsorbent particle.
2. Intraparticle resistance or intraparticle diffusion: Transport of the adsorbate from the external surface of the solid to the interior of the particle.
3. Reaction resistance: Molecules in the pores are adsorbed from the solution on to the solid phase. This stage is relatively fast, compared to the first two steps; hence, local equilibrium is usually assumed between these two phases.

The steps occur in series, therefore if one of them is relatively slow, it will be the rate controlling step. The second step, or the internal diffusion, may occur by diffusion through the fluid in the pores (pore diffusion), by diffusion in the adsorbed state along the pore surfaces (surface diffusion), or by a combination of the two (combined diffusion). Pore and surface diffusion are parallel processes, therefore if one process is much faster, it will control the rate of internal diffusion.

2.3.2 Fixed Bed Columns and Breakthrough Curves

The most efficient arrangement for conducting adsorption operations is the columnar continuous plug flow configuration known as a fixed bed. In this adsorption mode, the reactor consists of a packed bed of adsorbent through which the stream under treatment is passed. As the polluted stream travels through this bed, adsorption of the contaminants takes place and a purified effluent exits the column (Figure 2.2).

Figure 2-2 Mass transfer zone progression in a carbon column

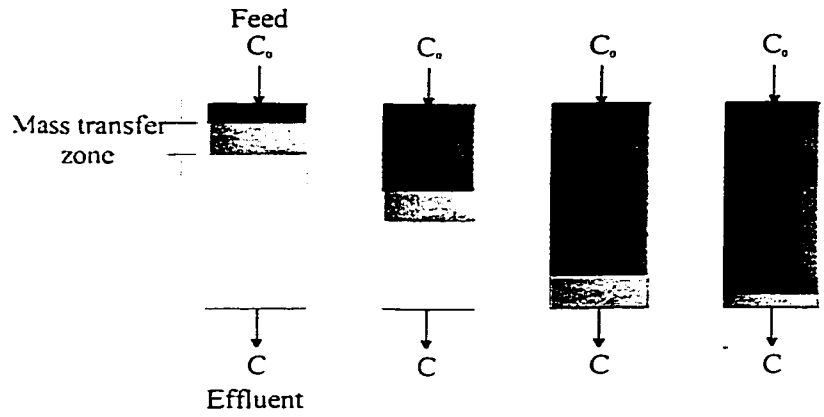

During the operation of such a column, the portion of the bed close to the inlet is continuously contacted by the concentrated feed stream, whereas the subsequent portions are exposed to adsorbate not adsorbed by an earlier portion. Thus, the adsorbate becomes fully loaded, i.e., saturated, at the inlet first and with time the saturation progresses downstream. The part of the bed that displays a gradient in solid concentration from zero to equilibrium is called the mass transfer zone (MTZ). As the name indicates, this is the active part of the bed where adsorption actually takes place. The concentration of pollutants in the stream also changes continuously throughout this part of the bed, from a value close to zero at the beginning of the MTZ to the feed concentration at the end.

As the saturated portion of the bed increases, the MTZ travels downstream and eventually exits the bed. This gives rise to a typical effluent concentration versus time profile, which is called the breakthrough curve (Figure 2.3). At breakthrough, the effluent concentration starts to rise and eventually reaches the effluent quality limit set by effluent regulations. This concentration is termed the breakthrough concentration c_b. When the effluent concentration becomes unacceptable, or after a predetermined time interval, the operation of the column is stopped and the spent adsorbent is either disposed or regenerated.

2.3.3 Development of Process Modeling of Fixed Bed Columns

The adsorptive performance of a carbon column is a consequence of both capacity and kinetics. The conventional approach to evaluating this performance is based on a two-step procedure: generation of equilibrium isotherms and operation of pilot columns. An isotherm indicates the capacity of a carbon for removing organic compounds from a particular water or wastewater. It is relatively easy to prepare; however, adsorption kinetics, which can affect greatly the efficiency of carbon use, is ignored in this test. With the operation of pilot

Figure 2-3 Breakthrough Curve of a GAC Column

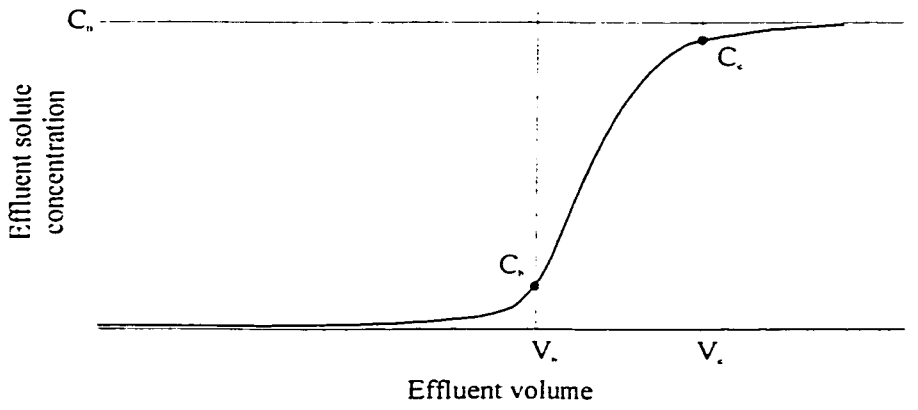

columns kinetics, i.e., contact time and the breakthrough curve shape, should be taken into account. These studies have been necessary because adsorption onto activated carbon is a highly complex operation. Unfortunately, this work can be expensive, time consuming, and dependent on value judgments.

Since the traditional process design procedure has such a drawback, research effort has been made to simulate the adsorption process using mathematical models. With the use of a proper theoretical model, it should be possible to reduce the need for pilot scale studies. Such a model could also assist in the analysis of laboratory, pilot, and full scale operating data. In practical applications, competitive adsorption, biological activity, and time-variant feed streams all serve to

complicate mathematical treatment of adsorbers. However, by gradually developing an understanding of the separate processes involved, a comprehensive model should eventually be possible.

2.3.3.1 General Considerations of Modeling

When developing a model to describe the performance of an activated carbon adsorption bed, the following aspects are generally considered:

1. Type of equilibrium isotherm.
2. The possible mechanism that describes the uptake rate onto the carbon.
3. Fluid phase concentration within the column.

Solutions of the model can be very complicated because of the unsteady state nature of the adsorption process. Consequently, simplified forms, especially those of the equation that describes the rate of adsorption, are often used. These simplified equations differ in the choice of the combination of diffusion resistances, namely the external or film resistance and the intraparticle resistances. In case of linear or irreversible isotherms, analytical solutions can normally be found. Meanwhile, numerical solutions have been described for virtually every possible combination of isotherm type and intraparticle transport mechanism. Weber and Chakravorti (1974) have tabulated most of these studies.

There are two ways of measuring the kinetic parameters of a proposed model, either in a batch kinetic experiment, or from the breakthrough behavior of an adsorption bed. An adsorption kinetic model must be able to describe both phenomena using an identical set of parameters.

2.3.3.2 Rate of Adsorption onto Activated Carbon

The equations that describe the rate of adsorption onto the carbon are based on the combination of adsorptive mass transfer resistances. The three steps involved in adsorption process, i.e., film diffusion, intraparticle diffusion, and reaction resistance, were addressed in Section 2.3.1.2. For the adsorption of dissolved organic compounds onto activated carbons, the

reaction resistance, which is the final step involved in the adsorption process, is generally quite rapid and commonly ignored as a possible rate-limiting step. That is, the rate of adsorption is assumed to be diffusion limited (Thacker and Snoeyink, 1981).

Intraparticle diffusion: The intraparticle diffusion is a combination of pore diffusion and surface diffusion. A general model that accounts for the resistance to mass transport due to the combined diffusion results from a mass balance on an adsorbent particle. It assumes constant diffusivities, and spherical particles. The mass balance produces the following equation:

$$\varepsilon_p \frac{\partial c}{\partial t} + \rho_c \frac{\partial q}{\partial t} = D_s \frac{\rho_c}{r^2} \frac{\partial}{\partial r}\left(r^2 \frac{\partial q}{\partial r}\right) + \frac{D_p}{r^2} \frac{\partial}{\partial r}\left(r^2 \frac{\partial c}{\partial r}\right) \qquad (2\text{-}4)$$

where

t is time, s

D_p is effective pore diffusion coefficient, cm^2/sec

D_S is effective surface diffusion coefficient, cm^2/sec

r is particle radii; variable, cm

c is liquid phase concentration in pores, g/cm^3

q is solid phase concentration, g/g

ρ_C is apparent adsorbent particle density, g/cm^3

ε_P is internal porosity of the adsorbent particle.

As addressed in Section2.3.1.2, pore and surface diffusions are parallel processes, therefore if one process is much faster, it will control the rate of internal diffusion. This provides grounds to simplify Equation (2-4). In fact, researches have almost always made the following two assumptions. The first one is to assume that the fluid phase accumulation in pores, which is the first term on the left hand side is negligible. This can be done because the concentration on the surface is much greater than that in the pore fluid (Peel, 1979, Thacker and Snoeyink, 1981). The second assumption is that either pore or surface diffusion are mathematically identical. Surface

diffusion is often referred to as the homogeneous solid diffusion. For the situation pore diffusion governs the rate of transport within the particle, only the second term on the right hand side is considered; similarly, if surface diffusion controls, only the first term on the right hand side is considered.

Besides the above assumptions, other forms of simplification are also used to describe the adsorption phenomena. The simplest of these methods is to replace the differential driving force expression of Equation (2-4) with a driving force expression that gives the rate in terms of an average or bulk parameter rather than a continuous gradient. The linear driving force model, Equation (2-5), and quadratic driving force model, Equation (2-6), are two forms of this approach:

$$\frac{d\bar{q}}{dt} = k_p a_p (q_s - \bar{q}) \qquad (2\text{-}5)$$

$$\frac{d\bar{q}}{dt} = k_p a_p \left(\frac{q_s^2 - \bar{q}^2}{2\bar{q}}\right) \qquad (2\text{-}6)$$

where

$\bar{q}$ is mean solid phase concentration in the particle, g/g

q_S is solid phase concentration at the particle's outer surface, g/g

k_p is pseudo mass transfer coefficient, cm/s

a_p is specific external surface area of adsorbent, cm^2/cm^3

Film diffusion: External resistance to mass transfer is due to a liquid film surrounding the adsorbent particle. When it is significant, it can be taken into account in a diffusion model by an appropriate boundary condition. For homogeneous solid diffusion, for example, such a boundary condition is the following equation, which arises from a mass balance that equates the rate of mass transfer through the surface film with the rate of mass transfer into the particle:

$$\rho_c D_s \left.\frac{\partial q}{\partial r}\right|_{r=R} = k_f (c - c_s) \qquad (2\text{-}7)$$

where

k_f is external film transfer coefficient, cm/s

c_S is liquid phase concentration at particle surface, mg/L

R is the radium of the particle, cm

2.3.3.3 Fluid Phase Concentration

To describe the adsorption in GAC column adsorbers, the above equations must be coupled with an equation describing the changes in liquid phase concentration along with the length of the column. The fluid phase equation is obtained from a mass balance over a differential bed segment of length dx:

$$\frac{\partial c}{\partial t} = D_z \frac{\partial^2 c}{\partial x^2} - v_s \frac{\partial c}{\partial x} - \left(\frac{1-\varepsilon}{\varepsilon}\right)\frac{3k_f}{R}(c - c_s) \qquad (2\text{-}8)$$

where

D_z is axial dispersion coefficient, cm^2/s

x is bed length variable, cm

ε is liquid volume fraction

R is radius of adsorbent particle, cm

v_S is interstitial liquid phase velocity, cm/s

Axial or longitudinal dispersion is a measure of the spreading of an initially sharp wavefront as it moves through a packed bed. Several researches have suggested that it can be neglected because the column length to particle diameter ratio in an adsorption column is large, and therefore D_z is small (Peel, 1979). If the axial dispersion term, which is the first term on the right hand side of the above equation, can be neglected, this equation will have a simple boundary condition and its solution involves less computation. Discussion of various forms of the kinetic models can be

found in the literature (Cooney, 1999; McKay, 1999; Sontheimer et al., 1988; Faust and Aly, 1987).

2.3.4 Dual Rate Kinetic Model

It has been recognized that in isotherm study, a rapid initial uptake of 60–80 % of the final capacity is followed by a slow uptake stage of over several weeks during which the remaining capacity was utilized (Peel, 1979). Based on this observed uptake behavior and a consideration of the physical structure of the activated carbon particle, a dual rate kinetic model or branched pore model has been devised to describe the intraparticle kinetics (Peel, 1979).

2.3.4.1 An Idealized Activated Carbon Pore Structure

The dual rate model assumes that activated carbon particles consist of two regions, one with macropores and the other with micropores. Macropores are defined as those pores whose pore radii are several times greater than the radii of the diffusing species. It is assumed that in macropores transport occurs by conventionally described diffusion mechanisms, either pore or surface, and that the presence of the pore walls has little or no effect on the diffusion rates. These larger pores are assumed to be homogeneously distributed throughout the particle and to provide a complex network of interconnected access channels to the interior. It is further assumed that the rapid initial uptake of substrate takes place within this region.

Micropores are defined as those pores whose radii are comparable to the sizes of diffusing species. This region encompasses all pores that are available for adsorption but not considered macropores. It is assumed that within the micropores transport rates are strongly hindered, either by the proximity of the walls or by the restraining effect of the adsorbate/adsorbent interactive forces. The exact mechanism of adsorption within these small pores is yet unclear. These pores are assumed to be homogeneously distributed throughout the particle and branch off the macropore network that is the source of adsorbate diffusing into the micropores. It is in these

small pores and fissures that the slow adsorption following the initial rapid uptake occurs (Peel, 1979).

2.3.4.2 Model Development

Figure 2-4 is a conceptual diagram of the branched pore model. To develop the model, it is assumed that the carbon particle can be divided into two homogeneously distributed regions. A fraction 'f' constitutes the macropore region, and a fraction '1-f' constitutes the micropore region. The carbon particles can be treated as spheres. A schematic diagram of an element of the adsorption bed of length dx is shown in Figure 2-5. The mechanisms through which adsorption onto the activated carbon occurs are assumed to be as follows:

1. External film transfer controls the rate of diffusion of adsorbate across the liquid boundary layer surrounding the particle. Surface diffusion mechanism is responsible for macropore transport. The accumulation in the liquid phase within the macropores is negligible.
2. The rate of transfer from the macropore to the micropore regions is described by the linear driving force between the local macro and micropore concentrations.
3. The adsorbent particles are small enough so that the fluid surrounding a single particle has a uniform concentration.
4. Axial dispersion is negligible.
5. Radial gradients do not exist fluid phase.

Figure 2-4 Conceptual Diagram of Branched Pore Model

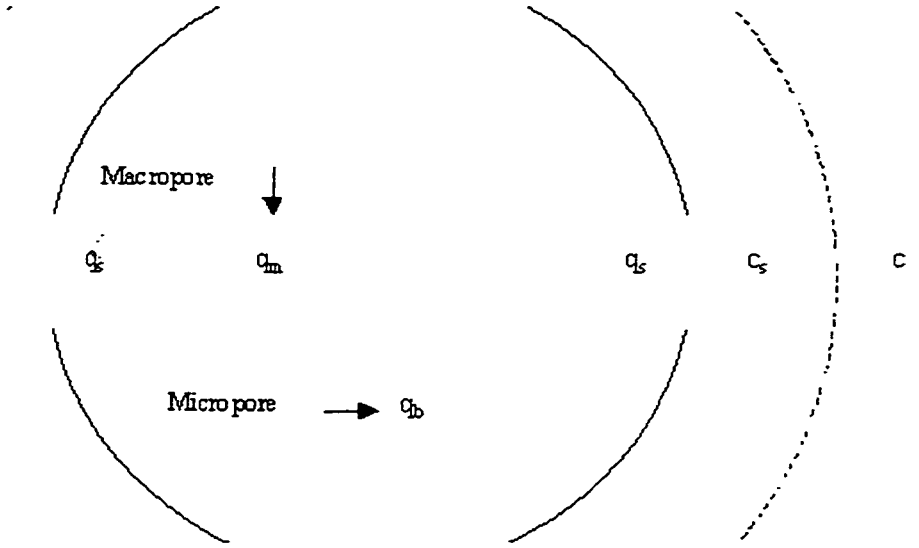

Figure 2-5 Differential Element of Adsorption Bed

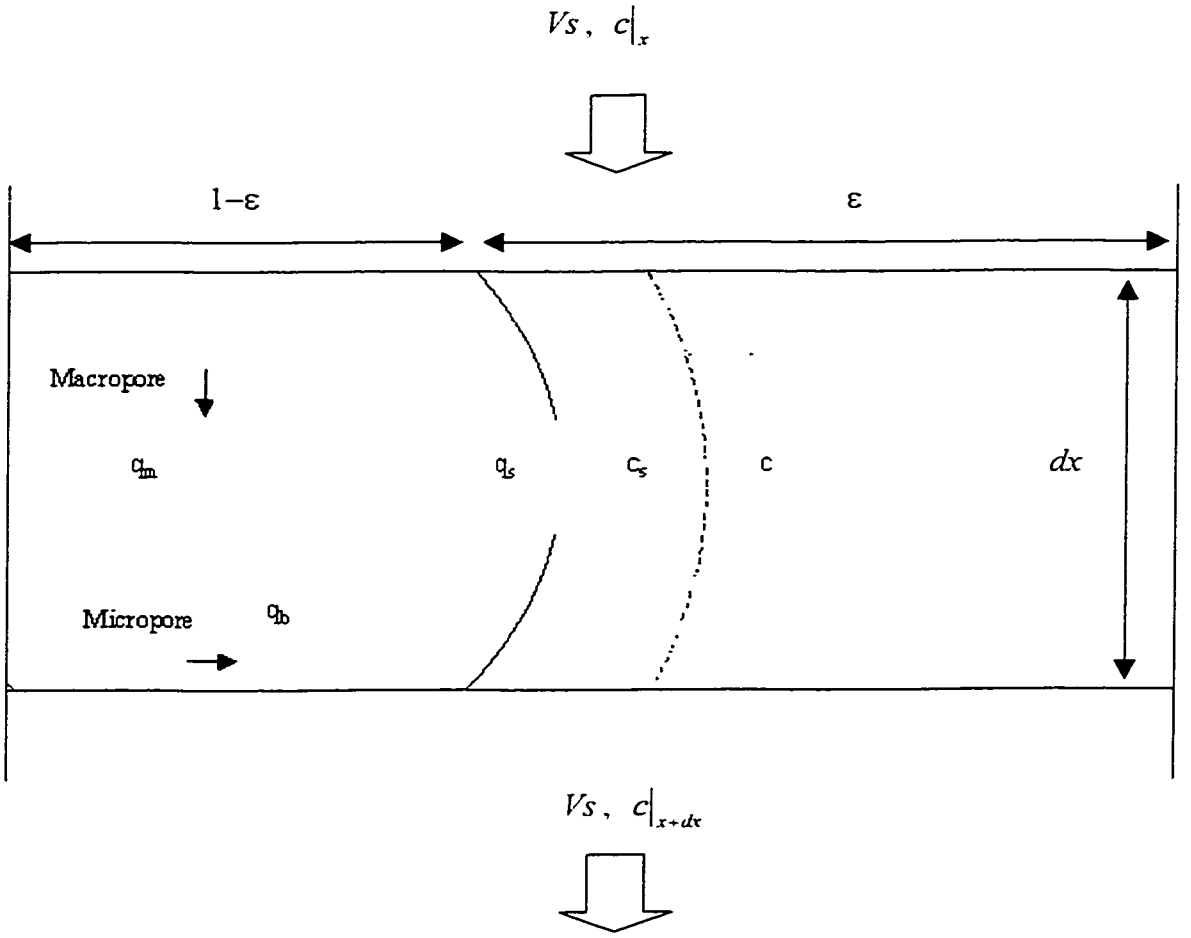

The mathematical formulation of the dual rate adsorption column model is as following:

Macropore mass balance

$$f\frac{\partial q_m}{\partial t} = \frac{fD_s}{r^2}\frac{\partial}{\partial r}(r^2\frac{\partial q_m}{\partial r}) - R_b \qquad (2\text{-}9)$$

Micropore mass balance

$$(1-f)W\frac{\partial \bar{q}_b}{\partial t} = k_b W(q_m - \bar{q}_b) = R_b \qquad (2\text{-}10)$$

Particle surface boundary condition

$$fD_s\rho_c\left.\frac{\partial q_m}{\partial r}\right|_R = k_f(c - c_s) \qquad (2\text{-}11)$$

Liquid phase mass balance

$$\frac{\partial c}{\partial t} = -v_s\frac{\partial c}{\partial x} - \frac{(1-\varepsilon)}{\varepsilon}\frac{3k_f}{R}(c - c_s) \qquad (2\text{-}12)$$

Freundlich isotherm

$$q_s = K_F(c_s(t))^n \qquad (2\text{-}13)$$

Other initial and boundary conditions

$$q_m(r,0) = 0 \qquad (2\text{-}14)$$

$$q_b(r,0) = 0 \qquad (2\text{-}15)$$

$$q_m(R,t) = K_F(c_s(t))^n \qquad (2\text{-}16)$$

$$\frac{\partial q_m}{\partial r}(0,t) = 0 \qquad (2\text{-}17)$$

where

f is fraction of total capacity available in macropores

k_b is micropore rate coefficient, s^{-1}

K_F is Freundlich isotherm constant

n is Freundlich isotherm exponent

ρ_b is packed density of adsorbent, g/cm^3

q_m is macropore solid phase concentration

q_b is branch pore solid phase concentration

q_s is solid phase concentration at the particles' external surface

It is important to note that if the fraction "f" in the model is set equal to unity, the model degenerates into the widely used external film resistance-surface diffusion mechanism model. This makes it possible to compare the numeric solution of the model with previously published analytical solutions. This model has been solved by Peel using Crank-Nicholson finite difference analogues. The solution was tested by successively decreasing the time and spatial increments to prove convergence. It was also proved to be correct by comparing it to a previous published analytical solution. A detailed account of the solution can be found in the literature (Peel, 1979).

Chapter 3

ACTIVATED SLUDGE PROCESS

The wastewater collected from a bleached Kraft pulp and fine paper mill was first treated using a laboratory-scale AST system that substantially removed its biological contents. Both influents and effluents of the ASP runs were analyzed for soluble COD (SCOD), soluble TOC (STOC), and pH. Influent and mixed liquor TSS and VSS were also analyzed for process control.

3.1 Experimental Materials and Method

3.1.1 Pulp and Paper Effluent

The wastewater treated in the AST systems was sampled from the primary sedimentation effluent lines of a bleached Kraft pulp and fine paper mill (Domtar at Cornwall, Ontario). The mill's products contained a wide variety of fine papers including coated printing Bristol, premium offset and copy papers. It produced bleached Kraft pulp from hardwoods for internal use and recycled pulp from old corrugated containers. The mill used chlorine dioxide bleaching followed by caustic extraction. The bleach sequence was DEDED (D=chlorine dioxide, E=caustic extraction).

Samples were collected using 200 L plastic barrels, transported to the laboratory within three hours after sampling, and then stored in freezers at −10 to −20°C. The samples were cooled to 0°C within 24 hours of sampling but did not freeze for several days. Soluble COD of the samples were between 300 and 800 mg/L, while soluble TOC were between 140 and 265 mg/L; pH was between 6.5 and 7.5.

3.1.2 System Configuration and Process Control

Two reactors, made of 6 mm clear Plexiglas™, were operated in parallel. Each reactor contained two sections that were separated by a baffle. One of the sections was an aeration tank filled with mixed liquor. The operation volume of this tank was 5 L. The other one was a sedimentation chamber used to separate the suspended activated sludge solids from the treated wastewater.

Influent was continuously fed to the aeration tank by a peristaltic pump through Tygon™ tubing. Air was introduced to the mixed liquor through stone diffusers to provide oxygen and mixing. Settled activated sludge in the sedimentation chamber was periodically taken through the port at the bottom of the chamber and recycled to the aeration tank. The reactors were operated at room temperature (23°C). Figure 3-1 shows the design of the reactors, Figure 3-2 shows the side view of a reactor, and Figure 3-3 shows the setup of the AST system.

Figure 3-1 Design of the Reactors

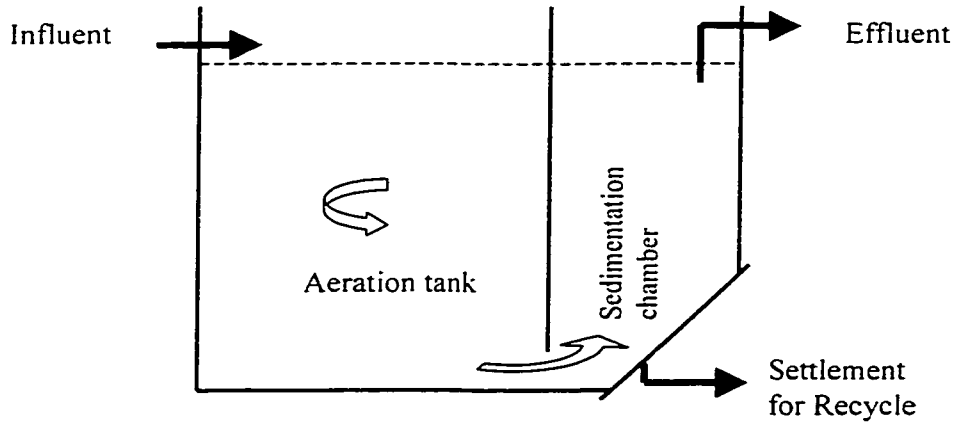

Figure 3-2 Side View of a Reactor in Operation (Graham, 1996)

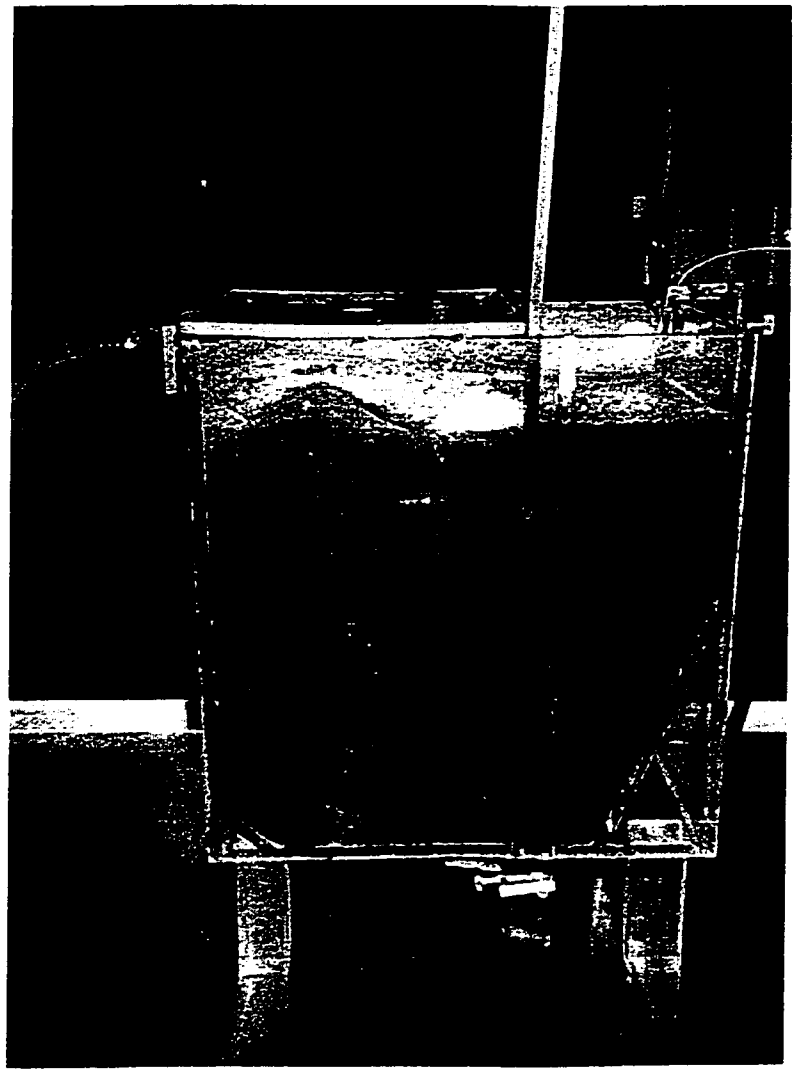

Figure 3-3 System Setup (Graham, 1996)

For feeding the reactors, frozen samples were thawed as needed and stored at 2°C. The tubing between the reservoir and the reactors was long enough to allow the temperature of the feed to increase to the room temperature. Phosphorus and nitrogen were added to the reservoir as forms of K_3PO_4 and $(NH_4)_2SO_4$ to maintain a degradable-COD and nutrients ratio, i.e., COD:N:P, at approximately 100:5:1.

Different operating conditions were maintained by controlling the solids retention time (SRT) and hydraulic retention time (HRT) of the system. Table 3-1 shows the operating conditions tested in this study. SRT is actually the sludge age (θ_c) of the system. The desired SRT was controlled by removing certain amount of mixed liquor every day. Wasting rate was calculated based on the following formula:

$$SRT = \frac{VX}{(Q - Q_W)X_e + Q_W X} \qquad (3\text{-}1)$$

where

V is aeration tank volume, cm^3

X is mixed liquor VSS, g/cm^3

Q is the flow rate, cm^3/d

Q_W is wastage rate, cm^3/d

X_e is effluent VSS, g/cm^3

The food-to-microorganism ratio (F/M) was also monitored for process control. It was calculated based on the following formula:

$$F/M = \frac{c_0}{\theta_H X} \qquad (3\text{-}2)$$

where

c_0 is influent COD or TOC concentration, mg/L

θ_H is hydraulic loading rate, d

Table 3-1 Operating Conditions for AST Process

Run	Feed COD (mg/L)	Feed TOC (mg/L)	HRT (hour)	SRT (day)
2	764 - 795	207 - 230	12	10
5	295 - 684	116 - 265	6	10
6	263 - 692	99 - 236	6	5

The AST process was operated for at least four weeks after it became steady for each set of operating conditions. Process effluents were stored in 200 L plastic barrels at −10°C until subsequent tests and treatment processes were conducted. Each barrel contained a mixture of effluents obtained in five consecutive days when the system was steady under a certain operating condition.

3.2 Results and Analysis

Both influents and effluents were analyzed for pH, soluble COD, and soluble TOC, which means that samples were filtered with *NALGENE*® 0.45μm CN membrane filters before COD and TOC analyses. In addition, effluents and mixed liquor were analyzed for TSS and VSS for process control. All the analyses were performed following standard methods (1971). The ferrous ammonium sulfate titrimetric method was used for COD analysis, and TOC analysis was carried out with FOLIO Instruments' DC-190 TOC analyzer. VSS and TSS samples were filtered with Whatman™ GF/C glass fiber paper. For TSS analysis, the samples were oven dried with the filters at 103°C for two hours before they were weighted.

Figures 3-4 to 3-6 summarize the analysis results of three runs operated under operating conditions summarized in Table 3-1. At SRT=10 d and HRT=12 h, COD removals were 71–79% and TOC removals were 57–66%; at SRT=10 d and HRT=6 h, COD removals were

46–70%, and TOC removals were 42–69%; finally, at SRT=5 d and HRT=6 h, COD removals were 48–60%, and TOC removals were 41–59%.

Figure 3-4 AST Process, Run 2

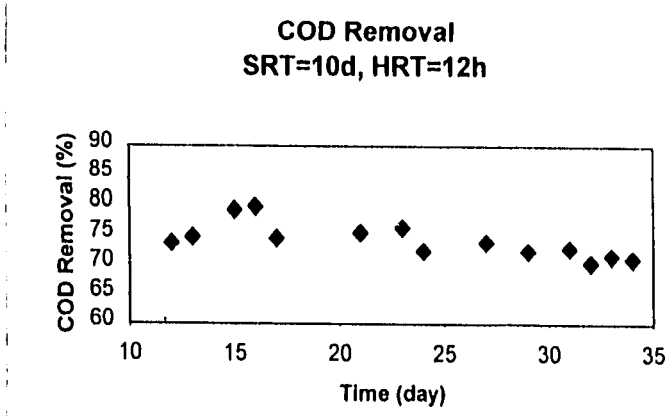

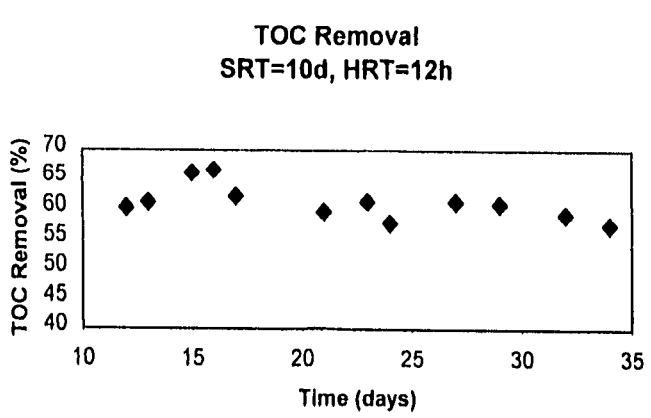

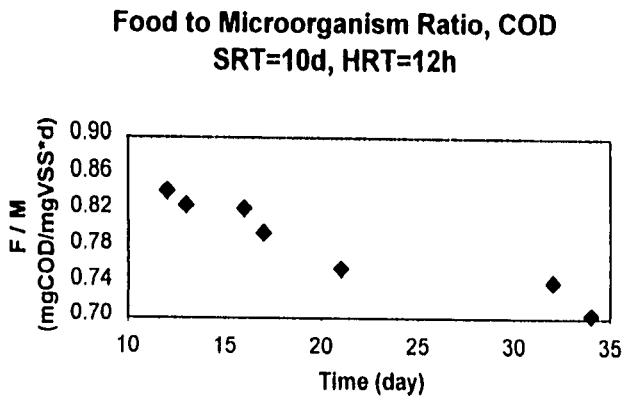

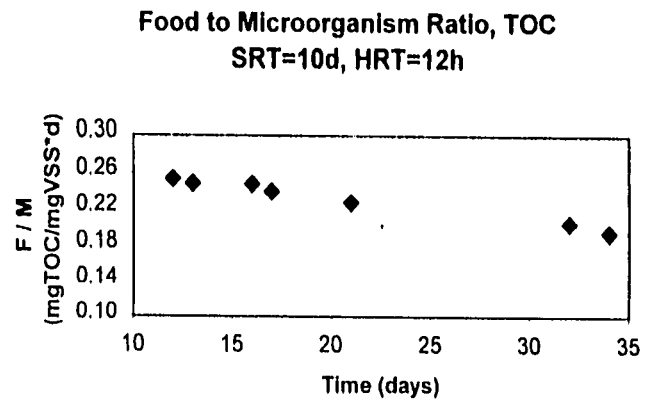

Figure 3-5 AST Process, Run 5

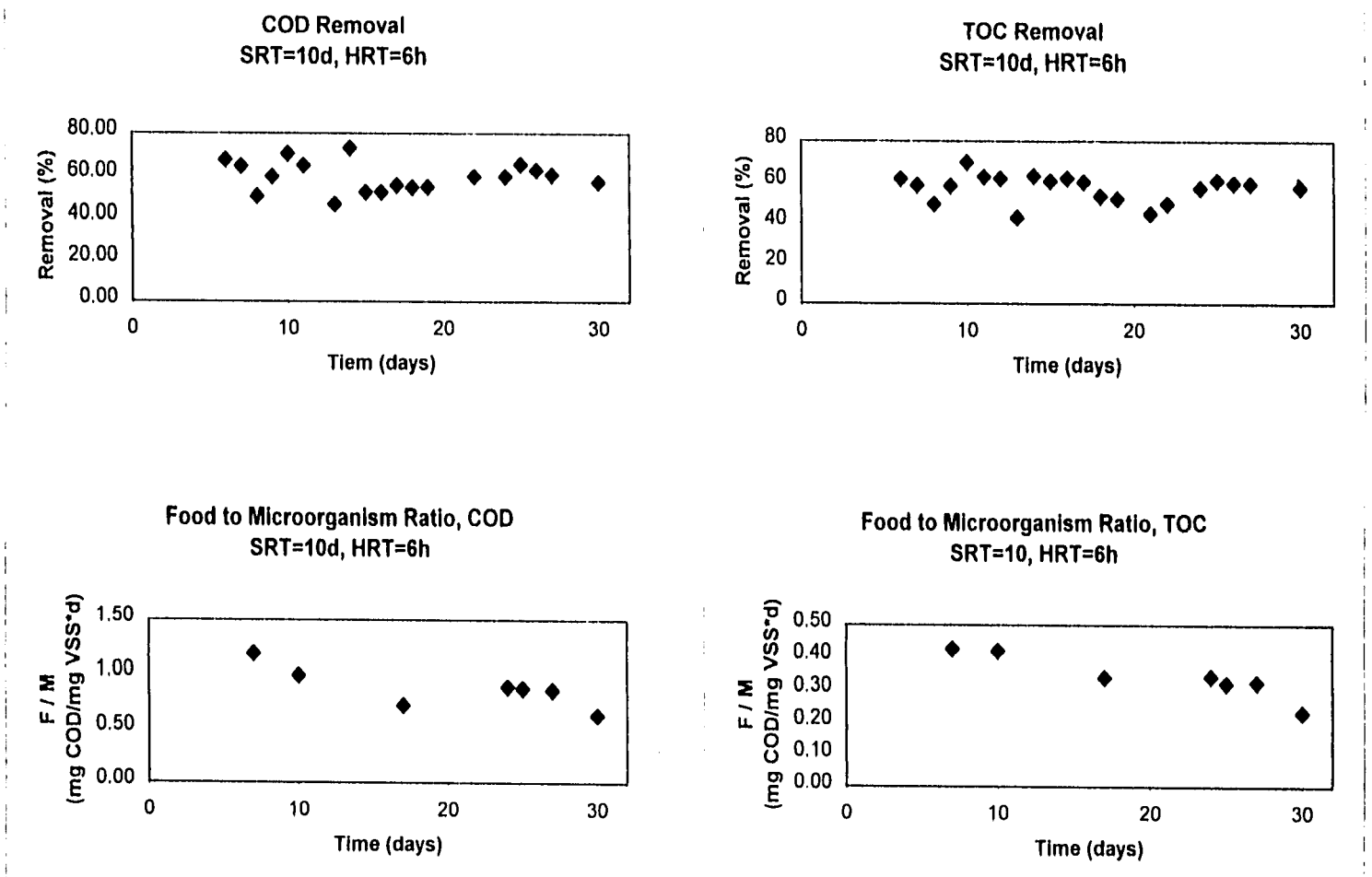

Figure 3-6 AST Process, Run 6

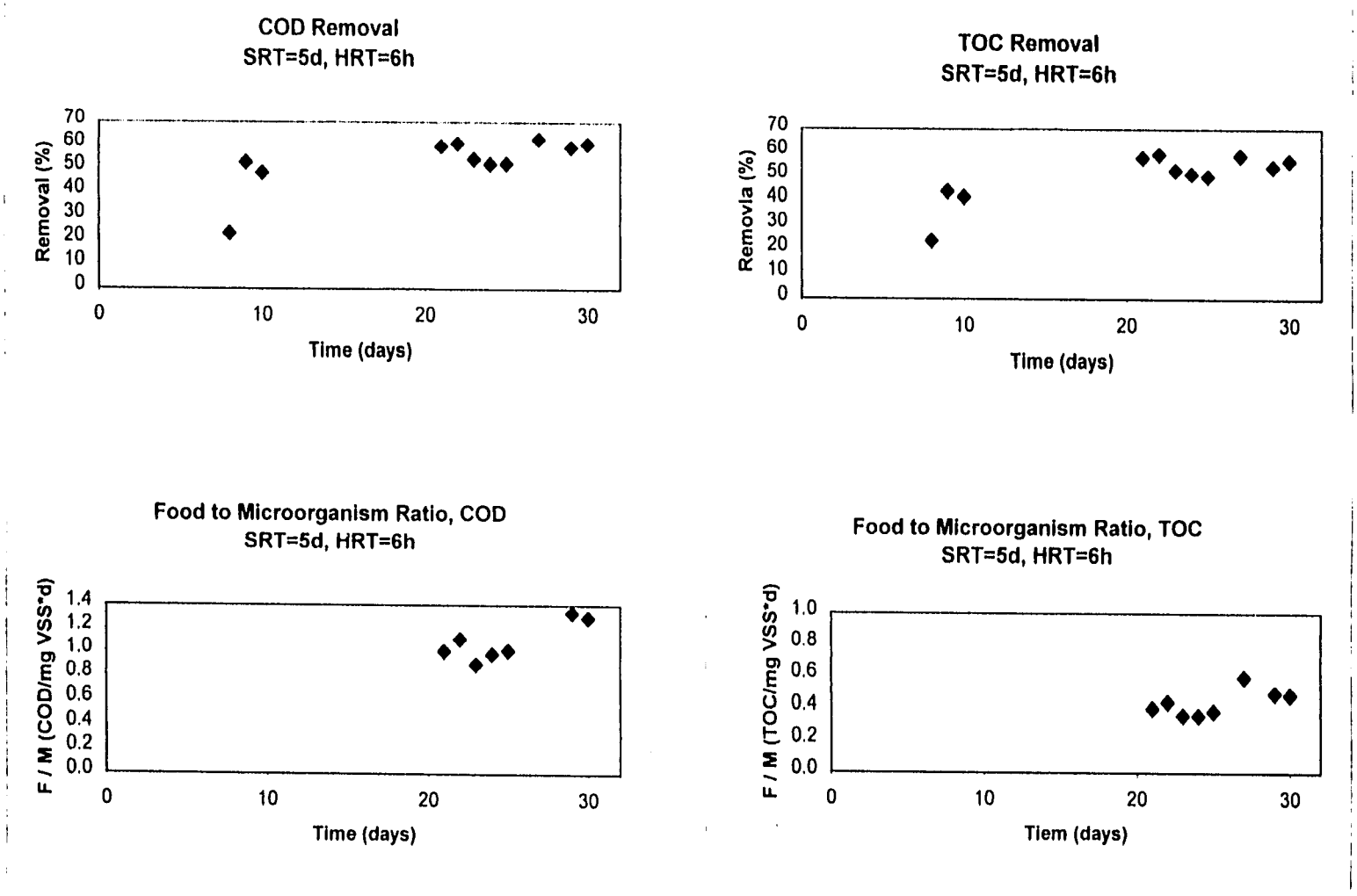

Chapter 4

ISOTHERM STUDY

The equilibrium isotherm describes the loading obtained in the activated carbon particles as a function of the solution equilibrium concentrations at a constant temperature. Isotherm studies were conducted for the feed of the AST system and for the AST effluents, which later served as the influents of GAC column experiments. The AST effluents were obtained under the operation conditions listed in Table 3-1.

The standard batch bottle-point technique was used for the isotherm study. Samples of known initial concentration were contacted with different amounts of activated carbon until equilibria were achieved. The GAC was ground to a powder before use in order to reduce the time to reach equilibrium. All samples were filtered before use and before being analyzed for COD and TOC.

4.1 Experimental Materials

Calgon® F400 GAC and wastewater samples were tested for adsorptive capacity before they were engaged in the column tests. Table 4-1 shows the specifications of the carbon. To prevent the leaching of the GAC, it was soaked for 24 hours in distilled-deionized water and then leached twice with boiling distilled-deionized water. After being decanted and then oven dried at 110°C for 24 hours, the GAC was pulverized and stored in a desiccator. Although there is concern that grinding the GAC will expose new areas of the carbon surface not previously accessible to the adsorbate, several studies found that adsorptive capacity was not affected by grinding (Randtke and Snoeyink, 1983).

Table 4-1 Specifications of F400 GAC

Item	Value
Iodine number, mg/g (Min.)	1000
Moisture, weight % (Max. %)	2
Abrasion Number (Min.)	75
Uniformity Coefficient (Max.)	1.9

Each wastewater sample was a mixture of AST effluents of five consecutive days within one run. It was filtered with *NALGENE*® 0.45μm CN membrane filters to remove suspended solids and bacteria before being tested in the isotherm study. The membrane filters were first washed with 200 mL distilled-deionized water before the filtration.

4.2 Experimental Procedure

It was assumed that adsorption equilibrium was achieved within 72 hours (Çeçen, 1993). A reference sample of the tested wastewater without carbon addition was included for each isotherm to test the possible degradation of the sample within the contact period. A blank, which was deionized distilled water without carbon addition, was also tested to measure the leaching of the bottle. Some isotherms were tested for the leaching of carbon by an additional bottle containing deionized distilled water and a carbon dosage of 400 mg/L.

Carbon dosages ranged from 100 to 4,000 mg/L. This was determined based on some preliminary experiments that showed that carbon dosages between 4,000 and 10,000 mg/L did not provide improved adsorption for the specific wastewater (Appendix A, Isotherm 1). The selected carbon dosage range provided data points that covered a broad range of equilibrium concentrations.

The experiment procedure for obtaining an isotherm is as following (Narbaitz, 1985):

1. Prepare the carbon and effluent sample as detailed in 3.4.1.
2. Measure the initial TOC and COD of the sample.

3. Wash and dry eleven 800 mL glass bottles.
4. Weigh each bottle.
5. Fill bottles 1 to 9 with sample to about 90% full.
6. Weigh each bottle with the sample it contained and then determine the net weight of the sample by subtracting the bottle weight (step 4) from the total weight.
7. Calculate the amount of activated carbon needed for each sample based on the target carbon dosage. Add adequate amount of activated carbon to each bottle.
8. Fill bottle 10 with distilled-deionized water to about 90% full. This control was used to measure the leaching from the bottle.
9. Fill bottle 11 with sample to 90% full, without adding activated carbon. This control was used to measure the degradation of sample in the contact period.
10. Repeat step 5 for bottles 10 and 11.
11. Seal all the bottles using Teflon lined caps.
12. Place the bottles in a tumbler that kept the carbon particles within the bottles in suspension and provide necessary mixing. The contact period was 72 h, and the room temperature was controlled at 23°C.
13. Upon the completion of the contact period, the activated carbon powder and the sample in bottle 1 to 9 were separated by pressure filtration using *NALGENE*® 0.45μm CN membrane filters that were prewashed with 200 ml distilled-deionized water.
14. Store the filtrates and samples taken from bottles 10 and 11 at 4°C until COD and TOC tests were conducted.

4.3 Results and Discussion

Six isotherm experiments were conducted, two for AST feed and four for AST effluents, in terms of bulk concentration parameters COD and TOC. While examining the influence of experimental materials on data, it was found that the degradation of AST effluent during the contact period was not measurable. The leaching of both bottles and carbon was found negligible (Appendix A). The experimental data were analyzed according to the following equation:

$$q_e = \frac{(c_0 - c_e)V}{M} \qquad (4\text{-}1)$$

where

V is the volume of the sample, L

c_0 is the initial liquid phase concentration, mg/L

c_e is the equilibrium liquid phase concentration, mg/L

M is the mass of activated carbon in the bottle, g

Adsorption for COD and TOC was found to conform to Freundlich isotherm:

$$q_e = K_F c_e^n \qquad (2\text{-}1)$$

The value of K_F is proportional to adsorption capacity, and the value of n is roughly an inverse indicator of the adsorption intensity (Wedler, 1976). As the value of n decreases, the adsorption intensity increases.

K_F and n were obtained by taking logarithm of both sides of equation 2-1 and then fitting the linear form of the isotherm, Equation 4-2, to the equilibrium data c_e and q_e.

$$\ln q_e = \ln K_F + n \ln c_e \qquad (4\text{-}2)$$

The least square method was used for the linear regression analysis. The confidence level of the analysis was 95%. Table 4-2 summarizes the output of the regression analysis, where the

Table 4–2 Summary of the regression analysis

Sample No.	COD			TOC		
	R square	Intercept	n	R square	Intercept	n
1	0.86	3.16 (2.44–3.89)	0.32 (0.14–0.49)	0.98	1.62 (1.22-2.09)	0.57 (0.46-0.67)
2	0.95	3.00(2.60-3.41)	0.45(0.35-0.56)	0.86	1.79(0.73-2.86)	0.51(0.22-0.80)
3	0.95	2.05(1.30-2.80)	0.68(0.49-0.87)	0.95	1.47(0.79-2.16)	0.71(0.49-0.93)
4	0.99	2.53(2.32-2.74)	0.51(0.46-0.55)	0.97	1.31(0.86-1.76)	0.69(0.57-0.81)
5	0.99	0.22(-0.66-1.10)	0.88(0.72-1.04)	N/A	N/A	N/A
6	0.94	0.71(-0.9-2.32)	0.92(0.58-1.25)	0.94	1.56(0.30-2.81)	0.68(0.35-1.01)

Table 4–3 Isotherms and AST operation conditions for the isotherm samples, COD

Sample No.	Source	COD (mg/L)	AST operation conditions	Residual (mg/L)	Isotherm
1	AST effluent	190	SRT = 10d, HRT = 12h	15	$q_e = 37.77c_e^{0.32}$
2	AST effluent	232	SRT = 10d, HRT = 12h	10	$q_e = 20.14c_e^{0.45}$
3	AST effluent	196	SRT = 10d, HRT = 6h	20	$q_e = 7.78c_e^{0.68}$
4	AST effluent	277	SRT = 5d, HRT = 6h	40	$q_e = 12.54c_e^{0.51}$
5	AST feed	546	N/A	120	$q_e = 1.25c_e^{0.88}$
6	AST feed	614	N/A	190	$q_e = 2.03c_e^{0.92}$

Table 4–4 Isotherms and AST operation conditions for the isotherm samples, TOC

Sample No.	Source	TOC (mg/L)	AST operation conditions	Residual (mg/L)	Isotherm
1	AST effluent	95.7	SRT = 10d, HRT = 12h	N/A	$q_e = 5.05c_e^{0.57}$
2	AST effluent	94.8	SRT = 10d, HRT = 12h	N/A	$q_e = 6.01c_e^{0..51}$
3	AST effluent	71.5	SRT = 10d, HRT = 6h	N/A	$q_e = 4.37c_e^{0..71}$
4	AST effluent	105.2	SRT = 5d, HRT = 6h	N/A	$q_e = 3.71c_e^{0.69}$
5	AST feed	N/A	N/A	N/A	N/A
6	AST feed	213.2	N/A	80	$q_e = 4.76c_e^{0.68}$

Figure 4-1 Equilibrium concentrations and linear regression analysis for isotherm 1

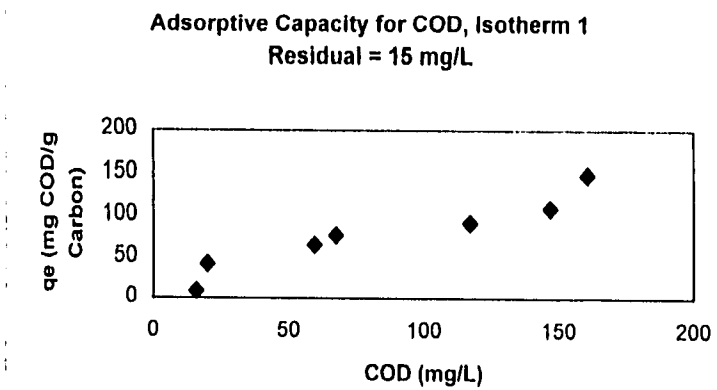

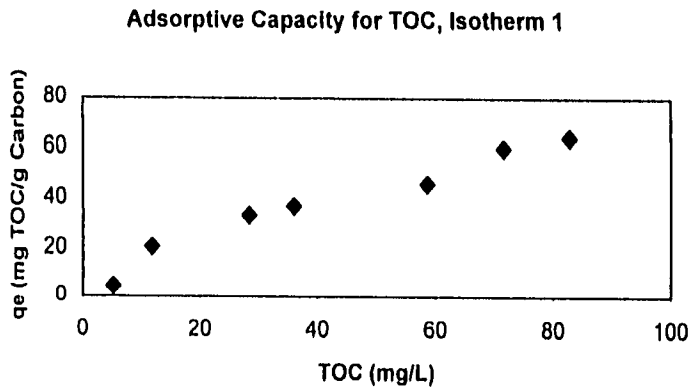

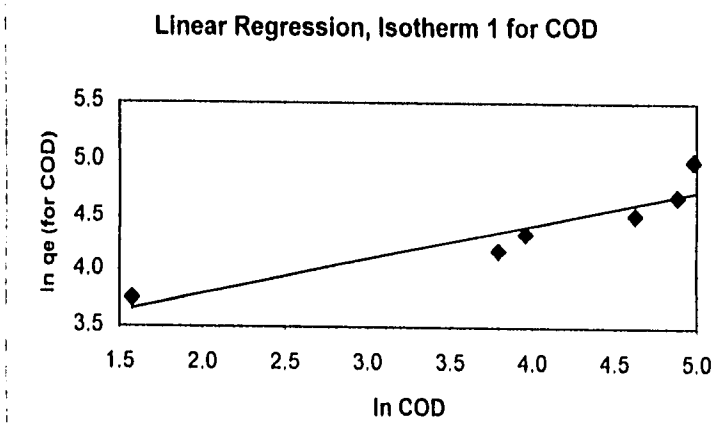

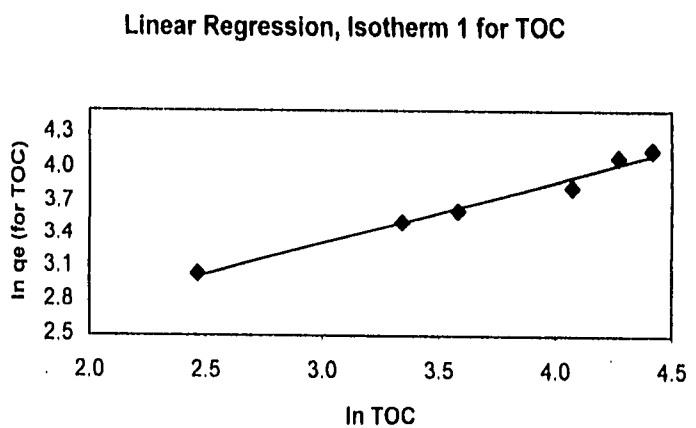

Figure 4-2 Equilibrium concentrations and linear regression analysis for isotherm 2

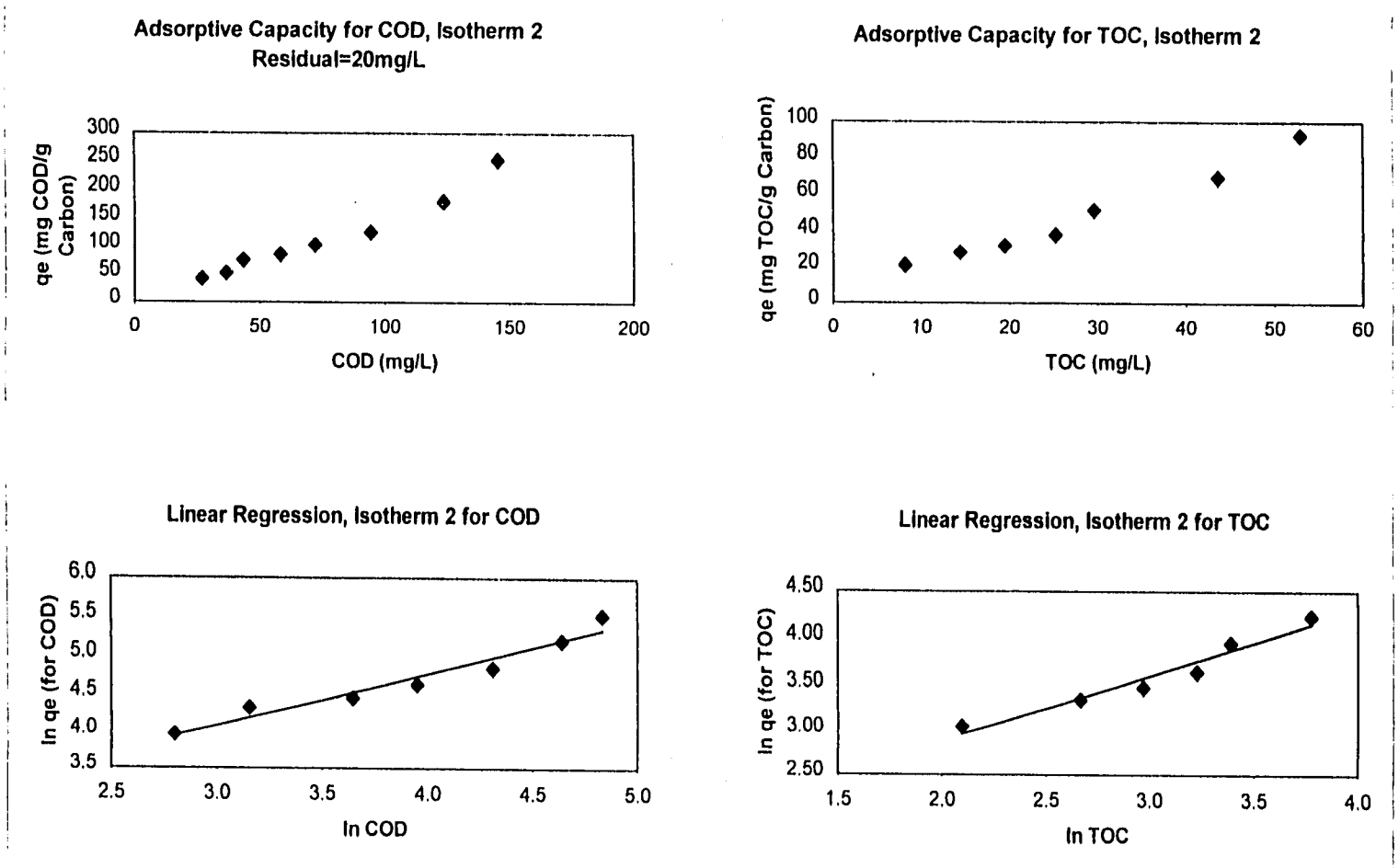

Figure 4-3 Equilibrium concentrations and linear regression analysis for isotherm 3

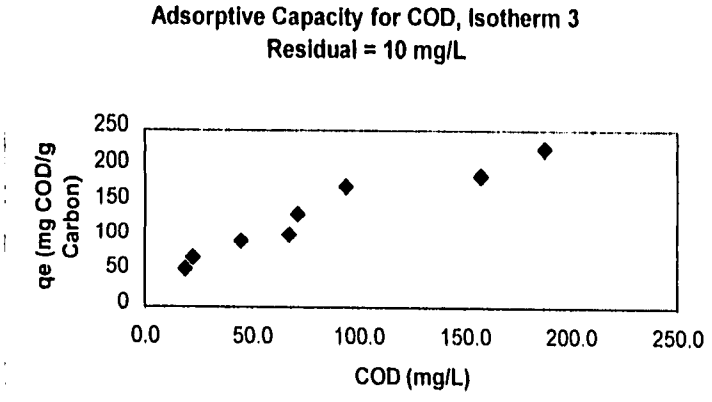

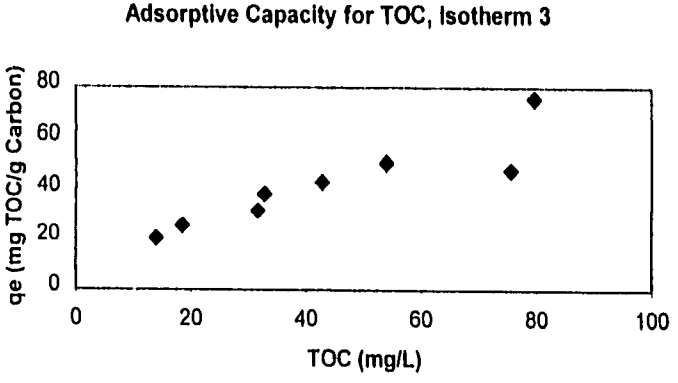

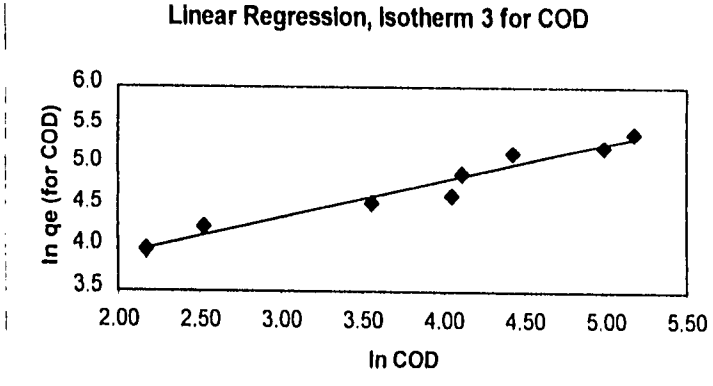

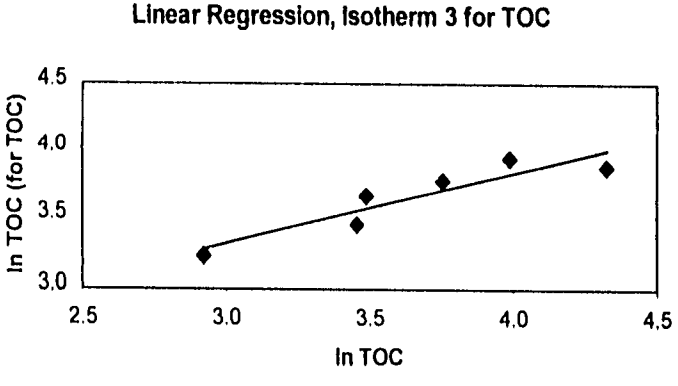

Figure 4-4 Equilibrium concentrations and linear regression analysis for isotherm 4

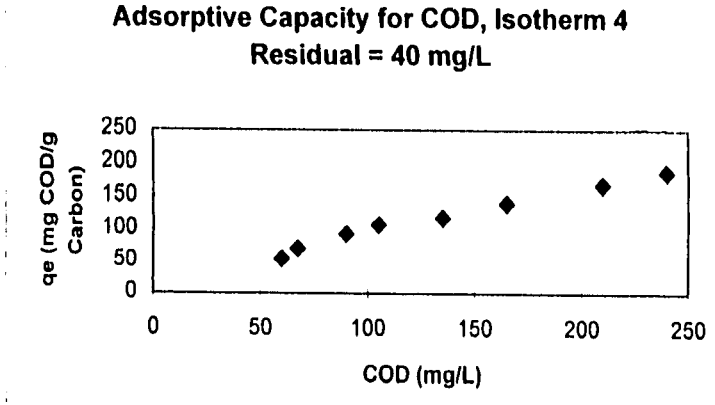

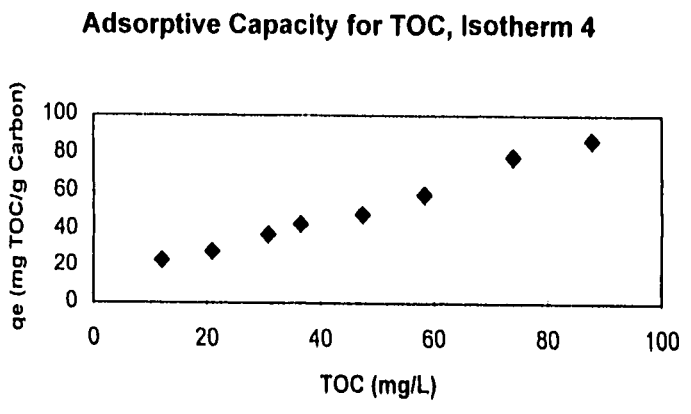

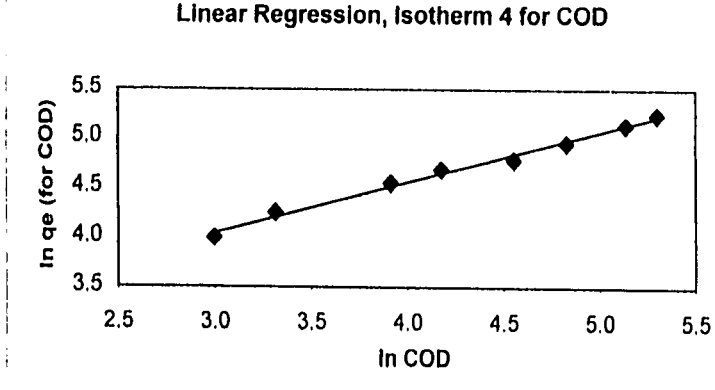

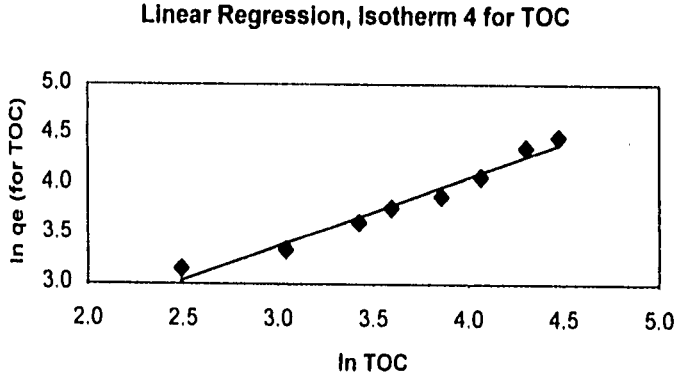

Figure 4-5 Comparison of Isotherms 1 to 4 for COD

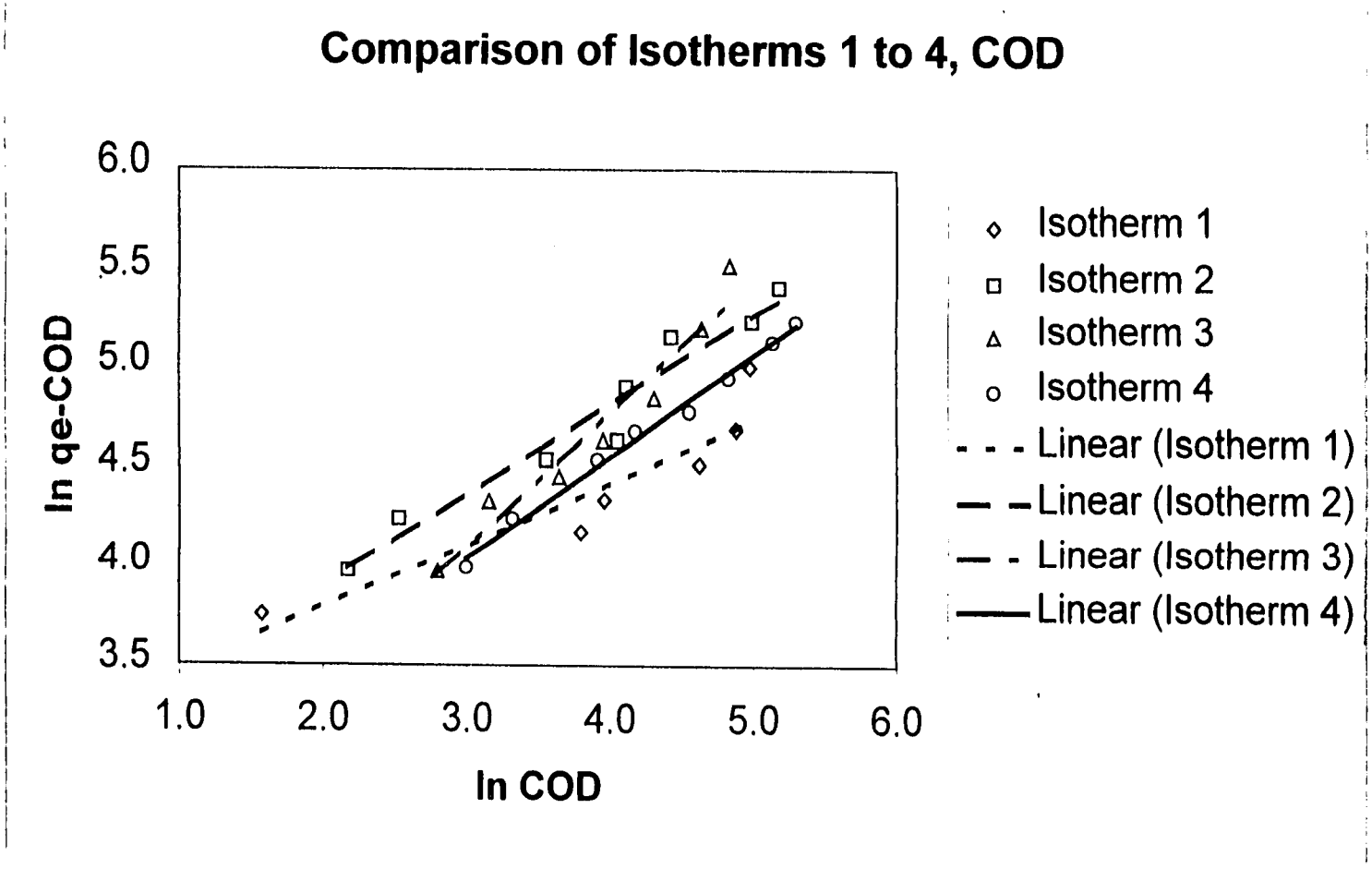

Figure 4-6 Comparison of Isotherms 1 to 4, TOC

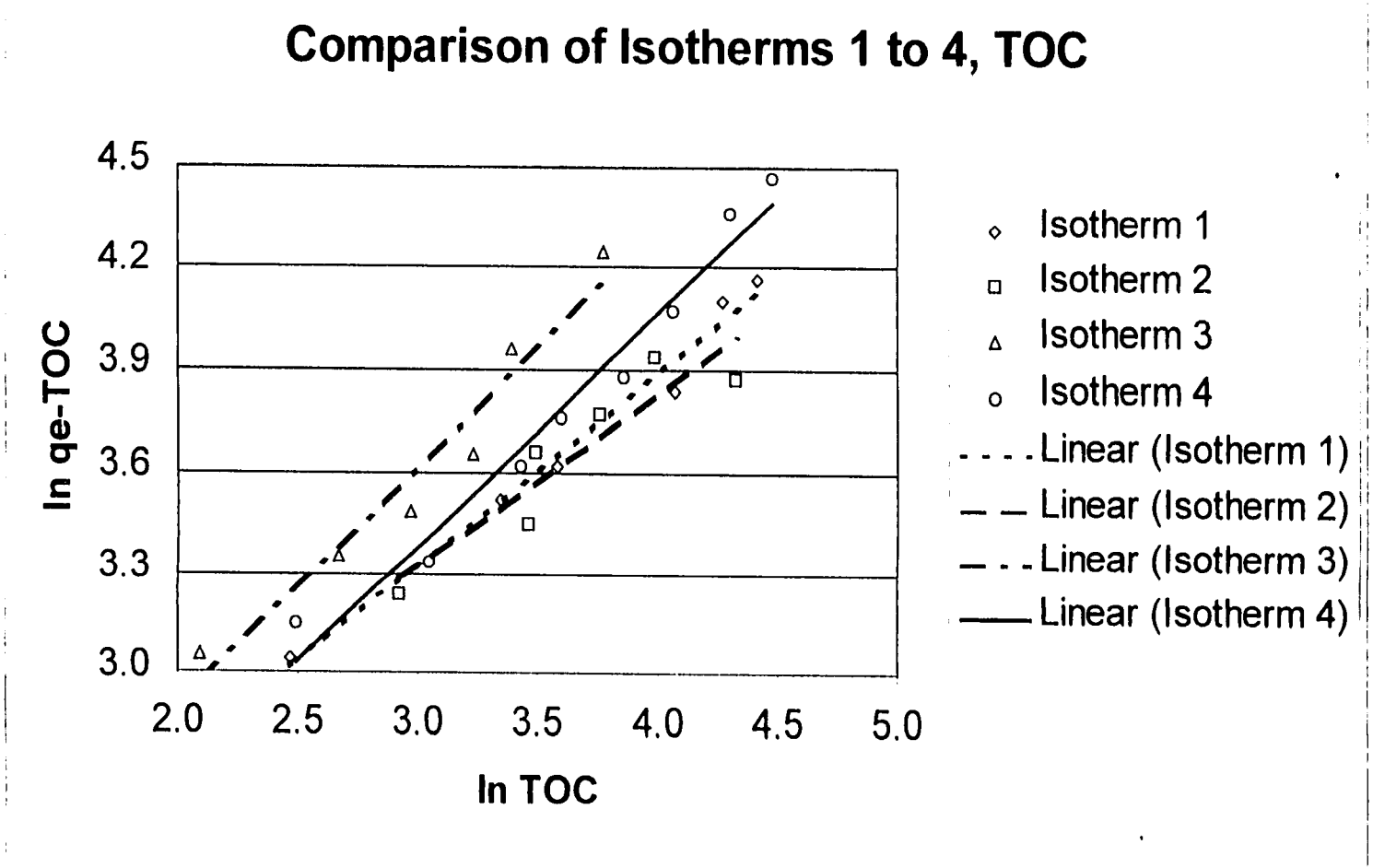

intercept and n are corresponding to lnK_F and n in Equation 4-2. The values in parentheses are confidence intervals. Tables 4-3 and 4-4 summarize the resulting isotherms. Figures 4-1 to 4-4 illustrate the linear regression analysis of the isotherms for the AST effluents. Figures 4-5 and 4-6 compare the isotherms for the AST effluents. Experimental data of all isotherms are detailed in Appendix A.

4.3.1 Discussion of Experimental Data

When the values of q_e were first calculated based on the total equilibrium concentrations as illustrated in Figures 4-1 to 4-4, a residual COD was clearly shown in the COD - q_e plot of each isotherm test. The magnitude of the residual was determined by the extrapolation of the isotherm to the zero loading, i.e., infinite carbon dosage in the COD – q_e plot (Benedek, 1980). It was found that the SRT of the AST process, in which a sample was pretreated, would affect the magnitude of COD residual in the isotherm experiment conducted for the sample. In other words, the SRT in the pretreatment process would affect the adsorbability of GAC for the COD of the sample.

When a sample was pretreated under lower SRT, the COD residual in the isotherm test conducted for the sample would be higher. As listed in Table 4-3, the SRT corresponding to isotherm 4 was one half of that of isotherms 1 to 3, and the residual resulted in isotherm test 4 was two to four times as high as that in isotherm tests 1 to 3. It was also shown in Table 4-3 that the COD residuals found in the isotherm tests conducted for AST feed were much higher than that found in the isotherm tests for AST effluents. Therefore, it was concluded that the GAC adsorbability for COD was higher, or the residual was lower, if the sample was pretreated under higher SRT in the AST process.

Unlike COD residuals, within the range of SRT controlled in the AST pretreatment processes in this study, the TOC residual, if measurable, was fairly low, less than 5 mg/L, and did not appear to a function of SRT. However, the TOC residual found in one of the

isotherm tests conducted for the AST feed was 80 mg/L, which accounted for 38% of the initial TOC of the feed and was much higher than those found in the isotherms conducted for AST effluents. Other factors including the HRT of the pretreatment process and the initial concentration of the isotherm experiment were also examined. However, no particular relationships between the residual value and these factors were found.

While examining the influence of experimental materials on data, it was found that the degradation of AST effluent during the contact period was not measurable. The leaching of both bottles and carbon was found negligible (Appendix A). When the residual value was determined, the COD equilibrium concentrations were corrected by subtracting the residual value from the raw data.

Linear regression analyses were performed, based on the corrected data, for the logarithm of q_e versus logarithm of equilibrium concentration plot to determine the values of parameters n and K_F. When the carbon dosage was very low, the percentage error of $c_0 - c_e$ (Equation 4-1), and therefore the percentage error of q_e, could be high. Justified by this, the data point corresponding to the lowest carbon dosage was not included in the linear regression of the isotherms (Benedek, 1980). Tables 4-3 and 4-4 summarize the analysis results. Figures 4-1 to 4-4 show the raw equilibrium concentrations and linear regression analysis for isotherms 1 to 4.

4.3.2 Discussion of the Isotherms

The isotherms listed in Tables 4-3 and 4-4 were obtained from the regression analysis of the adsorbable fraction of the equilibrium concentration. That is, the data were corrected by subtracting the residual from the equilibrium COD or TOC prior to the modeling. By doing this, it was assumed that the pretreatment process conditions, the SRT in particular, would not affect the analysis of the adsorbability of the GAC.

An earlier study conducted by Randtke and Snoeyink (1983) indicated that, unlike a truly single-solute system, wastewater was a heterogeneous mixture of organic contaminants. In such a complex system, the equilibrium isotherm would depend on the initial adsorbate concentration in an isotherm experiment. A higher initial adsorbate concentration would require a removal of a greater percentage of the adsorbate to reach a given equilibrium concentration, resulting in a greater removal of the more poorly adsorbed compounds. Therefore, the GAC adsorbability for the mixture of organic contaminants measured by the bulk parameter, i.e., COD or TOC, will decrease as the initial adsorbate concentration increased (Randtke and Snoeyink, 1983).

However, examining the AST effluents tested in this study, where COD ranged between 190 and 277 mg/L, and TOC ranged between 71.5 and 105 mg/L, it was found that the adsorbabilities of GAC for COD and TOC were not strong functions of the initial concentrations (Tables 4–3 and 4–4). As stated in section 4.3, the value of n in an isotherm was roughly an inverse indicator of adsorbability. Considering the isotherms 1 to 4 shown in Table 4–3, isotherm 4 had the highest initial COD, but the value of n was not the highest among the four. Isotherms 1 and 3 had almost the same initial COD, but the value of n of isotherm 3 was twice as high as that of isotherm 1. Taking consideration of the value of K_F of these two isotherms, the one that had a low value of n had a much higher value of K_F. This diminishes the differences between the adsorptive capacity calculated from the whole isotherm expression.

While comparing the COD isotherms obtained for AST effluents to that obtained for the AST feed, the values of n for the AST effluents were much lower than that for the AST feed. This indicated that the adsorbability of the GAC for COD of the AST effluents was much higher than that for the AST feed. This can be attributed to the adsorption of metabolic end product (MEP) in the AST effluent. Previous work indicated that a major portion of the

residual organics in the effluent of activated sludge systems is not the original substrate, but is MEP synthesized by the biomass (Daigger and Grady, 1979). Other studies showed that a significant fraction of the MEP is adsorbable (Randtke and McCarty, 1979).

The TOC isotherms obtained from different samples appeared very similar. The value of n of each TOC isotherm, including the one for the AST feed, fell into a very narrow range, as did the value of K_F. This indicated that the change of initial TOC within the range tested in this study did not affect the adsorption capacity of the GAC for TOC. Experimental data of isotherms for both the AST effluents and the AST feed are listed in Appendix A.

Comparing the COD and TOC isotherms for the same sample, when the values of n are close (isotherms for sample 3), the ratio of K_F value for COD to K_F value for TOC is close to 2. This is a typical COD:TOC ratio for the industrial wastewater (Droste, 1997).

Finally, comparison has also been conducted among the four isotherms obtained for AST effluents, measured in either COD or TOC, in terms of the confidence intervals of the coefficients, i.e., the *intercept* and n summarized in Table 4–2. It was observed from the regression analysis that the confidence intervals for the four sets of coefficients, are overlapped. This indicates that the isotherms describe similar adsorptive behaviors and can be represented by a single isotherm.

Chapter 5

ADSORPTION MODEL FOR FIXED-BED COLUMNS AND THE COLUMN EXPERIMENT

The dual internal mass transfer resistance model of Peel and Benedek (1981) offers great flexibility modeling GAC columns. It was chosen to model the GAC column runs in the current study because of the ready availability of the computer program for it, its great flexibility, and the excellent results obtained by Peel (1979). Also it is unlikely that newer models, such as the combined surface and pore diffusion model, would offer more flexibility as they do not contain more internal resistances.

Microcolumn experiments were performed to obtain the data that were used to estimate the mass transfer coefficients involved in the dual rate model. The column influents were obtained as described in Chapter 3. Various flow rates were tested. Based on the experimental data, computer programs PRECOS and REG-3 developed by Peel (1979), Narbaitz, and Benedek (Narbaitz and Benedek, 1983) were used to solve the model and perform the regression analysis for the estimation of the mass transfer coefficients.

5.1 Adsorption Model

The dual-rate column model was discussed in detail in Section 2.3.4.2. It provides the foundation of this study. In the dual rate model (Equations 2-9 through 2-17), the surface diffusion was considered being the predominant transport mechanism in the macropore, and a simple linear expression is assumed for transport within the micropore. Since both macropore and micropore concentrations were radially distributed, the numerical solution was very complicated and time consuming. In further research, Peel and Benedek (1981) investigated the simplified forms of the model, namely the linear driving force and quadratic driving force

(QDF) expressions. They have tested the solutions of the two simplified versions against the exact solution of the original model and chosen the QDF expression as the simplified model. In the QDF expression, the dual rate model was simplified by using quadratic driving force approximations to replace the continuous concentration profile within an activated carbon particle. The mathematical formulation of the driving force column model is as following:

Freundlich isotherm:

$$q_s = K_F c_s^n \tag{2-13}$$

Macropore mass balance

$$fW\frac{d\bar{q}_m}{dt} = k_m \rho_c \frac{3W}{R\rho_c}\left(\frac{q_s^2 - \bar{q}_m^2}{2q_m}\right) - R_b \tag{5-1}$$

Micropore mass balance

$$(1-f)W\frac{d\bar{q}_b}{dt} = k_b W(\bar{q}_m - \bar{q}_b) = R_b \tag{5-2}$$

Particle surface boundary condition

$$k_f(c - c_s) = k_m \rho_c \left(\frac{q_s^2 - \bar{q}_m^2}{2q_m}\right) \tag{5-3}$$

Liquid phase mass balance

$$\frac{\partial c}{\partial t} = -v_s\frac{\partial c}{\partial x} - \frac{(1-\varepsilon)}{\varepsilon}\frac{3k_f}{R}(c - c_s) \tag{5-4}$$

where

$\bar{q}_b$ is mean branch pore solid phase concentration

$\bar{q}_m$ is mean macropore solid phase concentration

k_m is macropore pseudo mass transfer coefficient, cm/s

W is mass of carbon, g

Coupled with the Freundlich isotherm described by Equation (2-13), Equations (5-1) to (5-4) describe the adsorption bed model. The model was solved using implicit finite difference expansions of the differential terms. The solution has proven to be a good approximation to the exact solution (Peel and Bendek, 1981). The QDF expression of the dual rate model was used in this study to simulate the performance of the GAC column.

5.2 Multicomponent and Bulk Parameter Modeling

As in the AST process, bulk concentration parameters soluble COD and TOC were used in the adsorption bed modeling. Using bulk parameters is necessary in many applications of activated carbon adsorption because it is often impossible to define a wastewater in terms of one or several components. Even when tens or hundreds of single compounds are identified, they still only comprise a small fraction of the total organic matter in the wastewater. In such a situation the only possible solution is to use bulk parameters.

However, using bulk parameters can impose limitations on the ability of a mathematical model to describe the adsorption behavior of GAC columns. When a complex wastewater is applied to a GAC column, problems such as early breakthrough of poorly adsorbed components and concentration of weakly adsorbed components in the effluent can occur. The second problem is caused by the displacement effect existing in the column. It is impossible to predict these effects using a bulk parameter approach (Peel, 1980).

In this study it was assumed that the concentration of any single component was much less than that of the gross concentration represented by COD and TOC. Therefore, COD and TOC would reflect the overall behavior of the system.

5.3 Microcolumn Experiment

One major issue in mathematical modeling of GAC column is to determine the mass transport parameters, namely film transfer coefficients and intraparticle coefficients. Traditionally, effective intraparticle diffusivities, i.e., surface and/or pore diffusivities

depending on the adsorption mechanism of choice, was often obtained by batch kinetic experiment. The film transfer coefficient k_f, on the other hand, were estimated using mathematical correlations. The potential errors that could be introduced by correlation procedures were estimated to be as high as 20% (Liu and Weber, 1981).

Peel et al. (1980) used a different approach based on a batch kinetic model to estimate the film transfer coefficient and other coefficients. The batch kinetic model was also derived from the dual rate adsorption mechanism. The only function that was different between these two models was the one that described the liquid phase mass balance, i.e., Equation 5-4. The equation appeared in the batch kinetic model as follows:

$$V\frac{dc}{dt} = -k_f \frac{W}{\rho_c}\frac{3}{R}(c - c_s) \qquad (5\text{-}5)$$

where V was the volume of the batch reactor. The batch kinetic model was fitted with batch experimental data. It was assumed that the liquid phase concentration at carbon surface was close to zero at the very first stage of adsorption – the first three minutes for o-chlorophenol. Then the coefficient k_f can be obtained from the logarithm of c versus t plot of the initial data based on Equation 5-5. Other coefficients involved in the model were estimated by fitting the whole model with the full set of batch kinetic data. This approach depended on the assumption of a zero liquid phase concentration at the carbon surface in the initial stage. Therefore, the accuracy of the film transfer coefficient k_f was largely affected by the precision of the data obtained within the first couple of minutes of the batch kinetic experiment.

As an alternative to these traditional methods, a microcolumn technique was introduced by Liu and Weber (1981). This technique has proved to be able to simultaneously determine the film transfer coefficients and effective intraparticle diffusivities with high precision.

5.3.1 Microcolumn Technique

A microcolumn is defined as a column of sufficiently short length that immediate concentration breakthrough occurs (Liu and Weber, 1981). Weber and Liu conducted sensitivity analysis of the film transport coefficient k_f and the effective surface diffusivity D_S on microcolumn breakthrough curves for *p*-bromophenol and dodecylbenzenesulfonate. They found that when the column length was made sufficiently short, the initial portions of breakthrough curves were dominated by film transfer mechanism regardless of the predominant mass transport type of overall process. Therefore, the effect of film transfer can be separated from that of intraparticle diffusion. By separately measuring k_f in the region where it is the controlling resistance, better estimates of D_S could be obtained. Liu and Weber also found that for the same degree of change in k_f and D_S, the response of microcolumn is more sensitive than that of a long column. Based on this observation, k_f can be determined by analyzing the initial portion of the breakthrough curve of a microcolumn run. Once k_f is determined. D_S can be searched using nonlinear regression analysis for the entire breakthrough curve. Liu and Weber also conducted the sensitivity study for the effect of the exponent of Freundlich isotherm on micro-column breakthrough curve. They found that with high value of n, for example 0.6 for PBP, both film transfer and solid diffusion occur simultaneously from the beginning of the breakthrough curve. Therefore, they indicated, the microcolumn technique was not particularly successful for adsorption systems with high values of n.

5.3.2 System Configuration and Experimental Materials

Microcolumns were made of clear Plexiglas™. The internal diameter of each column was 1.0 cm while the length was 60 cm. Such a column length provided enough space for carbon packing, supporting material packing, and freeboard height for backwashing. Columns were

operated in upright position and downflow mode. Each column had a bleeding port at the top to prevent the build up of air bubbles. Glass wool was used as supporting material for GAC particles and packed close to the lower end of the column. A peristaltic pump was used to provide constant flow to the column. Tygon™ tubing was used to connect the reservoir, the pump, and the column. The same type of tubing was used to discharge the effluent from the column. Figure 5-1 shows the setup of a microcolumn system.

Figure 5-1 Set up of the microcolumn system

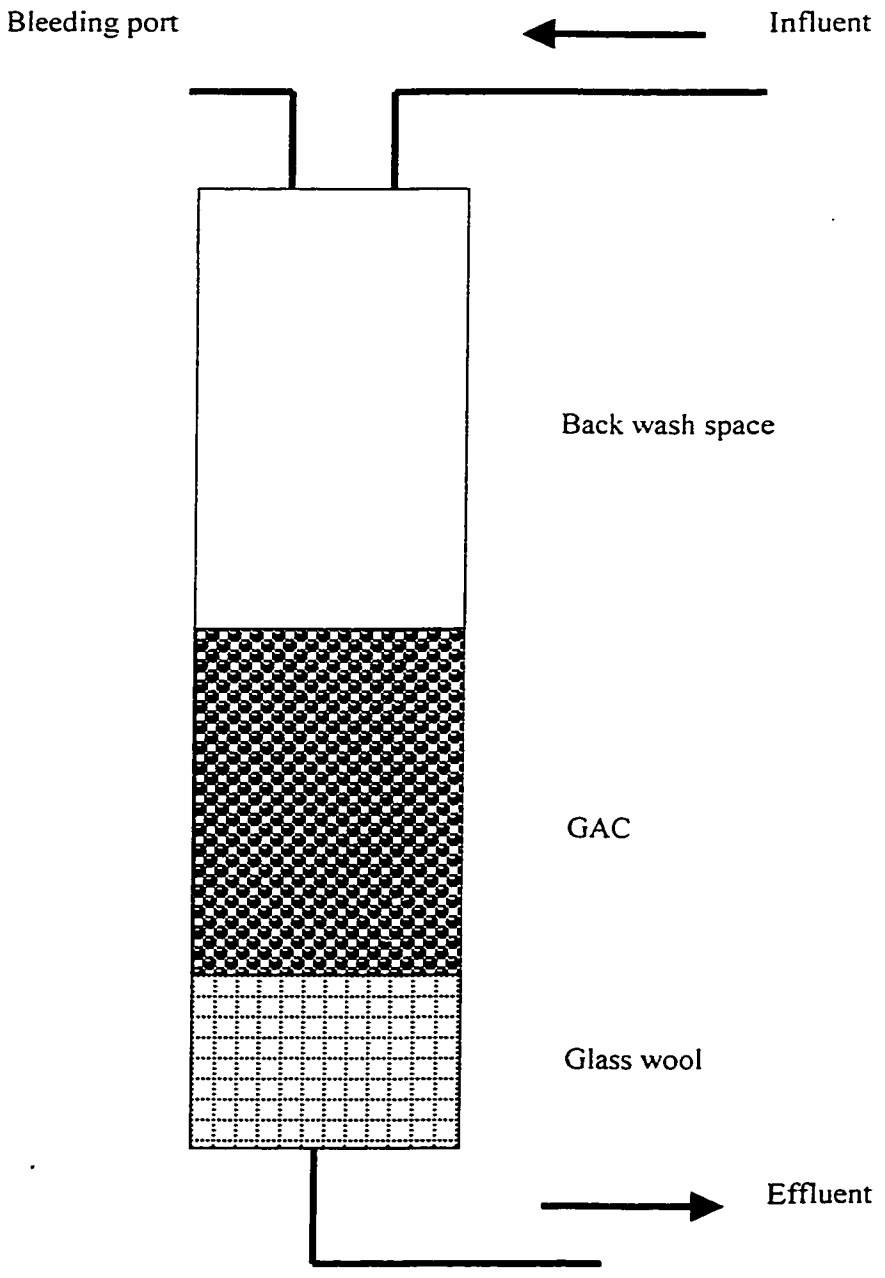

Calgon F400 GAC was chosen to be the adsorptive media and the preparation of the GAC followed the same procedure described in section 4.1 except that the GAC was not pulverized, but ground to smaller sizes. The initial F400 GAC particles had sieve sizes of 12×40. The 40×50 fraction of the ground carbon was used, which was corresponding to a particle size range of 0.0297 to 0.0420 cm. It was thoroughly washed to remove fine carbon and to reduce the effect of possible leaching of carbon. Then it was dried and stored as described in section 4.1. Among the seven column runs, one column was filled with 2.51 g GAC and had a bed length of 7.2 cm, and the rest columns were filled with 1.80 g GAC and had a bed length of 5.5 cm. The ratio of carbon bed length to average particle diameter was 150. The ratio of column diameter to the average particle diameter was 28.

When a column was filled with measured amount of GAC, the bed was first backwashed with deionized distilled water to remove air bubbles. A very small amount of fine carbon could be washed out during the backwash. However, since the GAC was well washed after it was ground, it was considered that most fine carbon had been removed and carbon lost during the backwash process was negligible. When air bubbles were removed, the carbon bed was allowed to settle and soaked in deionized distilled water before the experiment started.

AST effluents obtained earlier from the laboratory-scale system were tested in the microcolumn experiment. Refer to Table 3-1 for the characteristics and AST operation conditions of these effluents and Tables 4-2 and 4-3 for equilibrium isotherms of these effluents. A study conducted to treat a similar wastewater using the same laboratory AST system concluded that the average removal of soluble CBOD (carbonaceous biochemical oxygen demand) in this system was 98%, with a standard deviation of 1.1% (Graham, 1996). The biodegradable contents of the AST effluents were very low. As stated in Chapter 3, these AST effluents were frozen during storage to minimize degradation. Shortly before a

microcolumn run started, the sample used in the experiment was thawed and filtered with *NALGENE*® 0.45μm CN membrane filters to remove solids and bacteria. Then the filtrate was stored in a 20 L plastic reservoir at room temperature (23°C) until it was used in the column experiment. Experimental evidence found in the isotherm study stated in chapter 3 showed that the degradation of the AST effluents at room temperature within a period of 72 hours was negligible. Based on the facts stated above, it was assumed that the biodegradation within the column was negligible.

5.3.3 Process Control

The feed concentrations, i.e., COD and TOC, for each column run, except column 5, remained constant. To obtain a basis of model verification, column experiments were conducted using various flow rates, ranging from 0.065 mL/s to 0.133 mL/s. One major consideration in deciding the minimum flow rate was to guarantee sufficient volume of samples for analysis in the initial frequent sampling period. When a column test started, sampling started after the distilled water in which the carbon bed was soaked was completely pushed out of the bed by the influent wastewater. The effluent was sampled every 15 minutes during the first hour of experiment, and then less frequently. The operation was terminated when the effluent COD and TOC were unchanged in a period of six hours. Table 5-1 summarizes the carbon bed measurement and influent information of each column test.

Unlike the other single columns, columns 4 and 5 were operated in series, therefore, the influent COD and TOC of column 5 varied during the experiment. As the result, the column model was not fitted to the data obtained from column 5.

5.3.4 Discussion of the Column Effluent Data

As discussed in Section 4.3.1, a portion of the AST effluent COD was non-adsorbable in the isotherm experiment. The magnitude of the residual was mainly affected by the SRT in

the AST pretreatment process. The lower the SRT in the pretreatment process was, the higher the residual was found in the adsorption test. Refer to Table 4-3 for the residual values of samples corresponding to various SRT in the pretreatment process. The non-adsorbable portion of the influent concentration would pass directly to the effluent in an adsorption column and had no effect on the adsorption process. Therefore, it was subtracted from both the influent and effluent concentrations before analysis. Detailed microcolumn experimental data can be found in Appendix B.

Table 5-1 GAC Bed Dimension and Influent Characteristics

Item	Column 1	Column 2	Column 3	Column 4	Column 5	Column 6	Column 7
Carbon particles radium (cm)	0.0297 – 0.0420						
Carbon weight (g)	2.506	1.803	1.802	1.801	1.800	1.802	1.800
Internal column diameter (cm)	1.0						
Bed length (cm)	7.2	5.6	5.6	5.5	5.5	5.5	5.5
Bed density (g/cm^3)	0.44	0.41	0.41	0.42	0.42	0.42	0.42
Apparent particle density (g/cm^3)	0.75						
Volumetric flow rate (mL/s)	0.0658	0.068	0.133	0.082	0.082	0.105	0.105
Hydraulic loading rate (m/hr)	3.02	3.13	6.08	3.75	3.75	4.80	4.80
Retention time, or EBCT (s)	85.83	63.18	33.16	52.80	52.80	41.25	41.25
Carbon bed void fraction (%)	0.41	0.45	0.45	0.44	0.44	0.44	0.44
Feed concentration (COD / TOC mg/L)	178.5/80.5	151.5/82.5	151.5/82.5	207.0/88.0	N/A	278.7/85.7	169.8/71.6
SRT in AST process (d)	5	5	5	10	10	10	10
HRT in AST process (h)	6	6	6	6	6	6	12
Influent pH	7.35	7.35	7.35	7.00	7.00	7.50	7.50

5.4 Estimation of the Mass Transfer Coefficients in the Dual Rate Model

5.4.1 The Computer Program

The computer program used to solve the QDF dual rate model in this study was based on the FORTRAN program MASTER (McMaster Adsorption System Optimization Routines) developed by Narbaitz and Benedek (1983). MASTER solved the QDF dual rate model using implicit finite difference scheme. It also calculated the carbon usage rate for different design configurations and estimated the cost of GAC column systems. MASTER was revised to suit the PC platform in 1996 (Swyer, 1996).

This study used solely the simulation portion of MASTER, called PRECOS, to estimate mass transfer coefficients involved in the dual rate model and predict the carbon usage rate of a single column. The inputs of the program are listed in Table 5-2, which include the mass transfer coefficients, namely k_f, k_m, k_b, and f, and information regarding the column influent, the dimension of the carbon bed, and process control. The output of the program is the effluent concentration profile, i.e., a breakthrough curve, calculated based on the inputs of the program.

To determine the mass transfer coefficients, the first estimation of the mass transfer coefficients and the experimental data obtained from one microcolumn experiment were used as the input of PRECOS. The calculated breakthrough curve was fitted with the experimental data, and the input mass transfer coefficients were adjusted based on the analysis of the errors. A FORTRAN program called REG-3 developed by Narbaitz in 1997 was used in conjunction with MASTER to accomplish the non-linear regression analysis. REG-3 took the output of MASTER, calculated the average error and the sum of squares of the predicted breakthrough curve against the experimental data, and then adjusted the input values of mass transfer coefficients. This process iterated until the errors were below the predefined levels. Since the non-linear regression analysis was very sensitive to the initial input, the column

Table 5-2 Major Input Parameters of PRECOS

Symbol	Description
KF	External liquid film transfer coefficient, k_f(cm/s).
KM	Macropore mass transfer coefficient, k_m (cm/s).
FB	Micropore mass transfer coefficient, k_b (cm/s).
F	Fraction of total capacity available in the macropore f.
C0	Influent concentration, COD or TOC (mg/l).
CL	Length of the carbon bed (cm).
V	Volumetric flow rate (ml/s).
HLR	Hydraulic loading rate (m/hr).
RHOB	Packed bed density (g/cm^3).
RHOC	Apparent particle density (g/cm^3).
EQ1	Parameter calculated based on K_F (mg/g) and n of the Freundlich isotherm: $EQ1 = \frac{10^3}{10^{6n}} K_F$
EQ2	The value of n of the isotherm.
IERR	Number of experimental data points.
ARRE	Values of the experimental data.
	Various incremental steps required by the numerical method.

model was first manually fitted with the experimental data using PRECOS alone. The mass transfer coefficients resulted from the manual fitting process were then used as the input of REG-3. Minor changes were made to both PROCES and REG-3 to tailor the input and output formats to suit the requirements of this study.

5.4.2 Selection of the Isotherm

The influent of a microcolumn was pretreated in an AST system under a particular set of operation conditions. Among these operation conditions, the SRT had a considerable

influence on the adsorbability of GAC for COD indicated by the residual found in the equilibrium isotherm experiment. It was concluded in Section 4.3.2 that, the influence of the SRT on the adsorbability of GAC, and thereby the isotherm, could be eliminated by subtracting the residual from the equilibrium concentration. When fitting the dual rate model with the microcolumn experimental data, only the adsorbable fraction was evaluated. The isotherm chosen for the model was the one that fitted all microcolumn experimental data best.

5.4.3 Estimation of the Mass Transfer Coefficients

Typical values of the mass transfer coefficients for the particular type of wastewater were not available in the literature. Therefore, the values for some other simple or complex compounds were adopted as the initial input of the column model. Table 5-2 listed some of the values.

While manually fitting the dual rate model to the microcolumn experimental data using the computer program PRECOS, the input values of the mass transfer coefficients were adjusted according to the response of the output breakthrough curves. Sensitivity tests were conducted for k_f, k_m, and f. It was found that k_f significantly affected the earlier stage of the breakthrough curve. This conformed to the findings of Liu and Weber (1978) and Peel (1980). When the value of k_f was increased, the predicted effluent concentration at the beginning of the process would decrease, which indicated a slower approach to breakthrough. Figure 5-2 shows the response of the predicted breakthrough curve to the change of k_f when fitting the model with the experimental data of column 2.

Table 5-3 Typical Values of Freundlich Isotherm and Mass Transfer Coefficients

Coefficient	Phenol[1]	o-Chlorophenol[2]	TOC[3]	TOC[4]
n	0.21	0.098	0.75	1.02
K_F	78.1	204.2	137.5	103.6
k_f (cm/s)	2.7×10^{-3}	9.69×10^{-3}	9.62×10^{-4}	1.80×10^{-3}
k_m (cm^2/s)	5.32×10^{-8} (±6%)	3.81×10^{-8} (±7%)	1.56×10^{-7}	1.15×10^{-9}
k_b (1/s)	1.59×10^{-6} (±8%)	1.14×10^{-6} (±9%)	8.72×10^{-8}	6.65×10^{-8}
f	0.708 (±1%)	0.678 (±1%)	0.35	0.35

[1] [2]: The value of k_f was obtained from batch kinetics experiment. Peel, 1979.

[3]: For Bioresidual material generated by biologically degrading the pure compound phenol in an activated sludge system. The value of k_f was obtained from batch kinetics experiment. Peel, 1979.

[4]: For organic components in tap water. The value of k_f was obtained from batch kinetics experiment. Peel, 1979.

As indicated in Section 2.3.4.2, when the fraction f is set to unity, the model becomes the widely used external film resistance-surface diffusion mechanism model. The QDF dual rate model has shown to give very similar results to that of the surface diffusion model (Peel, 1979). Figure 5-3 shows the effect of k_m on the predicted breakthrough curve when fitting with the experimental data of column 2. At lower k_m values, the model gave higher effluent concentrations for the early and middle stretch of the breakthrough curve. Unlike the responds to k_f, the effluent concentration at the very beginning was not sensitive to k_m. This also conformed to Liu and Weber's finding (1981) that the initial portion of the breakthrough curve was always controlled by k_f.

The coefficient k_b was found to have an effect on the middle stretch of the breakthrough curve, as shown in Figure 5-4. An increase in k_b would result in a lower rate of breakthrough because the micropore capacity filled more quickly. The coefficient f had an effect on the middle stretch of the breakthrough curve. At lower f value, the micropore capacity becomes more important. Since the rate of adsorption in the micropore would be lower than that in the macropore, the effluent concentration tends to increase faster especially after the initial stage. Therefore, a more rapid breakthrough approach was predicted. Figure 5-5 shows the stated effect of f.

Figure 5-2 Effect of k_f on Predicted Breakthrough Curves for Column 2

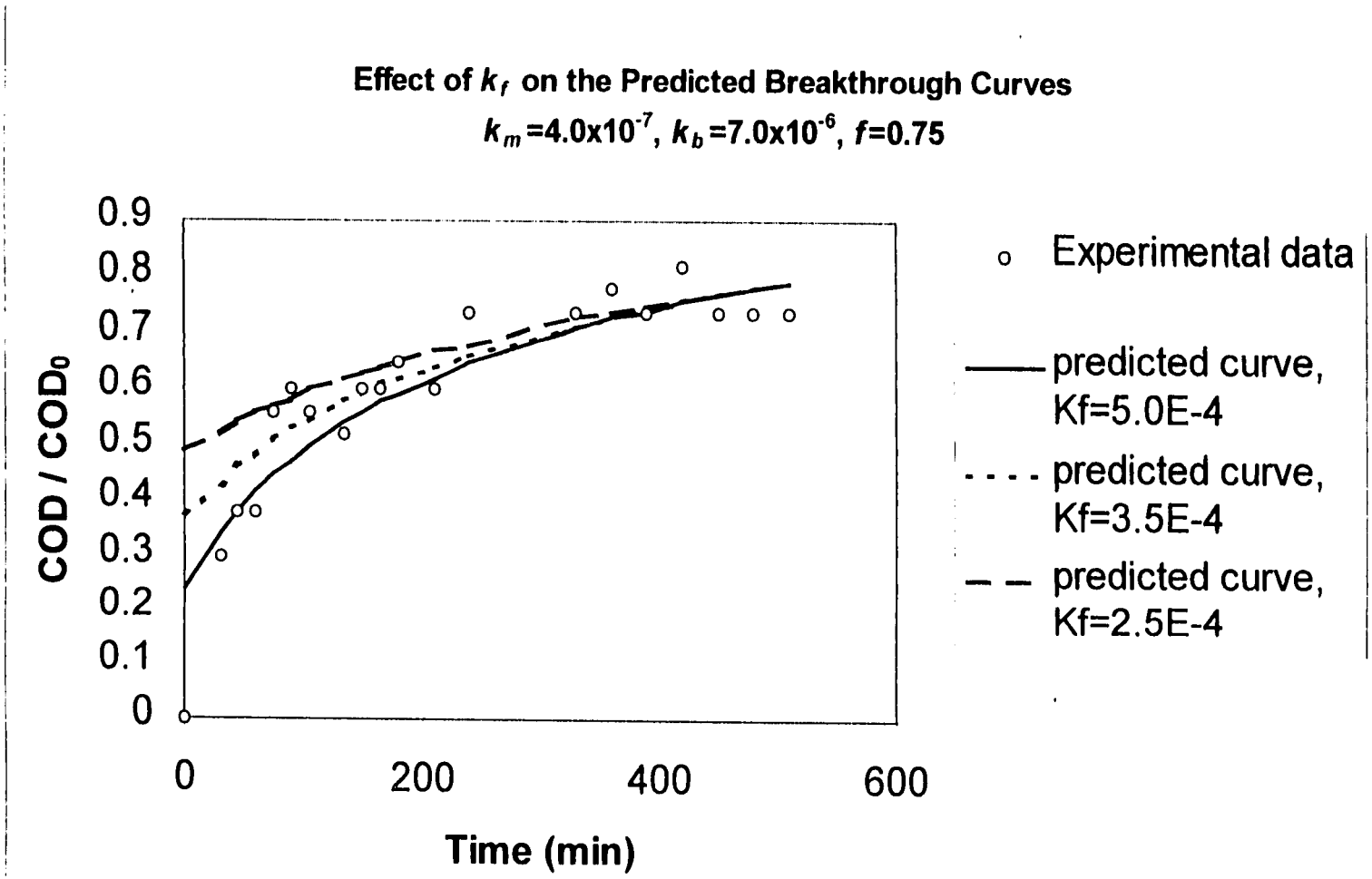

Figure 5-3 Effect of k_m on Predicted Breakthrough Curves for Column 2

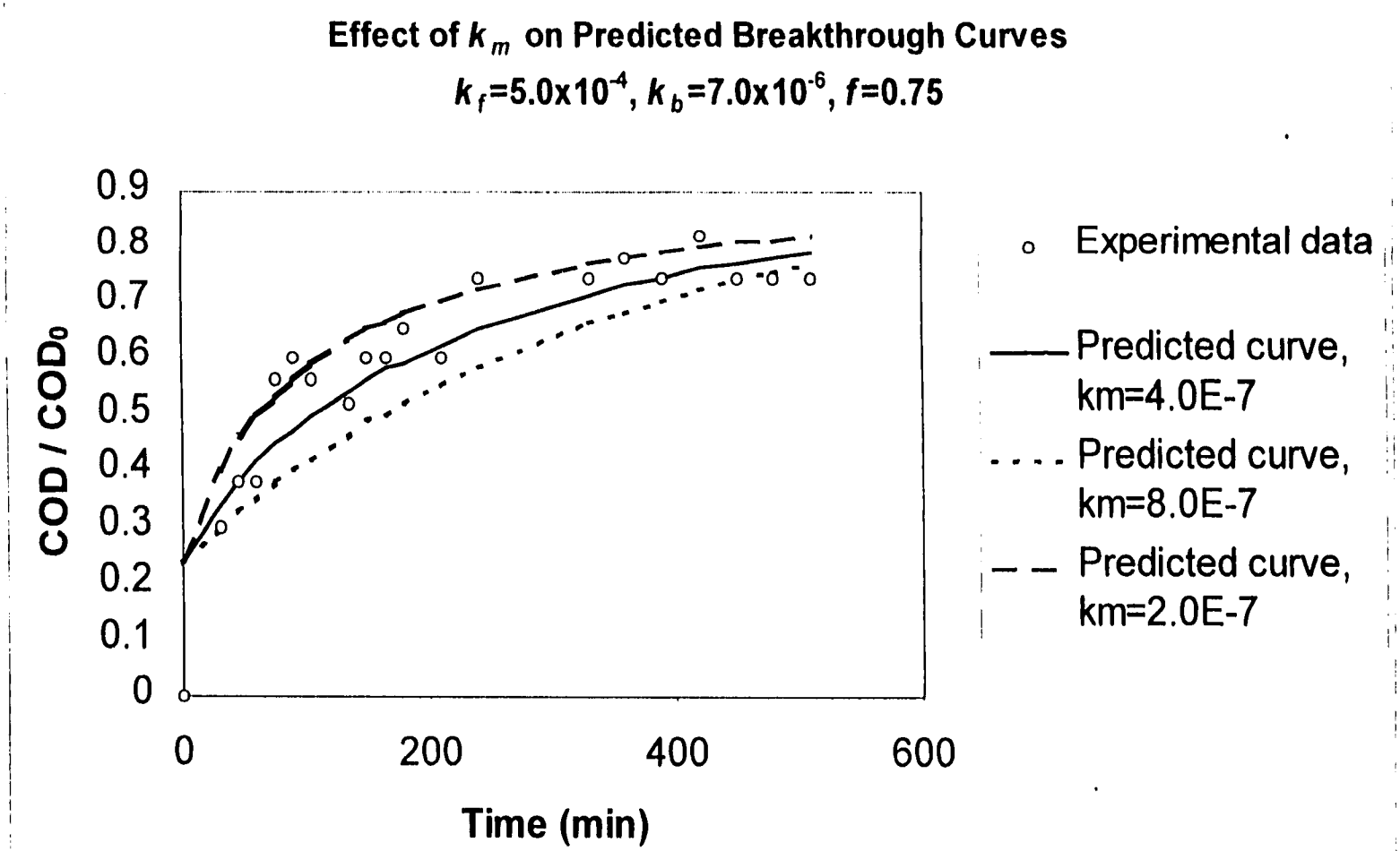

Figure 5-4 Effect of k_b on Predicted Breakthrough Curves for Column 2

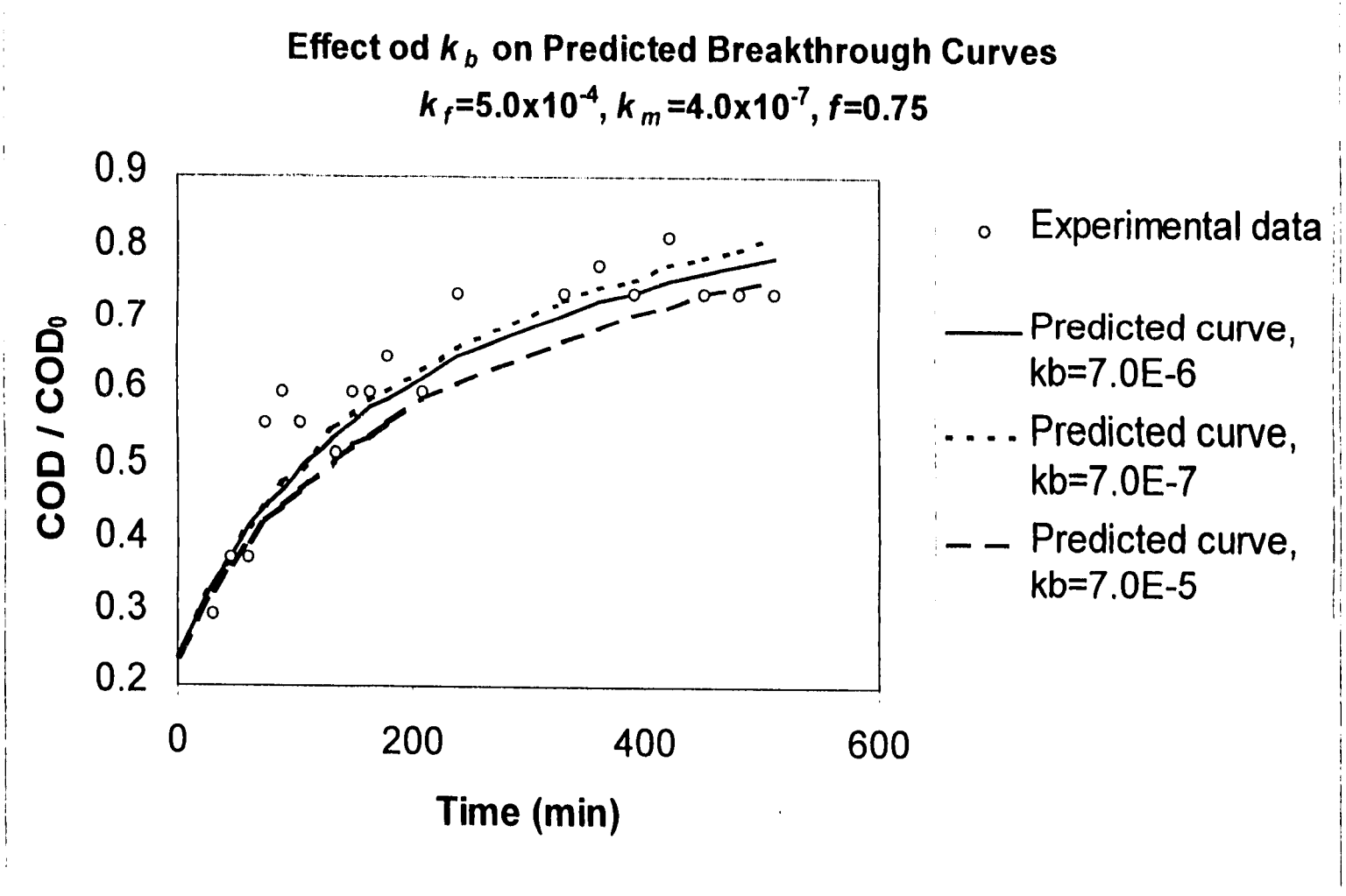

Figure 5-5 Effect of f on Predicted Breakthrough Curves for Column 2

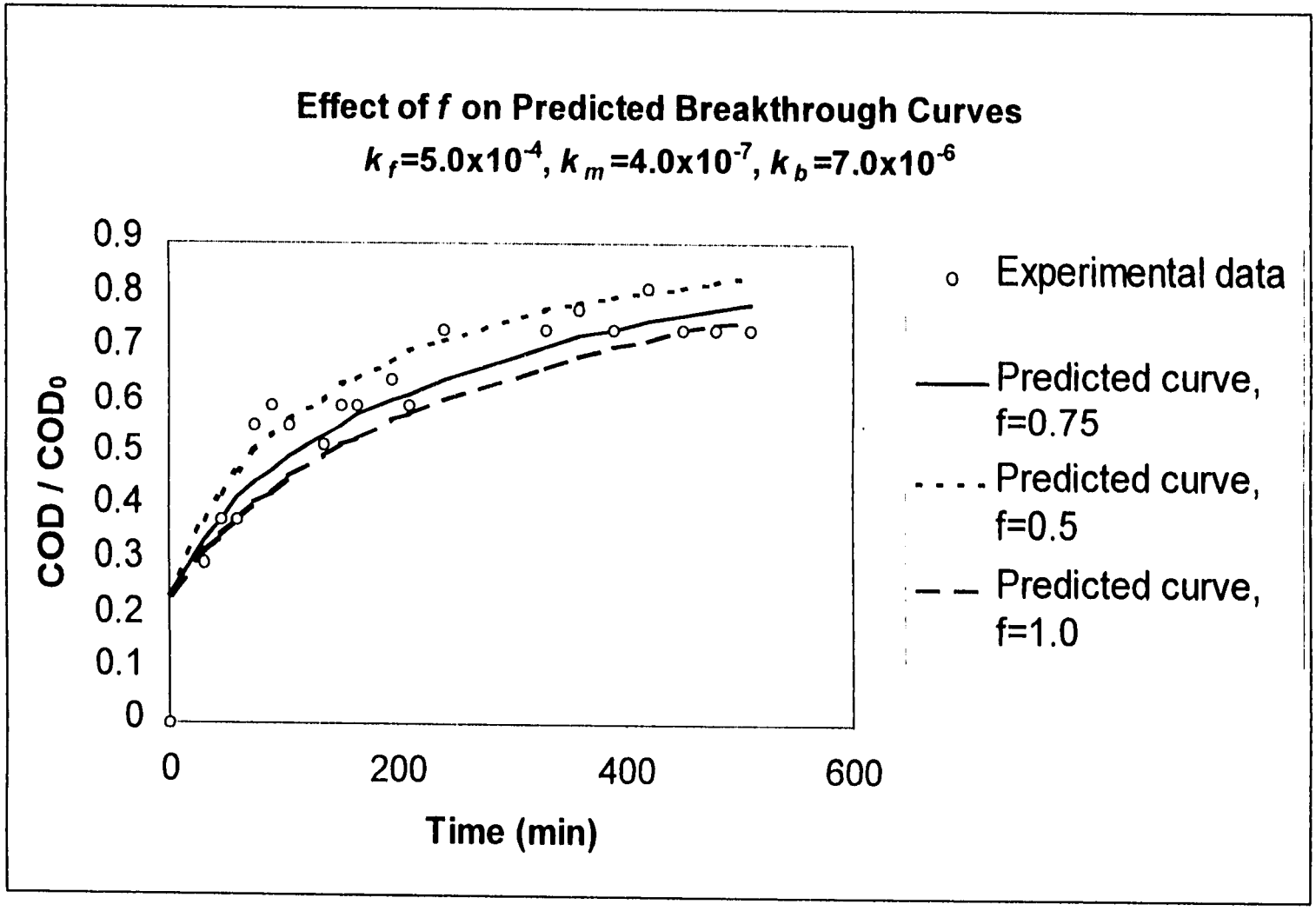

5.5 Results and Discussion

5.5.1 Adsorption of COD

Based on the sensitivity study, the dual rate adsorption model was first fitted with the experimental data of columns 1 and 2 simultaneously to determine the mass transfer coefficients of the model, namely k_f, k_m, k_b, and f. Isotherms obtained in Chapter 4 were used as the equilibrium expression included in the model. A set of mass transfer coefficients was determined for each isotherm so that the output of the model, i.e., the predicted breakthrough curve, for each microcolumn had good correspondence with the experimental data. The results are listed in Tables 5-4.

Table 5-4 Mass Transfer Coefficients for Adsorption of COD

Coefficient	Isotherm 1	Isotherm 2	Isotherm 3	Isotherm 4
n	0.32	0.45	0.68	0.51
K_F	37.77	20.14	7.78	12.54
k_f	5.5×10^{-4}	7.0×10^{-4}	not convergent	5.0×10^{-4}
k_m	3.0×10^{-11}	5.0×10^{-9}	not convergent	4.0×10^{-7}
k_b	7.0×10^{-10}	7.0×10^{-6}	not convergent	7.0×10^{-6}
f	0.10	0.75	not convergent	0.75

Mass transfer coefficients listed in Table 5-4 are within the range of Peel's results (Table 5-3). The set obtained by using isotherm 4 was chosen to predict the performance of columns 3, 5, 6, and 7 and to simulate the full scale GAC column operation. As stated in section 5.3.3, column 5 was operated in series with column 4, and its influent was changing during the operation. Therefore, the model was not fitted to the data obtained from column 5. Table 5-5 shows the average errors between the predicted breakthrough curves and the experimental data, calculated based on the following equation:

$$\eta = \frac{\sum_{1}^{N} \frac{\left| x_{predicted} - x_{observed} \right|}{x_{observed}}}{N} \qquad (5\text{-}6)$$

where

η is the average error

$x_{predicted}$ is the predicted effluent concentration

$x_{observed}$ is the experimental data

N is the total number of data

Table 5-5 Regression Analysis of Fitting the Model with Microcolumn Experimental Data

Error	Column 1	Column 2	Column 3	Column 4	Column6	Column 7
Average	0.154	0.078	0.138	0.085	0.084	0.058

The loading analysis was conducted for column 2 to compare the actual COD loading onto the carbon column to the theoretical maximum loading calculated using the isotherm. The column was run until the effluent COD was 74% of the influent COD. The maxium COD loadings were calculated for the equilibrium concentration of influent COD, which was 228 mg/L. The mass of carbon in column 2 was 1.80 g, and the time for the column to reach an effluent COD of 74% of the influent COD was 510 minutes. The result was listed in Table 5-6. More information about column 2 can be found in Appendix B.

Table 5-6 Results of Loading Analysis, COD

	Experimental	Isotherm 1	Isotherm 2	Isotherm 3	Isotherm 4
Loading (mg COD)	167	386	417	562	360

The actual loading was around 45% of the maximum loading calculated based on isotherms 1, 2, and 4. This indicates that it would take relatively long time after 75% breakthrough for the column to become saturated. As discussed in Section 4.3.2, isotherm 3

had a substantially high value of n comparing to the other three. This made the maximum COD loading calculated from this isotherm very high and, as a result, the loading achieved in the experiment accounted for even smaller fraction of the calculated saturation (theoretical) loading.

Figures 5-4 to 5-9 are the plots of microcolumn experimental data along with the simulated breakthrough curves. The mass transfer coefficients and experimental conditions for each microcolumn run are listed under the graph. The experimental data in the surrounding of operation time of 200 minutes had higher COD values than the predicted concentrations in every plot. This can be attributed to the early breakthrough of poorly adsorbed components in the wastewater.

Considering the drawbacks of using bulk parameters in modeling a multicomponent adsorption system, which was detailed in section 5.2, the ability of the dual rate model to predict the column adsorption process was generally very good. The values of mass transfer coefficient k_f obtained for isotherms 1, 2, and 4 were fairly consistent, while the others varied significantly. Compared with those listed in Table 5-3, the values of k_f found in this study were one to two orders lower than those found in the literature. This indicated that the adsorption for COD of the wastewater studied herein had a higher external film resistance. According to the sensibility study stated in Section 5.4.3, this lower k_f would produce a higher effluent concentration in the initial stage when simulating the column adsorption process.

While the three sets of mass transfer coefficients fitted the experimental data almost equally well, it was impossible to use isotherm 3 to obtain the mass transfer coefficients that fit the experimental data. This can be attributed to the higher value of n in isotherm 3. As stated in Section 5.4.3, for an adsorption system with higher value of n, both film transfer and solid diffusion occur simultaneously from the beginning of the microcolumn experiment. As

a result, the obtained data are not particularly helpful in predicting the film transfer coefficient k_f and therefore the other mass transfer coefficients. When the input parameters of the computer program, i.e., the first estimated coefficients obtained from fitting the microcolumn data, are not precise enough, the chance of getting an acceptable output from nonlinear regression analysis is small.

Figure 5-6 Fitting the Model with COD Data of Column 1

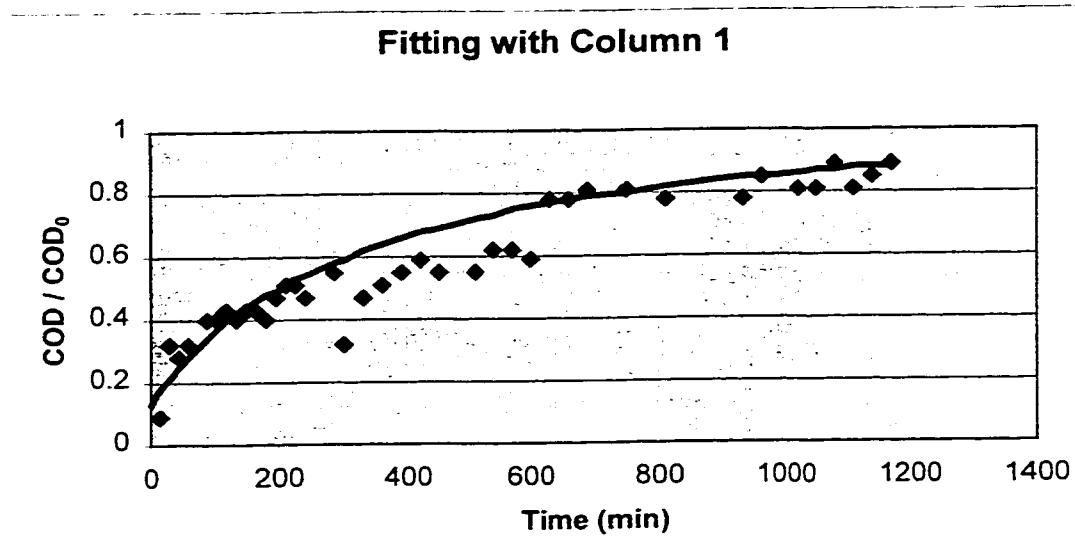

Influent COD: 228.5 mg/L, Hydraulic loading rate: 3.02 m/hr

$k_f = 5.0\times10^{-4}$, $k_m = 4.0\times10^{-7}$, $k_b = 7.0\times10^{-6}$, $f = 0.75$, $n = 0.51$, $K_F = 12.54$

Figure 5-7 Fitting the Model with COD Data of Column 2

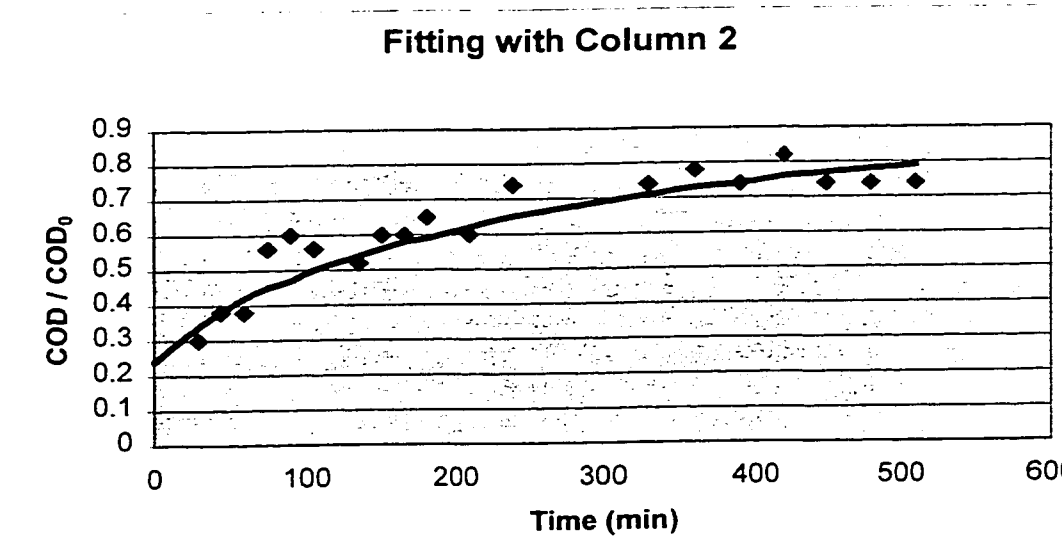

Influent COD: 186.8 mg/L, Hydraulic loading rate: 3.13 m/hr

$k_f = 5.0\times10^{-4}$, $k_m = 4.0\times10^{-7}$, $k_b = 7.0\times10^{-6}$, $f = 0.75$, $n = 0.51$, $K_F = 12.54$

Figure 5-8 Fitting the Model with COD Data of Column 3

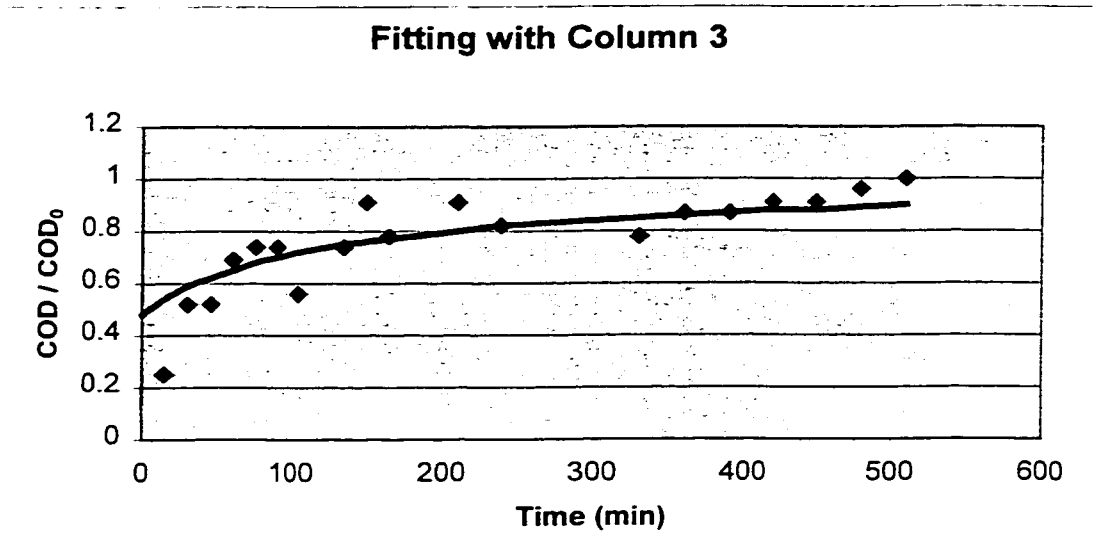

Influent COD: 186.8 mg/L, Hydraulic loading rate: 6.08 m/hr
$k_f = 5.0\times10^{-4}$, $k_m = 4.0\times10^{-7}$, $k_b = 7.0\times10^{-6}$, $f = 0.75$, $n = 0.51$, $K_F = 12.54$

Figure 5-9 Fitting the Model with COD Data of Column 4

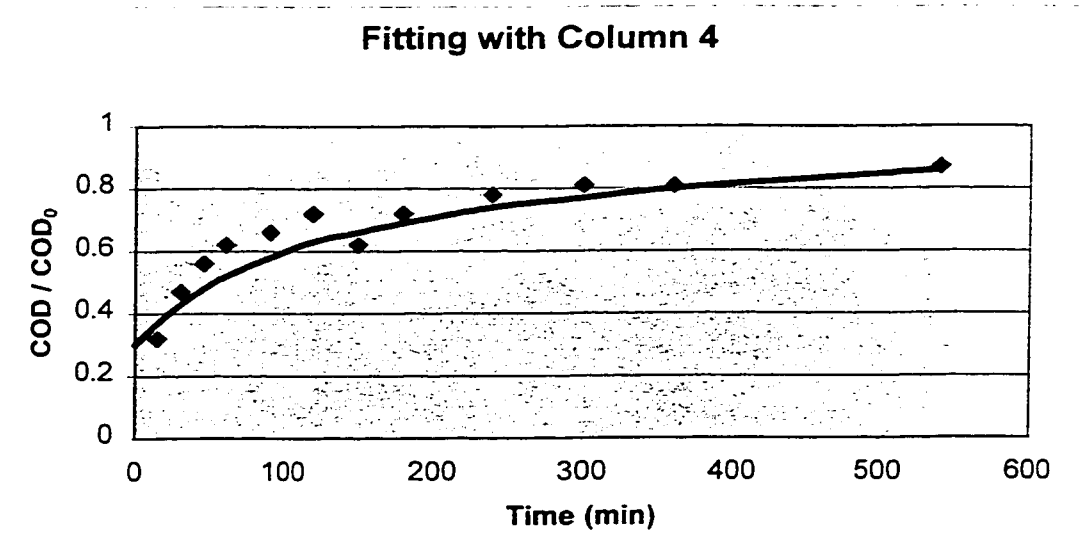

Influent COD: 227.00 mg/L, Hydraulic loading rate: 3.75 m/hr
$k_f = 5.0\times10^{-4}$, $k_m = 4.0\times10^{-7}$, $k_b = 7.0\times10^{-6}$, $f = 0.75$, $n = 0.51$, $K_F = 12.54$

Figure 5-10 Fitting the Model with COD Data of Column 6

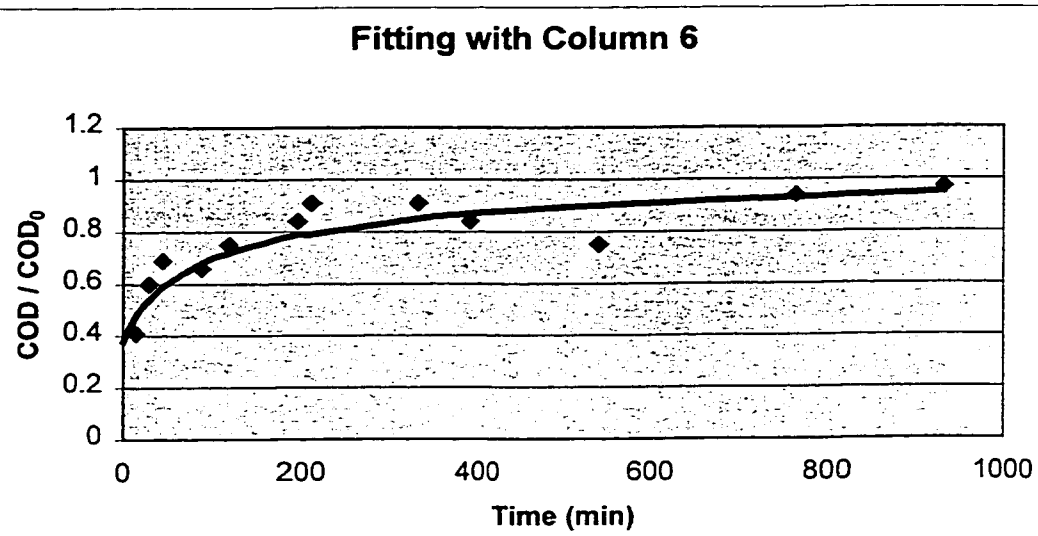

Influent COD: 248.7 mg/L, Hydraulic loading rate: 4.80 m/hr
$k_f = 5.0\times10^{-4}$, $k_m = 4.0\times10^{-7}$, $k_b = 7.0\times10^{-6}$, $f = 0.75$, $n = 0.51$, $K_F = 12.54$

Figure 5-11 Fitting the Model with COD Data of Column 7

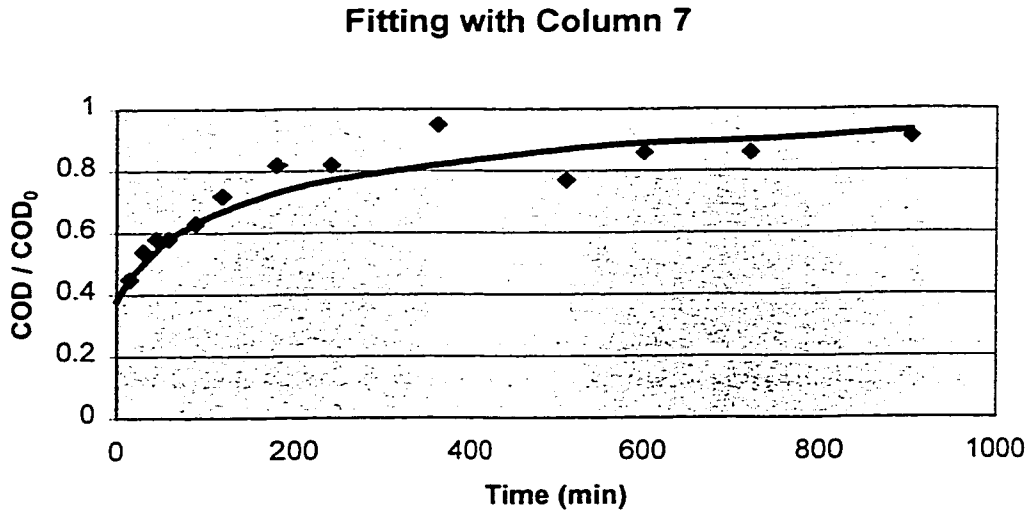

Influent COD: 248.7 mg/L, Hydraulic loading rate: 4.80 m/hr
$k_f = 5.0\times10^{-4}$, $k_m = 4.0\times10^{-7}$, $k_b = 7.0\times10^{-6}$, $f = 0.75$, $n = 0.51$, $K_F = 12.54$

5.5.2 Adsorption of TOC

Unlike the adsorption of COD, the simulation of the adsorption of TOC by the microcolumns was not as successful. Table 5-7 shows the results. The best set of coefficients obtained with isotherm 1 was used to fit microcolumns 1 and 2. The plots of experimental data along with the simulated breakthrough curves are shown in Figures 5-10 and 5-11. It is obvious that the predicted curve do not fit the experimental data well. While trying to lower the value of f and adjust other coefficients accordingly, the solution would not converge. The failure of using microcolumn data to estimate mass transfer coefficients for adsorption of TOC can be attributed to the high exponent values of adsorption isotherms as stated in section 5.5.1.

Table 5-7 Mass Transfer Coefficients for Adsorption of TOC

Coefficient	Isotherm 1	Isotherm 2	Isotherm 3	Isotherm 4
n	0.57	0.51	0.71	0.69
K_F	5.05	6.01	4.37	3.71
k_f	8.5×10^{-4}	not convergent	not convergent	not convergent
k_m	4.0×10^{-6}	not convergent	not convergent	not convergent
k_b	7.0×10^{-6}	not convergent	not convergent	not convergent
f	0.80	not convergent	not convergent	not convergent

The loading analysis was conducted for column 2 to compare the actual TOC loading onto the carbon column to the theoretical maximum loading calculated using the isotherm. The column was run until the effluent TOC reached 93% of the influent TOC. The maxium TOC loadings were calculated for the equilibrium concentration of influent TOC, which was 82.5 mg/L. The mass of carbon in column 2 was 1.80 g, and the time for the effluent TOC to reach 93% of the influent TOC was 510 minutes. See Appendix B for more information regarding column 2. The result was listed in Table 5-7.

Figure 5-12 Fitting the Model with TOC Data of Column 1

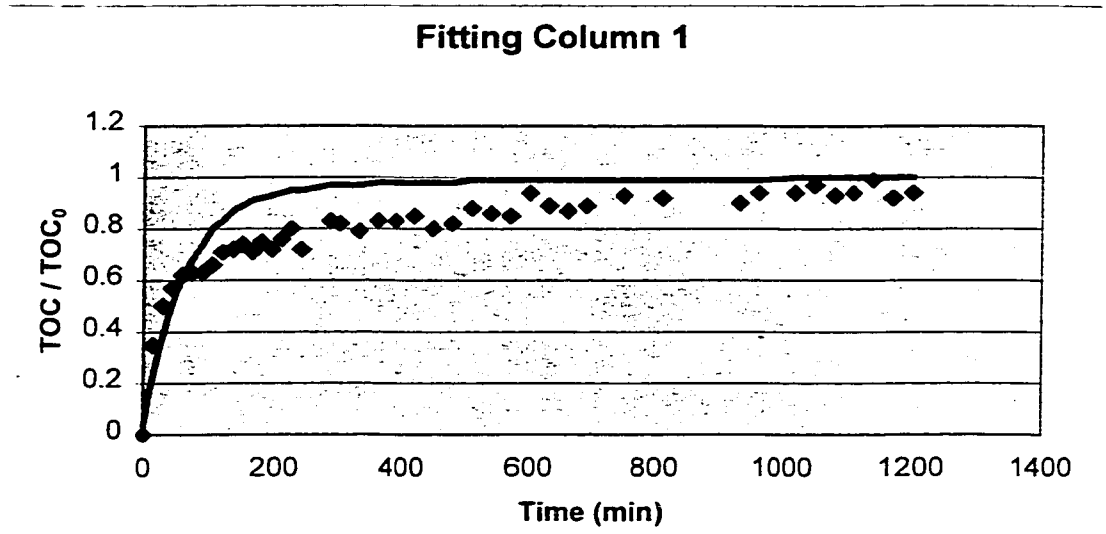

Influent TOC: 80.32 mg/L, Hydraulic loading rate: 3.02 m/hr
$k_f = 8.5\times10^{-4}$, $k_m = 4.0\times10^{-6}$, $k_b = 7.0\times10^{-6}$, $f = 0.85$, $n = 0.57$, $K_F = 5.05$

Figure 5-13 Fitting the Model with TOC Data of Column 2

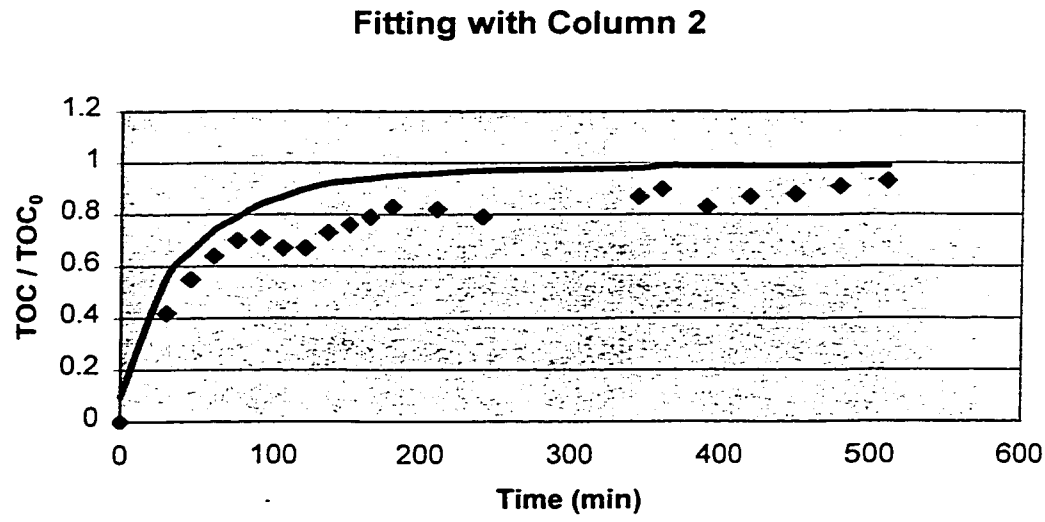

Influent TOC: 82.5 mg/L, Hydraulic loading rate: 3.13 m/hr
$k_f = 8.5\times10^{-4}$, $k_m = 4.0\times10^{-6}$, $k_b = 7.0\times10^{-6}$, $f = 0.85$, $n = 0.57$, $K_F = 5$

Table 5-8 Results of Loading Analysis, TOC

	Experimental	Isotherm 1	Isotherm 2	Isotherm 3	Isotherm 4
Loading (mg TOC)	38.5	112	103	180	140

Since the column was run until the effluent TOC reached 93% of the influent TOC, the actual TOC loading onto the carbon within the column should have been fairly close to the maximum loading calculated from the isotherm. However, it was observed that the actual loading measured from the experimental data was around only 30% of the maximum loading calculated from each of the four isotherms. This is very different from the analysis results obtained for COD.

There are no obvious explanations for this. The lack of agreement between the actual loading and the calculated maximum loadings, however, indicates that the isotherms did not describe the actual adsorptive behavior of the carbon. Therefore, by using these isotherms, the dual rate kinetic model did not describe the actual breakthrough behavior observed in the column experiment.

Chapter 6

PREDICTION AND OPTIMIZATION OF COLUMN PERFORMANCE

When the mass transfer coefficients and the isotherm have been chosen for the dual rate column model, it is possible to use the model to predict the performance of full-scale GAC columns. It was noted that the experiments conducted in this study to obtain the kinetic and equilibrium profiles were prepared in such ways that it was assumed that there was no biological activity taking place in the GAC columns. This is unlikely the case in industrial operations. However, considering the biostabilization provided prior to the column experiment by the AST treatment, the adsorption behavior would constitute the major mechanism in the unit operation. It was thoroughly investigated in the current study, and the microcolumn data were well described by the proposed model. Therefore, the performance prediction based on the model will provide a solid foundation for a feasibility study.

Optimizing the performance of GAC columns means to design the columns in such a way that the following two constraints are met (Droste, 1997):

1) The minimum empty bed contact time (EBCT), which is the total bed volume divided by the volumetric flow rate (V/Q), must be provided.
2) The carbon must be provided at a rate equal to the exhaustion rate R_e.

A complete design of a GAC column system, which is beyond the scope of this study, includes determination of design parameters such as the dimension of a column, number of columns, connection methods, i.e., series or parallel, and hydraulic factors. All these parameters need to be determined based on design variables EBCT and R_e along with the

economic factors. The EBCT will determine the amount of carbon required in a carbon column system. Previous studies showed that both the construction and operating costs of a GAC column system were related to the EBCT (Narbaitz and Benedek, 1981). Therefore, the estimation of the minimum EBCT and R_e is the baseline of the system design. The study carried out here applied the dual rate model to the traditional operating line method that was used to find the EBCT and R_e. The carbon usage rate for a fixed-bed GAC column system obtained here was also compared to the one obtained for a PACT™ system for a similar wastewater.

6.1 Operating Line Method for Process Design

Several design methodologies can be used to obtain the two design variables EBCT and R_e (Droste. 1997). The operating line method defined by Erkine and Schuliger (1971) was used in this study. An operating line is a plot of EBCT versus R_e for a desired breakthrough concentration at a certain hydraulic loading rate. The points on the operating line represent the possible values of EBCT and R_e for a specific GAC and wastewater system. An economic evaluation of the costs associated with different combinations of EBCT and R_e on the line can be performed to find the least cost design.

An operating line is constructed by analyzing the breakthrough curves obtained for different column lengths at a certain hydraulic condition, i.e., the hydraulic loading rate. Traditionally, a set of pilot-scale column experiments is required to obtain the needed breakthrough curves. It can be carried out using a set of columns of different lengths, or a column with sampling ports at different depths. The choices of the column lengths should include those on the order of the eventual design. Figure 6-1 is an example of a set of breakthrough curves, in the format of the fractional concentration versus time, obtained from such experiments. If the breakthrough concentration is defined as 0.28 C_0, then the time at which the dotted line

crosses a breakthrough curve defines the exhaustion time, or the regeneration time, for the column length that the breakthrough curve represents. The service time of a column is the regeneration time less of the filling time for the column. In practice, the filling time is generally ignored.

Figure 6-1 Breakthrough Curves for Different Column Length (Droste, 1997)

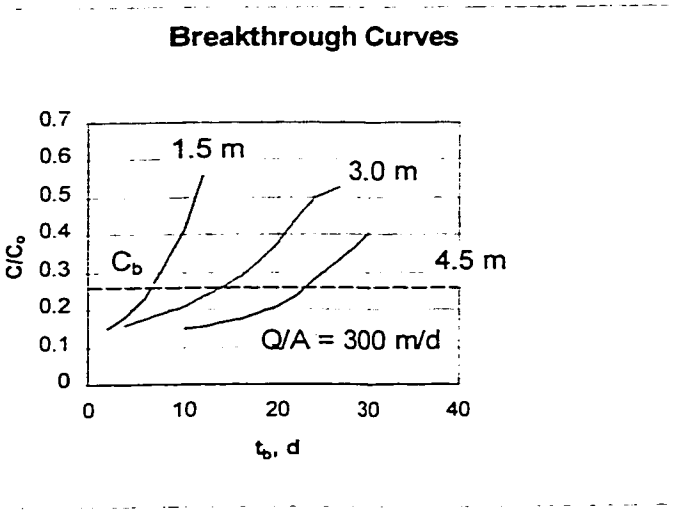

Figure 6-2 Operating Line and Theoretical Minimum EBCT (Droste, 1997)

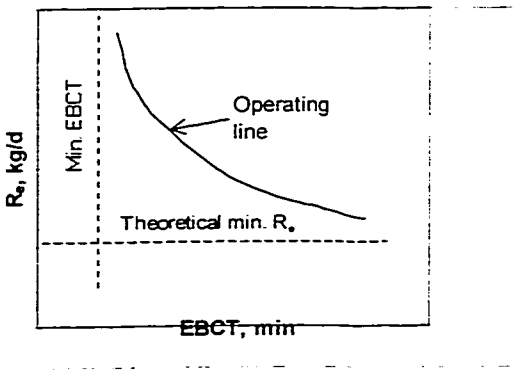

When the regeneration time of a column t_b is determined, the carbon exhaustion rate for the column can be calculated based on the following equation:

$$R_e = \frac{\rho_p \times A \times D}{t_b \times Q} = \frac{\rho_p \times D}{t_b \times HLR} \qquad (6\text{-}1)$$

Where:

ρ_p is the packed density of the carbon, kg/m^3

A is the cross sectional area of the column, m^2

D is the length of the column, m

Q is the volumetric loading rate, m^3/d

HLR is the hydraulic loading rate, m/h

Meanwhile, the EBCT can be determined based on the following equation:

$$EBCT = \frac{A \times D}{Q} = \frac{D}{HLR} \qquad (6\text{-}2)$$

Figure 6-2 shows the operating line obtained by plotting the R_e against EBCT for each column. The designer can choose any point on the operating line for a proper design. A more comprehensive analysis can be performed by applying different hydraulic loading rates and performing the economic analysis for each operating line.

The dotted line underneath the operating line indicates the theoretical minimum exhaustion rate $R_{e,mim}$. The $R_{e,mim}$ is based on the equilibrium isotherm for the carbon and the wastewater. The rate at which carbon is being exhausted is equal to the rate at which adsorbate is being removed.

$$R_{e,\min} q_\infty = Q(c - c_r) \qquad (6\text{-}3)$$

Therefore:

$$R_{e,\min} = \frac{Q(c - c_r)}{q_\infty} \qquad (6\text{-}4)$$

Where:

c_r is the non-adsorbable matter

q_∞ is the solids phase equilibrium concentration at $c_0 - c_r$

6.2 Application of the Dual Rate Model

Instead of conducting pilot-scale experiments, mathematically simulated columns, using the QDF dual rate model discussed in Chapter 5, were adopted to find the breakthrough curves required by the operating line method. As stated in Section 5.4.1, the computer program PRECOS solved the dual rate model and produced breakthrough curves based on the input column configuration and operating information. The R_e and EBCT for each simulated column were also calculated by PRECOS. The waste strength of the wastewater was measured in the COD.

Table 6-1 lists the input of the computer program PRECOS. The equilibrium and kinetic parameters involved in the model were obtained based on the experiments and analysis described in Chapters 4 and 5. The column configuration and operating conditions were chosen based on the typical industrial applications (Eckenfelder, 1981). The influent concentration was the typical value of the sample wastewater used in this study.
The breakthrough curves were obtained at different column lengths for each of the three hydraulic loading rates: 6.0, 8.0, and 12.5 m/hr. Figures 6-3, 6-4, and 6-5 show the output breakthrough curves and the operating lines obtained accordingly. Three breakthrough levels were examined for each column length: $COD/COD_0 = 0.1$, 0.2, and 0.5. The dotted line under operating lines in each figure indicated the theoretical minimum carbon exhaustion rate calculated based on adsorbable fraction of the influent COD (200 mg/L), using equation 6-4.

Table 6-1 Input of the Computer Model

Input item	Value
Isotherm	$q = 12.54c_e^{0.51}$
k_f	5.0×10^{-4}
k_m	4.0×10^{-7}
k_b	7.0×10^{-6}
f	0.75
Influent COD (COD_0)	230 mg/L
Volumetric loading rate	9600 m^3/d
Hydraulic loading rate	6.0 – 12.5 m/hr
Column length	40 – 600 cm
Carbon bed packed density	500 kg/m^3

Tables 6-2, 6-3, and 6-4 list the EBCT and R_e for three breakthrough levels for each hydraulic loading rate, calculated by PRECOS. Where *CL* is the column length in cm. The column influent listed in Table 6-1 was the total COD in the column influent. As discussed in Section 5.3.4, the dual rate model analyzed the adsorption process based on the adsorbable fraction of the column influent and effluent. Therefore, it was assumed that the pretreatment AST system had a SRT of 6 days and the non-adsorbable COD in the column influent was 30 mg/L. While solving the dual rate model, the input value of the column influent concentration was the total COD less the non-adsorbable portion. However, the non-adsorbable portion was added to the predicted effluent COD before the breakthrough curves were plotted. The carbon exhaustion rate was calculated for virgin carbon based on the breakthrough of total COD.

Figure 6-3 Predicted Breakthrough Curves and Operating Line HLR=12.5 m/hr

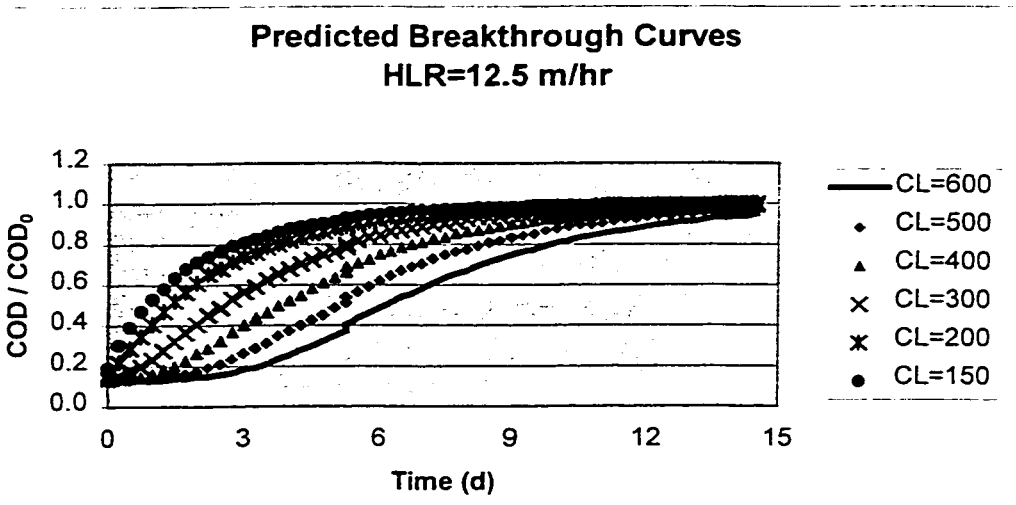

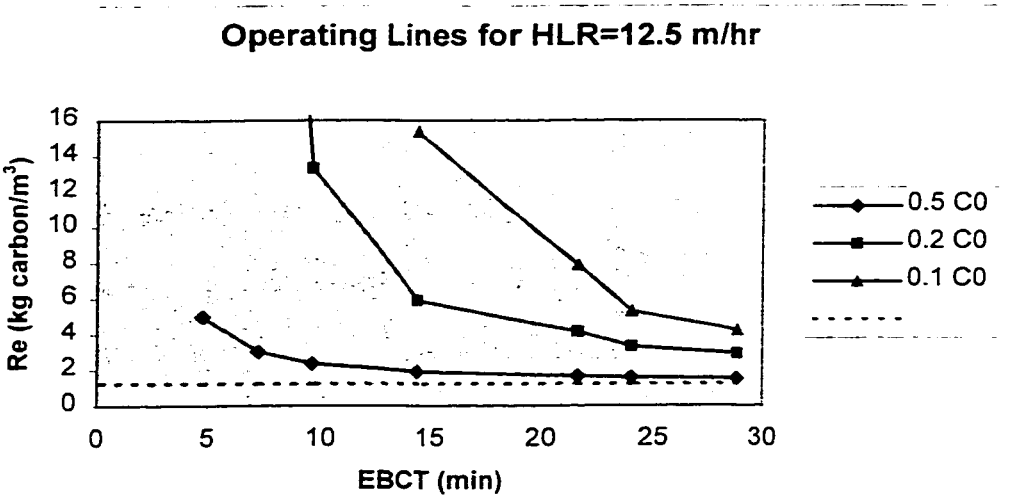

Figure 6-4 Predicted Breakthrough Curves and Operating Line
HLR=8.0 m/hr

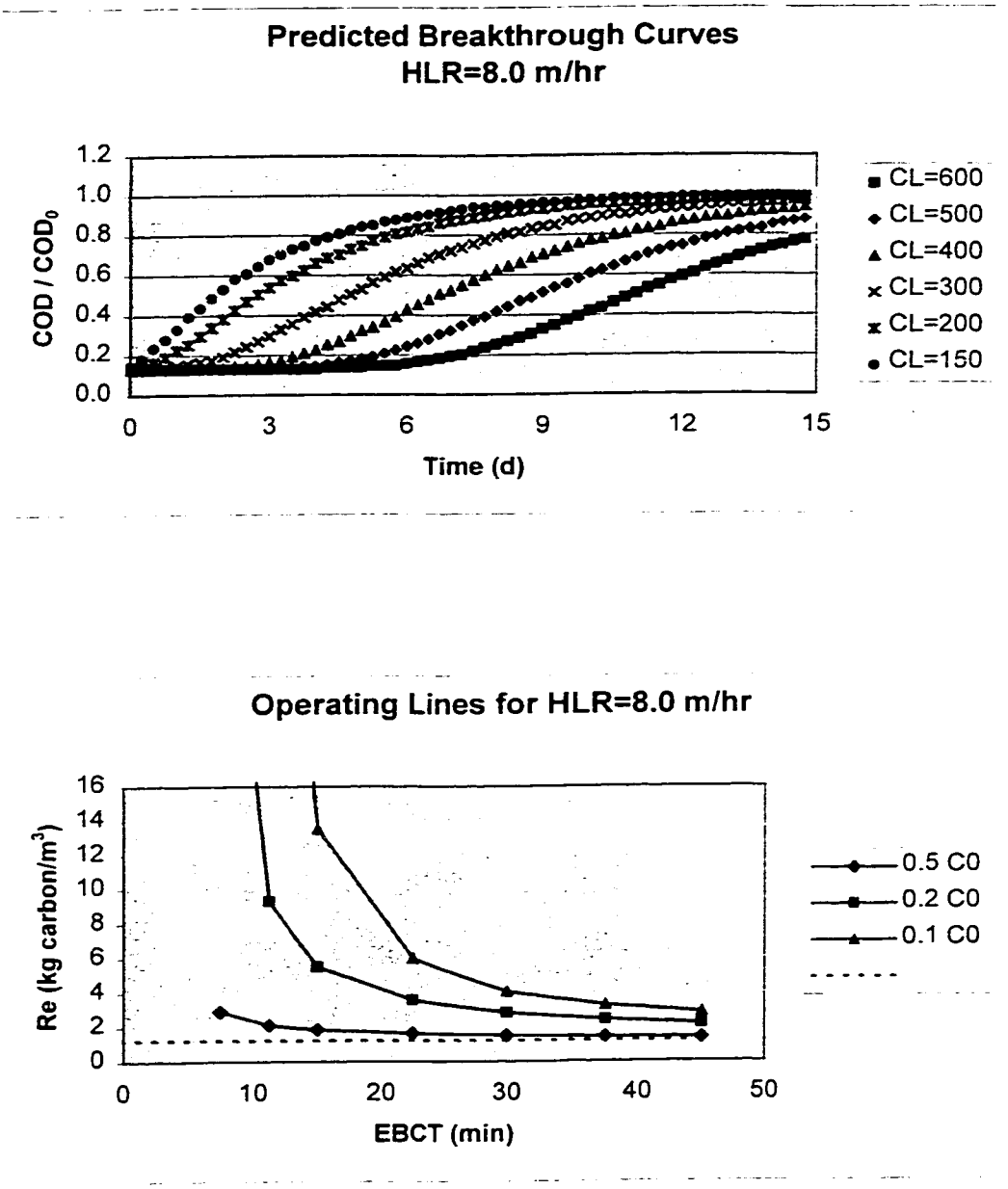

Figure 6-5 Predicted Breakthrough Curves and Operating Line HLR=6.0 m/hr

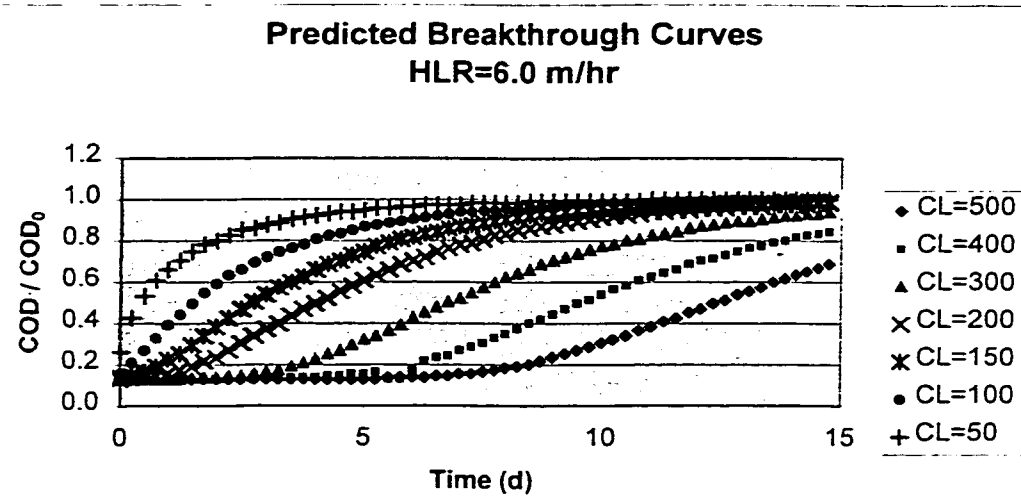

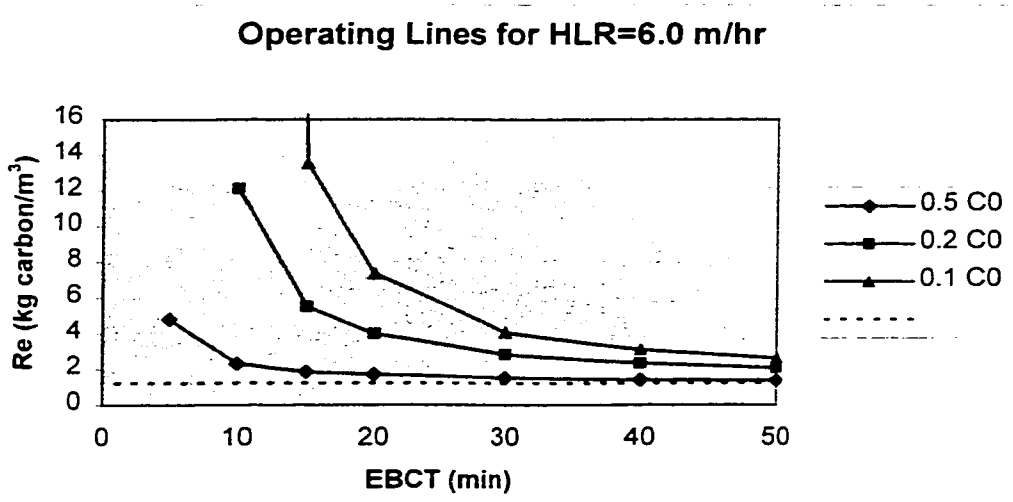

Table 6-2 Carbon Exhaustion Rate and EBCT, HLR=12.5 m/hr

Column length (m)	6.0	5.0	4.0	3.0	2.0	1.5	1.0
EBCT (min)	28.8	24.0	21.6	14.4	9.6	7.2	4.8
R_e (kg/m^3) for C/C_0=0.1	4.23	5.30	7.88	15.35	N/A	N/A	N/A
R_e (kg/m^3) for C/C_0=0.2	2.92	3.32	4.16	5.90	13.31	46.93	N/A
R_e (kg/m^3) for C/C_0=0.5	1.52	1.60	1.67	1.92	2.38	3.05	4.98

Table 6-3 Carbon Exhaustion Rate and EBCT, HLR=8.0 m/hr

Column length (m)	6.0	5.0	4.0	3.0	2.0	1.5	1.0
EBCT (min)	45.0	37.5	30.0	22.5	15.0	11.25	7.5
R_e (kg/m^3) for C/C_0=0.1	2.86	3.28	4.06	6.00	13.52	44.0	N/A
R_e (kg/m^3) for C/C_0=0.2	2.20	2.44	2.84	3.58	5.51	9.32	33.69
R_e (kg/m^3) for C/C_0=0.5	1.40	1.44	1.52	1.65	1.87	2.13	2.91

Table 6-4 Carbon Exhaustion Rate and EBCT, HLR=6.0 m/hr

Column length (m)	5.0	4.0	3.0	2.0	1.5	1.0	0.5
EBCT (min)	50.0	40.0	30.0	20.0	15.0	10.0	5.0
R_e (kg/m^3) for C/C_0=0.1	2.62	3.10	4.06	7.34	13.52	214.9	N/A
R_e (kg/m^3) for C/C_0=0.2	2.08	2.34	2.83	3.99	5.51	12.11	N/A
R_e (kg/m^3) for C/C_0=0.5	1.38	1.42	1.52	1.71	1.87	2.32	4.82

6.3 Results and Analysis

It is shown in Figures 6-3 to 6-5 that the predicted breakthrough curves do not begin at $COD/COD_0 = 0$. This can be attributed to the non-adsorbable portion of the influent COD. The predicted breakthrough curves for each hydraulic loading rate show a trend of trailing after the columns breakthrough 50% of the influent COD. This indicates that the adsorption zone within a column will be long (Section 2.3.2).

It has been observed from the operating lines in Figures 6-3 and 6-5 that the carbon usage rate is sensitive to the change of EBCT when the EBCT is short. The carbon usage rate will be greatly decreased by a small increase in EBCT at low EBCT level. At the higher EBCT range, for example, when EBCT is greater than 20 minutes at breakthrough of $0.5COD_0$ for each hydraulic loading rate, the carbon usage rate changes very little. For a certain hydraulic loading rate, an increase in EBCT will cause an increase in the length of the column. While an increase in EBCT will generally lower the operating cost of a column system, an increase in column length will increase the construction cost (Narbaitz and Benedek, 1981). Therefore, a proper combination of EBCT and carbon usage rate can only be determined after economic analysis.

At a certain hydraulic loading rate, the lower the desired effluent concentration is, the higher the carbon usage rate is for a certain EBCT value. When the breakthrough concentration is set to be 50% of influent COD, the carbon usage rate was very close to the theoretical minimum exhaustion rate of the carbon when the EBCT is greater than 20 minutes. If the hydraulic loading rate is 8 m/hr, for EBCT of 30 minutes and a breakthrough level of $0.5COD_0$, the carbon usage rate is 1.52 kg/m^3 wastewater, compared to the theoretical value of 1.07 kg/m^3, which was calculated based on Equation 6–4. The

corresponding column length will be 4.0 m, and the regeneration time of the system is 6.25 days.

For a certain EBCT and breakthrough level, the hydraulic loading rate of the column system will affect the carbon usage rate, especially at the lower EBCT range. The higher the hydraulic loading rate, the higher the carbon usage rate.

6.4 Fixed-bed GAC Column System and PACT™

The performance of the fixed-bed GAC column system in terms of COD removal and the carbon usage rate can be predicted based on the findings in Section 6.2 and Section 3.3. It should be noticed that the calculation is based on soluble COD. For a GAC column system with influent COD of 230 mg/L (30 mg/L of it is non-adsorbable), hydraulic loading rate of 8 m/hr, and EBCT of 30 minutes, when the column system is considered to breakthrough at 50% of influent COD, the carbon usage rate is 1.52 kg/m^3. If the COD removal in the AST pretreatment process is 60% (SRT = 6 days, HRT = 10 hours), then the overall COD removal is 80%. Using the GAC column system as the post treatment process, the overall COD removal will be increased to 80% from 60% obtained in the AST system.

Assume the PACT™ system is used in the treatment of the same wastewater, and the same isotherm applied. Suppose the PACT™ system have the same influent COD, and the COD removal attributed to the conventional AST mechanism is 60% of the influent COD. The theoretical carbon dosage required for an overall COD removal of 80% can be calculated by using the isotherm. The resulting carbon dosage will be 0.96 kg/m^3. The detailed calculation can be found in Appendix C.

In a study conducted with a PACT™ system (Graham, 1996), Calgon™ powdered activated carbon (PAC) was added to the traditional AST system in order to improve the treatment of a similar pulp and paper mill wastewater. When the PAC dosage was 1.0 g/L,

which was equivalent to a carbon usage rate of 1.0 kg/m^3, the COD removal was 78.4 to 88.1%, compared to the COD removal of 62.5% in a reference AST system for the same feed. The SRT and HRT of both the PACT™ and AST systems were 5 days and 8 hours, respectively (Graham, 1996).

Previous studies (Schultz, Keinath, 1984) speculated that the enhanced treatment in the PACT™ system, compared with the conventional AST process, could be attributed to the enhanced bioactivity and metabolic end product adsorption occurred in the PACT™ system. The enhanced bioactivity was the ability of PAC to increase the biological assimilation of organics by an activated sludge system. It was not directly related to the adsorptive capacity of PAC. However, it could improve the overall COD removal in the PACT™ system than would have by using column adsorption system as the post treatment process of the AST system. Since metabolic end product adsorption could occur in both PACT™ and AST followed by GAC column systems, further study is needed to identify its effect on COD removal in the two systems.

Although the PACT™ system could have the above advantage, the fact that the PACT™ system appears to be more effective seems to contradict the basic adsorption theory. A direct comparison between the two systems based on experiments is needed. As stated in Section 6.3, the predicted carbon usage rate in the GAC column was 1.52 kg/m^3 while the theoretical maximum carbon usage rate was 1.07 kg/m^3. This indicates that the column was not very efficient in terms of the carbon usage. One reason that could cause this was that the microcolumn experiment was not efficient. The inefficiency of small scale columns was also found in previous studies (Hand et. al., 1989). Since the coefficients of the dual rate model were determined based on the microcolumn experiment data, the predicted capacity of a full-scale column could be under estimated. It is also noticed that the comparison conducted in

this study was based on 50% COD removal in the adsorption process. A sensitivity study in terms of the carbon usage rate at various percentages of COD removal is needed.

Chapter 7

CONCLUSIONS AND RECOMMENDATIONS FOR FUTURE STUDY

The QDF dual rate column model has proved to be able to describe the adsorption process of GAC column system for soluble COD in the treatment of biotreated pulp and paper mill wastewater. The computer program PRECOS was used to solve the model. Microcolumn experiments were performed. The mass transfer coefficients involved in the model were estimated by fitting the model with microcolumn experimental data.

Isotherm studies were carried out for both AST effluents and the feed of AST systems to determine the equilibrium relationship between the GAC and the wastewater. It was found that the adsorptive capacity of GAC for COD in AST effluents was substantially higher than that for COD in the feed of AST systems. This was because that the metabolic end product in the AST effluents were more adsorbable than the original components in the feed of AST systems. Laboratory scale AST experiments were conducted to remove the biodegradable contents in the wastewater. At SRT=10 d and HRT=12 hr, COD removals were 71–79%; at SRT=10 d and HRT =6 hr, COD removals were 46–70%; and at SRT=5 d and HRT=6 hr, COD removals were 48–60%. At the three operating conditions, the TOC removals were 57–66, 42–69, and 41–59% respectively.

The QDF dual rate column model was used to simulate the performance of GAC column system over a wide range of operating conditions. It provided sufficient information for system design using the operating line method. When the performance of a GAC column system as predicted, the overall COD removal of the combination of the AST system and the GAC column system was compared with that of a PACT™ system. It was found that for an

overall COD removal of 80%, the carbon usage rate of the PACT™ system was 30% lower than that of the GAC column system. The better performance of the PACT™ system seems to contradict the basic adsorption theory. One possibility was that the actual efficiency in terms of carbon usage of a full-scale GAC column system could be higher than predicted based on the microcolumn experiment. A direct comparison between the two systems based on experiments is needed. A sensitivity study in terms of the carbon usage rate at various percentages of COD removal is also needed.

Since this study was intended to evaluate the adsorption process in an ideal environment, biological activities were eliminated from the GAC adsorption processes. In the future study, the biological activity should be considered in the process modeling because it will directly affect the adsorptive capacity of the carbon. The activated carbon based biological fluidized column can also be studied for the treatment of pulp and paper mill effluents.

APPENDIX A ISOTHERM EXPERIMENTAL DATA

Isotherm 1

Sample pretreatment: AST effluent, SRT=10 d, HRT=12 h. Filtered with 0.45 μm filters.
Initial COD: 190.41 mg/L
Initial TOC: 95.67 mg/L
Initial pH: 7.16

Bottle No.	Carbon dosage (mg/L)	COD (mg/L)	Corrected COD[1] (mg/L)	Solid phase COD[2] (mg/g carbon)	TOC (mg/L)	Solid phase TOC (mg/g carbon)
1	0	190	175		95.67	
2	200	160	145	148	82.8	64.35
3	400	146	131	109	71.57	60.25
4	800	117	102	91	58.63	46.30
5	1600	67	52	76	35.95	37.33
6	2000	59	44	65	28.32	33.68
7	4000	19	4	42	11.79	20.97
8	20000	15	1	8	5.18	4.52
9	Control-0	0			0.748	
10	Control-0	0			0.846	

[1]: Corrected liquid phase COD obtained by subtracting the residual from the raw value.
[2]: Calculated based on the corrected liquid phase COD.

Isotherm 2

Sample pretreatment: AST effluent, SRT=10 d, HRT=12 h. Filtered with 0.45 μm filters.
Initial COD: 262.5 mg/L
Initial TOC: 94.78 mg/L
Initial pH: 7.00

Bottle No.	Carbon dosage (mg/L)	COD (mg/L)	Corrected COD[1] (mg/L)	Solid phase COD[2] (mg/g carbon)	TOC (mg/L)	Solid phase TOC (mg/g carbon)
1	0	232	222		94.78	
2	200	187	177	225	79.67	75.55
3	400	157	147	187	75.57	48.03
4	800	93	83	173	53.97	51.01
5	1200	71	61	134	42.76	43.35
6	1600	67	57	103	32.79	38.74
7	2000	45	35	93	31.69	31.55
8	3000	22	12	70	18.58	25.40
9	4000	18	8	53	14.04	20.19
10	Control-0				0.53	

[1]: Corrected liquid phase COD obtained by subtracting the residual from the raw value.
[2]: Calculated based on the corrected liquid phase COD.

Isotherm 3

Sample pretreatment: AST effluent, SRT=10 d, HRT=6 h. Filtered with 0.45 μm filters.
Initial COD: 196.00 mg/L
Initial TOC: 71.50 mg/L
Initial pH: 7.10

Bottle No.	Carbon dosage (mg/L)	COD (mg/L)	Corrected COD[1] (mg/L)	Solid phase COD[2] (mg/g carbon)	TOC (mg/L)	Solid phase TOC (mg/g carbon)
1	0	196	176		71.50	
2	200	145	125	252	52.94	92.80
3	400	123	103	181	43.62	69.70
4	800	94	74	126	29.63	52.34
5	1200	72	52	103	25.20	38.58
6	1600	58	38	86	19.48	32.51
7	2000	43	23	76	14.40	28.55
8	3000	36	16	53	8.13	21.12
9	4000	26	6	42	6.77	
10	Control-0				0.89	

[1]: Corrected liquid phase COD obtained by subtracting the residual from the raw value.
[2]: Calculated based on the corrected liquid phase COD.

Isotherm 4

Sample pretreatment: AST effluent, SRT=5 d, HRT=6 h. Filtered with 0.45 μm filters.
Initial COD: 277.50 mg/L
Initial TOC: 107.20 mg/L
Initial pH: 7.00

Bottle No.	Carbon dosage (mg/L)	COD (mg/L)	Corrected COD[1] (mg/L)	Solid phase COD[2] (mg/g carbon)	TOC (mg/L)	Solid phase TOC (mg/g carbon)
1	0	277	237		105.20	
2	200	240	200	187	87.78	87.10
3	400	210	170	168	73.91	78.23
4	800	165	125	140	58.31	58.61
5	1200	135	95	118	47.34	48.22
6	1600	105	65	107	36.46	42.96
7	2000	90	50	93	30.78	37.21
8	3000	67	27	70	20.93	28.09
9	4000	60	20	54	12.09	23.28
10	Control-0				0.50	

[1]: Corrected liquid phase COD obtained by subtracting the residual from the raw value.
[2]: Calculated based on the corrected liquid phase COD.

Isotherm 5

Sample pretreatment: AST feed. Filtered with 0.45 μm filters.
Initial COD: 566.67 mg/L
Initial TOC: N/A
Initial pH: 7.22

Bottle No.	Carbon dosage (mg/L)	COD (mg/L)	Corrected COD[1] (mg/L)	Solid phase COD[2] (mg/g carbon)
1	0	546	426	
2	200	468	348	390
3	400	458	338	219
4	800	400	280	182
5	1600	333	213	132
6	2000	298	178	123
7	4000	228	108	79
8	20000	128	8	20
9	Control-0	0		
10				

[1]: Corrected liquid phase COD obtained by subtracting the residual from the raw value.
[2]: Calculated based on the corrected liquid phase COD.

Isotherm 6

Sample pretreatment: AST feed. Filtered with 0.45 μm filters.
Initial COD: 679.88 mg/L
Initial TOC: 256.00 mg/L
Initial pH: 7.10

Bottle No.	Carbon dosage (mg/L)	COD (mg/L)	Corrected COD[1] (mg/L)	Solid phase COD[2] (mg/g carbon)	TOC (mg/L)	Corrected TOC[3] (mg/L)	Solid phase TOC[4] (mg/g carbon)
1	0	614	424		213.20	133.20	
2	50	559	369	1,114	203.25	123.25	199.00
3	200	515	325	498	191.49	111.49	108.55
4	400	446	256	420	166.25	86.25	117.38
5	800	394	204	275	150.02	70.02	78.98
6	1,200	37	189	195	128.55	48.55	70.54
7	2,000	305	115	154	117.35	37.35	47.93
8	4,000	260	70	88	93.21	13.21	30.00
9	6,000	227	37	64	83.49	3.49	21.62
10	0	4			0.96		

[1] [2]: Corrected liquid phase COD obtained by subtracting the residual from the raw value.
[3] [4]: Calculated based on the corrected liquid phase COD.

APPENDIX B Microcolumn Experimental Data

Experimental Conditions and Parameters for Column 1, 2 and 3

Item	Symbol	Column 1	Column 2	Column 3
Carbon particle radium (cm)	R	0.035		
Carbon weight (g)	W	2.506	1.803	1.802
Column cross section radius (cm)	CR	0.50		
Column length (cm)	CL	7.20	5.50	5.50
Packed bed density (g/cm^3)	RHOB	0.44	0.41	0.41
Apparent particle density (g/ cm3)	RHOC	0.75		
Volumetric flow rate (ml/s)	V	0.0658	0.068	0.133
Hydraulic loading rate (m/hr)	HLR	3.02	3.13	6.08
Initial COD (mg/L)	COD_0	228.5	186.8	
Initial TOC (mg/L)	TOC_0	80.32	82.5	
pH	pH	7.35	7.35	
Pretreatment conditions	Pretreated by AST process. SRT=5 d, HRT=6 h.			

Effluent Data for Column 1

t (min)	COD (mg/L)	CODcr[1] (mg/L)	COD/ COD_0[2]	TOC (mg/L)	TOC/ TOC_0	t (min)	COD (mg/L)	CODcr[3] (mg/L)	COD/ COD_0[4]	TOC (mg/L)	TOC/ TOC_0
0	228	178	0	80.32		420	150	100	0.56	68.22	0.85
15	50	7	0.04	28.49	0.35	450	143	93	0.52	64.01	0.80
30	100	50	0.28	39.9	0.50	480				65.89	0.82
45	93	43	0.24	45.74	0.57	510	143	93	0.52	70.50	0.88
60	100	50	0.28	49.9	0.62	540	157	107	0.60	68.88	0.86
75				50.53	0.63	570	157	107	0.60	68.30	0.85
90	114	64	0.36	50.72	0.63	600	150	100	0.56	75.80	0.94
105	114	64	0.36	53.31	0.66	630	186	136	0.76	71.18	0.89
120	121	71	0.4	57.15	0.71	660	186	136	0.76	69.97	0.87
135	114	64	0.36	57.73	0.72	690	193	143	0.80	71.09	0.89
150	121	71	0.4	59.09	0.74	750	193	143	0.80	74.46	0.93
165	121	71	0.4	57.28	0.71	810	186	136	0.76	74.27	0.92
180	114	64	0.36	60.24	0.75	930	186	136	0.76	72.46	0.90
195	128	78	0.44	57.69	0.72	960	200	150	0.84	75.70	0.94
210	136	86	0.48	60.93	0.76	1020	193	143	0.80	75.59	0.94
225	136	86	0.48	64.13	0.80	1050	193	143	0.80	77.88	0.97
240	128	78	0.44	58.02	0.72	1080	207	157	0.88	74.86	0.93
285	143	93	0.52	67.06	0.83	1110	193	143	0.80	75.87	0.94
300	100	50	0.28	66.11	0.82	1140	200	150	0.80	79.62	0.99
330	128	78	0.44	63.36	0.79	1170	207	157	0.88	73.63	0.92
360	136	86	0.48	67.00	0.83	1200				75.88	0.94
390	143	93	0.52	66.27	0.83						

[1] [3]: Effluent COD corrected by subtracting the residual from the raw effluent COD.

[2] [4]: Calculated based on the corrected data.

Effluent Data for Column 2

t (min)	COD (mg/L)	CODcr[1] (mg/L)	COD/ COD_0[2]	TOC (mg/L)	TOC/ TOC_0
0		151		82.5	
15					
30	80	45	0.30	34.95	0.42
45	93	58	0.38	45.57	0.55
60	93	58	0.38	52.74	0.64
75	120	85	0.56	57.56	0.70
90	126	91	0.60	58.95	0.71
105	120	85	0.56	55.53	0.67
120				55.14	0.67
135	113	78	0.52	60.42	0.73
150	126	91	0.60	62.54	0.76
165	126	91	0.60	64.83	0.79
180	133	98	0.65	68.23	0.83
210	126	91	0.60	67.61	0.82
240	146	111	0.74	65.01	0.79
330	146	111	0.74	71.79	0.87
360	153	118	0.78	73.85	0.90
390	146	111	0.74	68.80	0.83
420	160	125	0.82	72.18	0.87
450	14	111	0.74	72.40	0.88
480	146	111	0.74	75.28	0.91
510	146	111	0.74	76.56	0.93

[1]: Effluent COD corrected by subtracting the residual from the raw effluent COD.
[2]: Calculated based on the corrected data.

Effluent Data for Column 3

t (min)	COD (mg/L)	CODcr[1] (mg/L)	COD/ COD_0[2]	TOC (mg/L)	TOC/ TOC_0
0	186	151		82.5	
15	73	38	0.25		
30	113	78	0.52	34.95	0.42
45	113	78	0.52	45.57	0.55
60	140	105	0.69	52.74	0.64
75	146	111	0.74	57.56	0.70
90	146	111	0.74	58.95	0.71
105	120	85	0.56	55.53	0.67
120				55.14	0.67
135	146	111	0.74	60.42	0.73
150	173	138	0.91	62.54	0.76
165	153	118	0.78	64.83	0.79
180				68.23	0.83
210	173	138	0.91	67.61	0.82
240	160	125	0.82	65.01	0.79
330	153	118	0.78	71.79	0.87
360	166	131	0.87	73.85	0.90
390	166	131	0.87	68.80	0.83
420	173	13	0.91	72.18	0.87
450	173	138	0.91	72.40	0.88
480	180	145	0.96	75.28	0.91
510	186	151	1.00	76.56	0.93

[1]: Effluent COD corrected by subtracting the residual from the raw effluent COD.
[2]: Calculated based on the corrected data.

Experimental Conditions and Parameters for Column 4, 5[1], and 6

Item	Symbol	Column 4	Column 5	Column 6
Carbon particle radium (cm)	R	0.035		
Carbon weight (g)	W	1.801	1.800	1.802
Column cross section radius (cm)	CR	0.50		
Column length (cm)	CL	5.50	5.50	5.50
Packed bed density (g/cm^3)	RHOB	0.42	0.42	0.42
Apparent particle density (g/ cm3)	RHOC	0.75		
Volumetric flow rate (ml/s)	V	0.082	0.082	0.105
Hydraulic loading rate (m/hr)	HLR	3.75	3.75	4.80
Initial COD (mg/L)	COD_0	227.00	N/A	248.70
Initial TOC (mg/L)	TOC_0	88.00	N/A	85.70
pH	pH	7.00	N/A	7.50
Pretreatment conditions	Pretreated by AST process. SRT=5 d, HRT=6 h.			

[1]: Column 5 was operated in series with column 4.

Effluent Data for Column 4

t (min)	COD (mg/L)	CODcrl[1] (mg/L)	COD/ COD_0[2]	TOC (mg/L)	TOC/ TOC_0
0	227	207		88.00	
15	86	66	0.32		
30	116	96	0.47	43.34	0.49
45	136	116	0.56	53.95	0.61
60	149	129	0.62	55.32	0.63
75				59.52	0.68
90	155	135	0.66	57.79	0.66
105				60.27	0.68
120	168	148	0.72	62.25	0.71
135				63.64	0.72
150	149	129	0.62	66.66	0.76
165				69.23	0.79
180	168	148	0.72	63.87	0.73
210				70.56	0.80
240	181	161	0.78	70.63	0.80
270				76.31	0.87
300	188	168	0.81	74.31	0.84
360	188	168	0.81	76.71	0.87
450				79.79	0.91
540	201	181	0.87	75.86	0.86

[1]: Effluent COD corrected by subtracting the residual from the raw effluent COD.
[2]: Calculated based on the corrected data.

Effluent Data for Column 5 [1]

t (min)	COD (mg/L)	CODcr[2] (mg/L)	COD/ COD_0[3]	TOC (mg/L)	TOC/ TOC_0
0	227	207		88.00	
15	25	5	0.03		
30				21.39	0.24
45	64	44	0.22	22.87	0.26
60	71	51	0.25	28.73	0.33
75				32.15	0.37
90	71	51	0.25	38.58	0.44
105				39.20	0.45
120					
135				45.50	0.52
150	116	96	0.47	50.12	0.57
165				48.75	0.55
180	129	109	0.53	52.73	0.60
210					
240	129	109	0.53	56.00	0.64
270				55.35	0.63
300	149	129	0.62	59.40	0.68
360	155	135	0.66	63.33	0.72
450				68.02	0.77
540	168	148	0.72	64.66	0.73

[1]: Column 5 was operated in series with column 4.
[2]: Effluent COD corrected by subtracting the residual from the raw effluent COD.
[3]: Calculated based on the corrected data.

Effluent Data for Column 6

t (min)	COD (mg/L)	CODcr[1] (mg/L)	COD/ COD_0[2]	TOC (mg/L)	TOC/ TOC_0
0	278	248		85.7	
10	131	101	0.41	28.03	0.33
30	178	148	0.60	48.16	0.56
45	201	171	0.69	57.13	0.67
90	193	163	0.66	56.99	0.66
120	216	186	0.75	66.28	0.77
180	240	210	0.84	71.05	0.83
210	255	225	0.91	71.9	0.84
330	255	225	0.91	75.79	0.88
390	240	210	0.84	77.27	0.90
540	216	186	0.75	81.09	0.95
750	263	233	0.94	82.24	0.96
930	271	241	0.97	82.17	0.96

[1]: Effluent COD corrected by subtracting the residual from the raw effluent COD.
[2]: Calculated based on the corrected data.

Experimental Conditions and Parameters for Column 7

Item	Symbol	Column 7
Carbon particle radium (cm)	R	0.035
Carbon weight (g)	W	1.800
Column cross section radius (cm)	CR	0.50
Column length (cm)	CL	5.50
Packed bed density (g/cm^3)	RHOB	0.42
Apparent particle density (g/ cm3)	RHOC	0.75
Volumetric flow rate (ml/s)	V	0.067
Hydraulic loading rate (m/hr)	HLR	3.06
Initial COD (mg/L)	COD_0	169.8
Initial TOC (mg/L)	TOC_0	71.6
pH	pH	7.5
Pretreatment conditions	SRT=10 d, HRT=12 h	

Effluent Data for Column 7

t (min)	COD (mg/L)	CODcr[1] (mg/L)	COD/ COD_0[2]	TOC (mg/L)	TOC/ TOC_0
0	169	159		71.6	
15	81	71	0.45	31.24	0.44
30	96	86	0.54	38.67	0.54
45	103	93	0.58	43.74	0.61
60	103	93	0.58	47.11	0.66
90	110	100	0.63	49.17	0.69
120	125	115	0.72	51.98	0.73
180	140	130	0.82	53.74	0.75
240	140	130	0.82	50.73	0.71
360	162	152	0.95	56.49	0.79
510	132	122	0.77	60.71	0.85
600	147	137	0.86	59.24	0.83
720	147	137	0.86	64.9	0.91
900	155	145	0.91	64.48	0.90

[1]: Effluent COD corrected by subtracting the residual from the raw effluent COD.
[2]: Calculated based on the corrected data.

APPENDIX C THEORETICAL CARBON USAGE RATE OF PACT™

Assume the influent COD of a PACT™ system is 575 mg/L. The COD removal that can be attributed to the conventional AST mechanism is 60%. Then the COD concentration that is subject to PAC adsorption is 230 mg/L. Assume 30 mg/L of the 230 mg/L COD is non-adsorbable and is added to the effluent concentration. To achieve an overall COD removal of 80% of the influent COD, The equilibrium liquid concentration will be 85 + 30 = 115 mg/L.

Assuming that the aeration basin is completely mixed and the detention time is sufficient to reach equilibrium, then we can assume that the loading achieved by the PAC exiting the system will be in equilibrium with the water exiting the system. The calculation for the carbon usage rate will be based on the adsorbable portion of the equilibrium concentration, i.e., 85 mg/L.

Isotherm:

$$q_e = 12.45 \times 85^{0.51} = 120(mg/g)$$

Mass balance in the PACT™ reactor:

$$Q(c_{in} - c_{out}) = M_c q_e$$

$$\frac{M_c}{Q} = \frac{(200-85)(mg/L)}{120(mg/g)} = 0.96(g/L) = 0.96(kg/m^3)$$

where

M_C is the carbon dosage for a day (g/d)

Q is the flow rate (L/d)

REFERENCE

Ball, D.G. (1996) "Comparison of the PACT and Activated Sludge Processes, for the Treatment of a Kraft Pulp Mill Wastewater", M.A.Sc. Thesis, Civil Engineering Dept., U. of Ottawa, Ottawa, Ontario

Benedek, A. (1980) "Carbon Evaluation and Process Design", Proceedings of the Physical chemical Treatment, Activated Carbon Adsorption in Pollution Control, Ontario, Canada

Bryant, C.W., Amy, G.L., Neill, R., and Ahmad, S. (1988) "Partitioning of Organic Chlorine Between Bulk Water and Benthal Interstitial Water Through a Kraft Mill Lagoon", Wat. Sci. Tech., Vol. 20, No. 1, p 73

Bryant, C.W., Avenell, J.J., and Barkley, W.A. (1992) "The Removal of Chlorinated Organics from Conventional Pulp and Paper Wastewater Treatment System", Wat. Sci. Tech., Vol.26, No. 1–2, pp 417–425

Callaham, W.F. and Pincince, A.B. (1977) "Physical-chemical Treatment System at Fitchburg, Massachusetts", presented at TAPPI Environ. Conf., Chicago, Illinois

Çeçen, F. (1993) "Adsorption Characteristics of a Biotreated Pulp Mill Effluent", Wat. Sci. Tech., Vol. 28, No. 2, pp 1–10

Çeçen, F., Urban, W., and Haberl, R. (1992) "Biological and Advanced Treatment of Sulfate Pulp Bleaching Effluents", Wat. Sci. Tech., Vol. 26, No. 1–2, pp435–444

Chen, H.T. (1981) "Pilot Plant Evaluation of Three Tertiary Technologies for Pulp and Paper Mill Effluent Treatment", presented at TAPPI Environ. Conf.

Cooney D.O. (1999) "Adsorption Design for Wastewater Treatment", Lewes Publishers, Boca Raton, Florida

Crittenden, J.C. and Weber, W.J.Jr. (1978) "Model for Design of Multicomponent Adsorption System", Jr. Envi. Eng. Division, EE6, pp 1175–1195

Crittenden, J.C. and Weber, W.J.Jr. (1978) "Predictive Model for Design of Fixed-bed Adsorbers: Single-component Model Verification", Jr. Envi. Eng. Defision. EE3, pp 433–443

Daigger, G.T. and Grady, C.P.L. (1979) "A Model for the Bio-Oxidation Process Based on Product Formation Concepts", Wat. Res., Vol. 11, p 1094

Droste, R.L. (1997) "Theory and Practice of Water and Wastewater Treatment", John Wiley & Sons, Inc., Toronto, Ontario

Eckenfelder, W.W.Jr., (1981) "Application of Adsorption to Wastewater Treatment", Proceedings of International Conf. on Application of Adsorption to Wastewater Treatment, Vanderbilt University, School of Engineering, Continuing Education, Enviro Press. Inc., Boston, Massachusetts

Environment Canada (1996) "Pulp and Paper Mill Effluent Chlorinated Dioxins and Furans Regulations, Compliance and Enforcement Report–Vol. 1", webpage of Environment Canada

Faust S.D. and Aly O.M. (1987) "Adsorption Processes for Water Treatment", Butterworth Publishers, Boston, MA

Graham, B.R. (1996) "Comparison of Powdered Activated Carbon and Activated Sludge Treatment of a Kraft Pulp Mill Wastewater", M.A.Sc. Thesis, Civil Engineering Dept., U. of Ottawa, Ottawa, Ontario

Hall, E.R. and Randle, W.G. (1992) "AOX Removal from Bleached Kraft Mill Wastewater: A Comparison of Three Biological Treatment Processes", Wat. Sci. Tech. Vol. 26, No. 1–2, pp 387–396

Hand, D.W, Crittenden, J.C., Arora, H., Miller, J.M., and Lykins, B.W.Jr. (1989) "Designing Fixed-bed Adsorbers to Remove Mixtures of Organics", JAWWA, Vol.81, No.1, pp 67–77

Jackson-Moss, C.A., Maree, J.P., and Wotton, S.C. (1992) "Treatment of Bleach Plant Effluent with the Biolofical Granular Activated Carbon Process", Wat. Sci. Tech., Vol. 26. No. 1–2, pp 437–444

Kallas J. and Munter R. (1994) "Post-treatment of Pulp and Paper Industry Wastewaters Using Oxidation and Adsorption Processes", Wat. Sci. Tech., Vol. 29, No. 5–6, pp 259–272

Kantardjieff, A. and Jones, J.P. (1997) "Practical Experiences with Aerobic Biofilters in TMP, Sufite, and Fine Paper Mills in Canada", Wat. Sci. Tech., Vol. 35, No. 2–3, pp 227–234

Kringsted, K.P. and Lindstorm, K. (1984) "Spent Liquors from Pulp Bleaching", Environ. Sci. Tech. Vol. 18, 236A

LaFand, R.A. and Rerguson, J. (1991) "Anaerobic and Aerobic Biological Treatment Processes for Removal of Chlorinated Organics from Kraft Bleaching Wastes", TAPPI Environ. Conf., Proceedings, Book 2, pp797–805, San Antonio, Texas, US

Liu, K. and Weber, W.J.Jr. (1981) "Characterization of Mass Transfer Parameters for Adsorber Modeling and Design", Jr. WPCF. Vol. 53, No. 10, pp 1541–1550

McCubbin, N. (1992) "Municipal and Industrial Strategy for Abatement Best Available Technology Study, Pulp and Paper Sector", Ontario Ministry of the Environment, PIBS1847, Queen's Printer, Toronto, Ontario

McKay, C. (1999) "Use of Adsorbents for the Removal of Pollutants form Wastewaters", CRC Press, Boca Raton, Florida

Mobius, C.H. and Cordes-Tolle, Mo (1994) "Advanced Treatment of Paper Mill Wastewaters". Wat. Sci, Tech. Vol. 29, No. 5-6, pp 273–282

Narbaitz, R. and Benedek, A. (1981) "The Effect of Operating Parameters on Carbon Usage", Proceedings of International conference on Application of Adsorption to Wastewater Treatment, Nashville, Tennessee

Narbaitz, R. M. (1985) "Modeling the Competitive Adsorption of 1, 1, 2-Trichloroethane with Naturally Occurring Background Organics onto Activated Carbon", a thesis for the degree of Doctor of Philosophy, McMaster University, Hamiton, Ontario

Narbaitz, R.M. and Benedek, A. (1983) "Least Cost Process Design for Granular Activated Carbon Adsorbers", Jr. WPCF, Vol.55, pp 1244–1251

Okazaki, M. and Kage, H. (1989) "predition of the Breakthrough Curve of a Packed Bed Adsorber Used for Treatment of Unknown Multisolute Wastewaters", Chem. Eng. Proc. Vol. 26, pp 247–255

Peel, R.G. (1979) "The Roles of Slow Diffusion and Bioactivity in Adsorption Column Modeling", Ph.D. thesis, McMaster University, Hamilton, Ont. Canada

Peel, R.G. and Benedek, A. (1981) "A Simplified Driving Force Model for Activated Carbon Adsorption", Can. Jr. Chem. Eng. Vol. 9, pp 688–692

Randle, W.G., Hall, E.R., and McKinlay, A.Y. (1991) "Optimization of Biological Treatment Systems for Enhanced Removal of AOX and Chlorophemolic Compounds", TAPPI Emviron. Conf. Proceedings, Book 1, pp 433–443, San Antonio, Texas

Randtke, S.J. and McCarty, P.L. (1979) "Removal of Soluble Secondary Effluent Organics", Jr. Env. Eng. Div. ASCE, 105, p 727

Randtke, S.J. and Snoeyink, V.L. (1983) "Evaluating GAC Adsorption Capacity", Jr. AWWA, Vol.75, pp 406–413

Rovel J.M., Trudel J.P., Lavallée P., and Schroeter I. (1994) "Paper Mill Effluent Treatment Using Biofiltration", Wat. Sci. Tech., Vol. 29, No. 10-11, pp217–222

Saunamäki, R., Jokinen, K., Jarvinen, R., and Savolainen, M. (1991) "Factors Affecting the Removal and Discharge of Organic Chlorine Compounds at Activated Sludge Treatment Plants", Wat. Sci. Tech., Vol. 24, No. 3–4, pp295–237

Schultz, J.R. and Keinath, T.M. (1984) "Powdered Activated Carbon Treatment Process Mechanisms", Jr. WPCF, Vol. 56, No. 2, pp 143–150

Sinclair, S.F. (1990) "Controlling Pollution from Canadian Pulp and Paper Manufactures: A Federal Perspective", Environment Canada, Ottawa

Sontheimer, Crittenden, and Summers (1988) "Activated Carbon for Water Treatment", 2nd edition, DVGW-Forschungsstelle, Engler-Bunte Institute, University of Karlsruhe, Germany

Springer, A.M. (1986) "Industrial Environmental Control, Pulp and Paper Industry", J.Wiley and Sons

"Standard Methods for the Examination of Water and Wastewater" (1971) 13th ed., APHA, AWWA, WPCF, American Public Health Association, Washington, DC.

Swyer, R. (1996) "Optimization of GAC Adsorption for Small Water Treatment Plants", a thesis for the degree of M.Eng., University of Ottawa, Ottawa, Ontario

Thacker, W.E., Snoeyink, V.L., and Crittenden, J. (1981) Modeling of Activated Carbon and Coal Gasification Chey Adsorbents in Single-Solute and Bisolute Systems", UILU-WRC-81-0161, Univ. of Illinois at Urbana-Champaign, Water Resources Center, Illinois

Verreault, M. (1992) "Biophysical Treatment of Wastewater from Fine Papermaking Operations Using the PACT™ System", presented at TAPPI Environ. Conf.

Vuoriranta, P. and Remo, S. (1994) "Bioregeneration of Activated Carbon in a Fluidized GAC Bed Treating Bleached Kraft Mill Secondary Effluent", Wat. Sci. Tech., Vol. 29, No. 5–6, pp 239–246

Wasserlauf, M. (1975) "Toxicity Temoval from Kraft Mill Effluents by Activated Carbon", Proceedings of the physycal-chemical Treatment, Activated Carbon Adsorption in Pollution Control Technology Seminar, Toronto, Canada

Weber, W.J.Jr. (1972) "Physicochemical Processes for Water Quality Control", John Wiley and Sons Inc., New York, N.Y.

Weber, W.J.Jr. and Chakravorti, R.K. (1974) "Pore and Solid Diffusion Models for Fixed-bed Adsorbers", AICHE, Jr., Vol. 20, No. 2, p228

Wedler, G. (1976) "Chemisorption: An Experimental Approach", Butterworths Publishers, Inc., Boston, Mass., pp 22-32